COMPARISON OF WIND-DRIVEN RAIN TEST METHODS FOR RESIDENTIAL FENESTRATION

By

CARLOS R. LOPEZ

A THESIS PRESENTED TO THE GRADUATE SCHOOL
OF CIVIL ENGINEERING AT THE UNIVERSITY OF FLORIDA IN PARTIAL
FULFILLMENT OF THE REQUIREMENTS FOR THE DEGREE OF
MASTER OF ENGINEERING

UNIVERSITY OF FLORIDA

2009

To my parents, Amanda Duarte and Alfonso Lopez

ACKNOWLEDGMENTS

Without the help of the oversight committee this research project would not have been possible. I would like to thank: Alside, American Architectural Manufacturers Association (AAMA), American Forest & Paper Association (AFPA), APA–The Engineered Wood Association, Architectural Testing Inc., Atrium Companies Inc., Cast-Crete Corporation, C.B. Goldsmith and Associates Inc., CEMEX, Certified Test Labs, Do Kim & Associates, DuPont, Fenestration Manufacturers Association (FMA), Florida Building Commission, Florida Home Builders Association (FHBA), General Aluminum, Henkel, Institute for Business and Home Safety (IBHS), James Hardie, JBD Code Services, JELD-WEN Windows and Doors, Lawson Industries Inc., Marvin Windows and Doors, Masonry Information Technologists Inc., MI Windows and Doors, NuAir Windows and Doors, Painter Masonry Inc., PGT Industries, PPG Industries, Protecto Wrap Company, Silver Line Windows and Doors, Simonton Windows, TRACO, and WCI Group Inc.

I would also like to thank my faculty advisor, Forrest J. Masters, Ph.D., and committee members Kurtis R. Gurley, Ph.D. and David O. Prevatt, Ph.D., P.E. for their advice and guidance.

This research was supported by the National Science Foundation (CMMI- 0729739) and the State of Florida Department of Community Affairs.

TABLE OF CONTENTS

LIST OF TABLES

Table page

LIST OF FIGURES

Figure page

Abstract of Thesis Presented to the Graduate School
of Civil Engineering at the University of Florida in Partial Fulfillment of the
Requirements for the Degree of Master of Engineering

COMPARISON OF WIND-DRIVEN RAIN TEST METHODS FOR RESIDENTIAL FENESTRATION

By

Carlos R. Lopez

December 2009

Chair: Forrest J. Masters
Cochair: Kurtis R. Gurley
Major: Civil Engineering

While recent changes in building codes have resulted in better structural performance during tropical cyclones, water intrusion through the building envelope continues to be a recurring issue. As a result, industry and code officials have voiced a need to reevaluate the standardized test methods in place for product approval.

Under the oversight of a task force that includes representatives from product manufacturing, homebuilding, architecture, engineering, insurance, code development and test laboratories, these methods have been investigated through a series of tests that examines full scale wall/window specimens subjected to simulated wind driven rain (WDR) scenarios. These WDR events were simulated using a pressure chamber, in which full-scale residential wall systems were subjected to uniform, linearly varying, and cyclic pressure loads while the façade was wetted. The specimens were also subjected to dynamic loads using a new turbulent wind load simulation apparatus developed at the University of Florida (UF). It was discovered that the static and cyclic pressure testing procedures used in the experiment described herein replicated the results observed in the dynamic pressure test reasonably well. Holistic testing of the

specimens also yielded results that demonstrate the importance of testing products as an assembly rather than in isolation.

CHAPTER 1
INTRODUCTION

Since 1980, ninety natural hazard events have cost the U.S. more than one billion dollars individually [1]. The most costly of these events are tropical cyclones (see figure 1.1, data from [1]). One-third of these hurricanes have caused an excess of one billion dollars in damages They are more destructive than tornadoes, snow storms, and terrorism combined, accounting for 47.5% of insured losses since 1984 (figure 1-2, data from [6] and [7]) and amounting to approximately $1.09 trillion dollars of damage since 1900 [3].

Florida, which is the most hurricane prone state in the U.S., is affected by 40% of all U.S. landfalling hurricanes. Two of the three Saffir Simpson Hurricane Scale (SSHS) Category 5 storms on record have made landfall in Florida, and 39% of major storms have affected this state [4]. Of the 10 most costly hurricanes impacting the U.S., eight made landfall in Florida (see table 1.1) [4]. Between 1987 and 2006, $138 billion in insurance claims were paid to policy holders [6, 7].

Florida's susceptibility to hurricanes is also a function of its population density, which has grown 85% (approximately $9.7 to 18.3 million) from 1980 to 2008, and expected to further grow from 18.3 million current residents to 28.7 million residents in 2030 [5a]. The implications of such a rapid increase in population is represented by the possibility of the next Category 5 storm yielding damages exceeding $80 billion dollars [6, 7] if it strikes a major population center.

Preventative measures must be taken in order to lessen the effect of tropical cyclones on residential structures. Thus, industry and code officials have voiced a need to reevaluate the standardized test methods in place for the product approval of fenestration products. The research herein addresses the mitigation of water ingress through wall systems with integrated

fenestration. It focuses on the water penetration resistance test methods used in the product approval process for building codes in hurricane-prone areas. This chapter presents a brief historical perspective on recent hurricane impacts, discusses water ingress through fenestration, and provides an overview of the scope of work for this research.

Recent Hurricane Impacts

On August 24, 1992, Hurricane Andrew struck southeast Florida with sustained wind speeds of 64.72 m/s (145 mph) and set the record as the most costly catastrophe of the 20th century. It caused $26.5 billion in damage and is second only to hurricane Katrina, which was responsible for $81.0 billion in damage [4]. The damage of Hurricane Andrew was quantified in a report commissioned by then Florida Governor Lawton Chiles as (Executive order 92-291, 1992):

- 135,446 homes damaged or destroyed
- 82,000 businesses damaged or destroyed
- 7,800 businesses closed
- 86,00 people unemployed

The devastation brought on by Hurricane Andrew raised many questions about building performance. Many government agencies subsequently began to investigate the effectiveness of the building codes and code compliance. The Federal Emergency Management Agency (FEMA) assembled a team to survey the failures and found problems with inadequate designs, poor workmanship, misapplication of building materials, improper review of construction permit documents, shortages of inspection staff, as well as deficient training of inspecting staff [9]. These findings led to changes that intended to improve the wind resistance of new buildings in Florida, including a tripling of the number of roofing inspectors in Dade County [6, 7]. New standards were also implemented in the building code, such as the incorporation of window and

door standards that mandate the use of hurricane shutters or impact resistant glass, as well as a mandatory review of plans by certified engineers [6, 7].

With the exception of Hurricane Opal (1995), Florida went without a notable landfall during the next 10 years. In 2004 a record 27 disaster proclamations were issued for hurricanes [10]. Florida was affected most severely, experiencing Hurricanes Charlie, Frances, Ivan, and Jeanne [10]. The damage in parts of Florida was magnified by the concurrence of both time and location of Charley, Frances and Jeanne (see figure 1-4). Jeanne and Frances followed almost identical paths and overlapped regions of Florida already affected by Hurricane Charley. The three storms were separated by 28 days (Landfalls: Charley August 13th, Frances September 5th, and Jeanne September 25th [11]).

The most active season in recorded history occurred the following year. The 2005 hurricane season was one that exceeded many previous records [4]. Tropical storms formed beyond the end of the Atlantic hurricane season as far as January 2006 (Zeta: Dec 30th to Jan 6th [11]). Seven major hurricanes and a record four hurricanes reached Category 5 strength on the Saffir-Simpson scale (Emily, Katrina, Rita, and Wilma [11]). Hurricane Katrina holds the record for costliest disaster at $81.0 billion dollars [4]. Together the 2004 and 2005 produced 7 of the 9 costliest hurricanes to occur in the U.S. These seasons had a combined 43 named storms, 15 of which made landfall on the United States costing an estimated $142 billion dollars in damage.

FEMA Mitigation Assessment Teams were tasked to investigate building performance and found that main wind force resisting systems designed to post-Andrew building codes were effective in withstanding extreme wind loads [10]. However, extensive damage occurred to component and cladding systems, particularly through water ingress. In report FEMA 490, the majority of building damage was attributed to “insufficient wind resistance of building envelope

systems which allowed wind-driven water infiltration into buildings, resulting in contents damage and loss of function." Furthermore, the authors stated that "the performance of building envelope systems in high wind events requires attention. Design guidance and code changes are needed." This research specifically addresses this concern with regard to performance of the window-wall systems, i.e., the window, wall, and interface (defined by the installation technique).

Water Penetration Resistance Requirements for Residential Fenestration

There are many field and laboratory test methods that evaluate the water penetration resistance of fenestration. These include static pressure tests (e.g., TAS 202-94 [47], ASTM E331-00 [41], Procedure A of ASTM E1105-05 [43], and ASTM E547-00 [42]), cyclic static pressure tests (e.g., TAS 203-94 [48], JIS A 1517 [46],and Procedure B of ASTM E1105-05 [43]), cyclic pressure tests (e.g. ASTM E2268-04 [44]), and dynamic tests (e.g., AAMA 501.1-05 [39]). These tests stipulate a performance criterion, such as a maximum allowable accumulation of water that overflows the innermost plane of the product. Most standards stipulate that the corresponding load condition be equal to 15% of the structural design pressure (AAMA/WDMA/CSA 101/I.S.2/A440 [38], TAS 202-94 [47]).

The principal question in this research is whether these conditions and the experimental design are representative of hurricane conditions. Moreover, since windows are currently tested in isolation, how do they perform when they are integrated into a finished wall system that might propagate leaks into the cavity between the window and the rough opening of the wall? The literature is scarce on the subject of holistic testing (i.e. testing of construction assemblies rather than products in isolation) which is highly problematic considering the wide variety of window options, installation methods, and finished wall systems available today. A thorough understanding of the interaction of these products is essential due to the increasing number

products available. Consider that the numbers of new windows produced each year has increased from 2 per 100 people in 1900 to 11.1 in 2000 [13].

Scope of Research

The objectives of this study are as follows:

- Develop a testing procedure that holistically evaluates the performance of the building system, i.e. a finished wall with an integrated window
- Evaluate existing fenestration testing protocols by analyzing these results with those attained from the full scale Hurricane Simulator at the University of Florida (See Masters et al. [49] , and Testing Apparatuses in Chapter 4).
- Examine the differences in water penetration behavior given various operable window assemblies.

To carry out this research, modified water penetration test methods were conducted on sixteen full size wall specimens that varied in window size, window material, operator type, wall construction, exterior finish, and sill type were constructed for evaluation. Each specimen underwent four individual rounds of testing using static, cyclic, dynamic, and static load sequences. The static and cyclic pressure tests were based on existing test methods. Water penetration was quantified and compared with results from testing using the Hurricane Simulator (detailed in Chapter 6). Testing using the Hurricane Simulator is used as the basis for comparison, given that the wind loading is calibrated to data collected in the field by the Florida Coastal Monitoring Program (FCMP) since 1999. The specimens were then subjected to a second static pressure test (using the exact pressure loading and wetting as the first static test), to determine if damage occurred during the first three tests. Specimens were loaded with both positive and negative pressure to compare their relative results. Finally, results from these tests were used to quantify the difference in water penetration resistance between different operator types.

Chapter 2 reviews the literature on the topic of wind-driven rain ingress through residential windows. An overview of existing water penetration resistance test methods is given in Chapter 3. Chapter 4 summarizes the experimental procedure. Specimen design and construction is explained in Chapter 5. Results of the research project are discussed in Chapter 6. Chapter 7 contains conclusions and suggestions for new test methods and future research.

Table 1-1. Ten Costliest Mainland United States Tropical Cyclones, 1900-2006

Rank	Hurricane	Impact	Year	Internal Pressure mbar	Category	Damage USD	2006 USD
1	Katrina	FL, LA	2005	920	3	81.0B	85.1B
2	Andrew	FL, LA	1992	922	5	26.5B	58.6B
3	Wilma	FL	2005	950	3	20.6B	21.6B
4	Charley	FL	2004	941	4	15.0B	17.1B
5	Ivan	FL,AL	2004	946	3	14.2B	16.2B
6	Hugo	SC	1989	934	4	7.0B	16.0B
7	Agnes	Fl	1972	980	1	2.1B	18.1B
8	Betsy	Fl, LA	1965	948	3	1.4B	18.7B
9	Rita	LA,TX	2005	937	3	11.3B	11.9B
10	Frances	FL	2004	960	2	8.9B	10.2B

Table 3a and table 3b from NWS TPC-5 [4]

Table 1-2. Saffir Simpson Scale

Category	Winds		Central Pressure		Surge		Damage
	m/s	mph	mbar	in Hg	m	ft	
1	33.1-42.5	74-95	>979	>28.9	1.2-1.8	4-6	Minimal
2	42.9-49.2	96-110	965-979	28.5-28.9	1.8-2.4	6-8	Moderate
3	49.6-58.1	111-130	945-964	27.9-28.5	2.4-3.7	9-12	Extensive
4	58.6-69.3	131-155	920-944	27.2-27.9	3.7-5.5	13-18	Extreme
5	69.3	>155	<920	<27.2	>5.5	>18	Catastrophic

Table 3a from NWS TPC-5 [4]

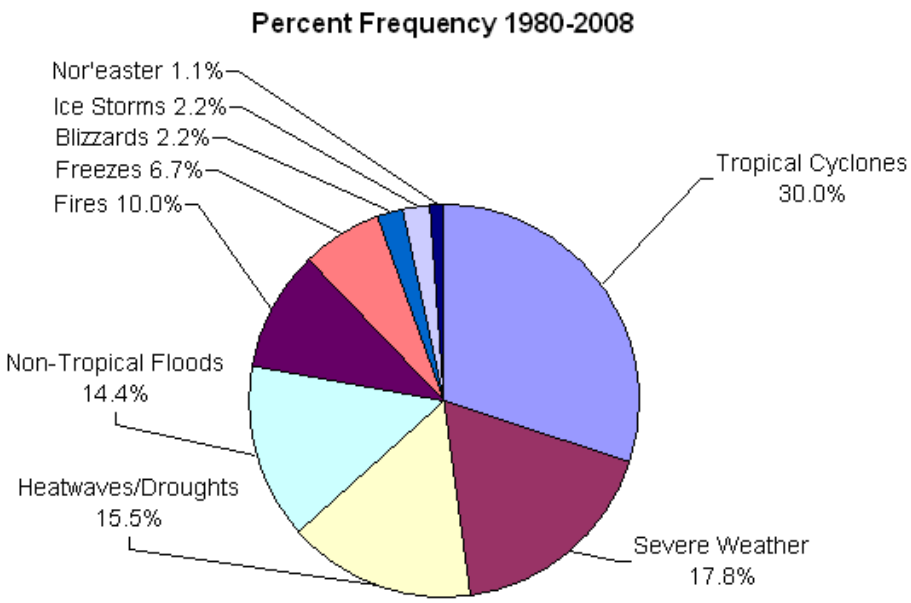

Figure 1-1. Percent of Natural Disasters Over 1.0 Billion Dollars

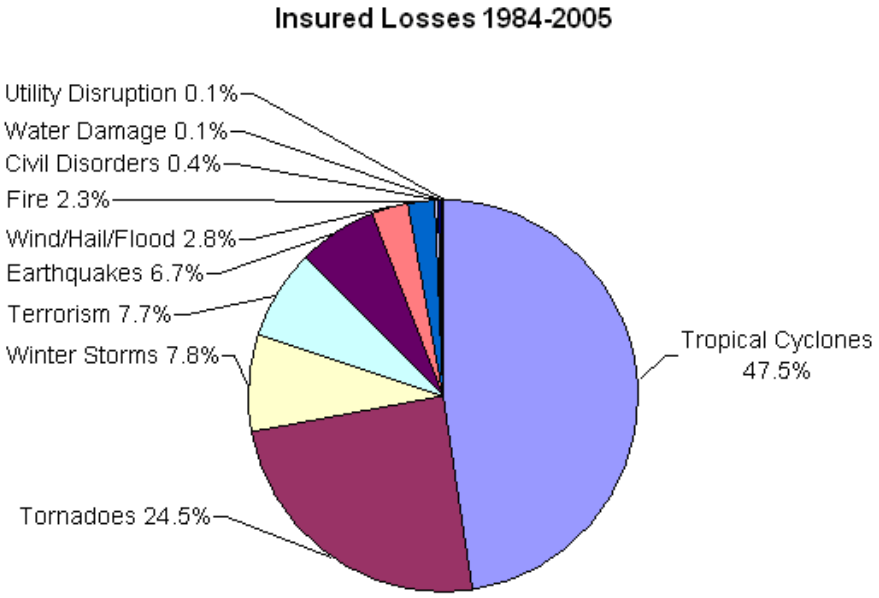

Figure 1-2. Allocation of Insured Losses Since 1984

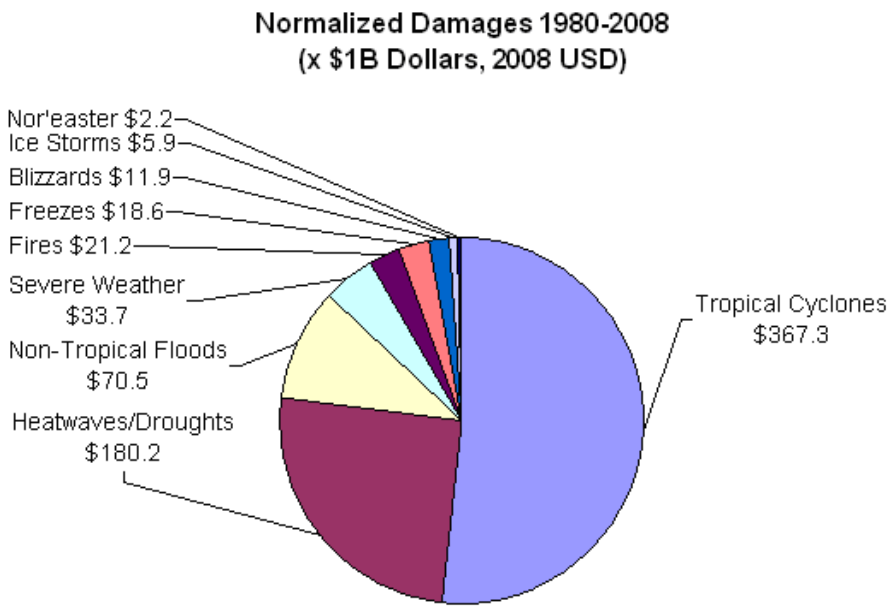

Figure 1-3. Normalized Losses Since 1980

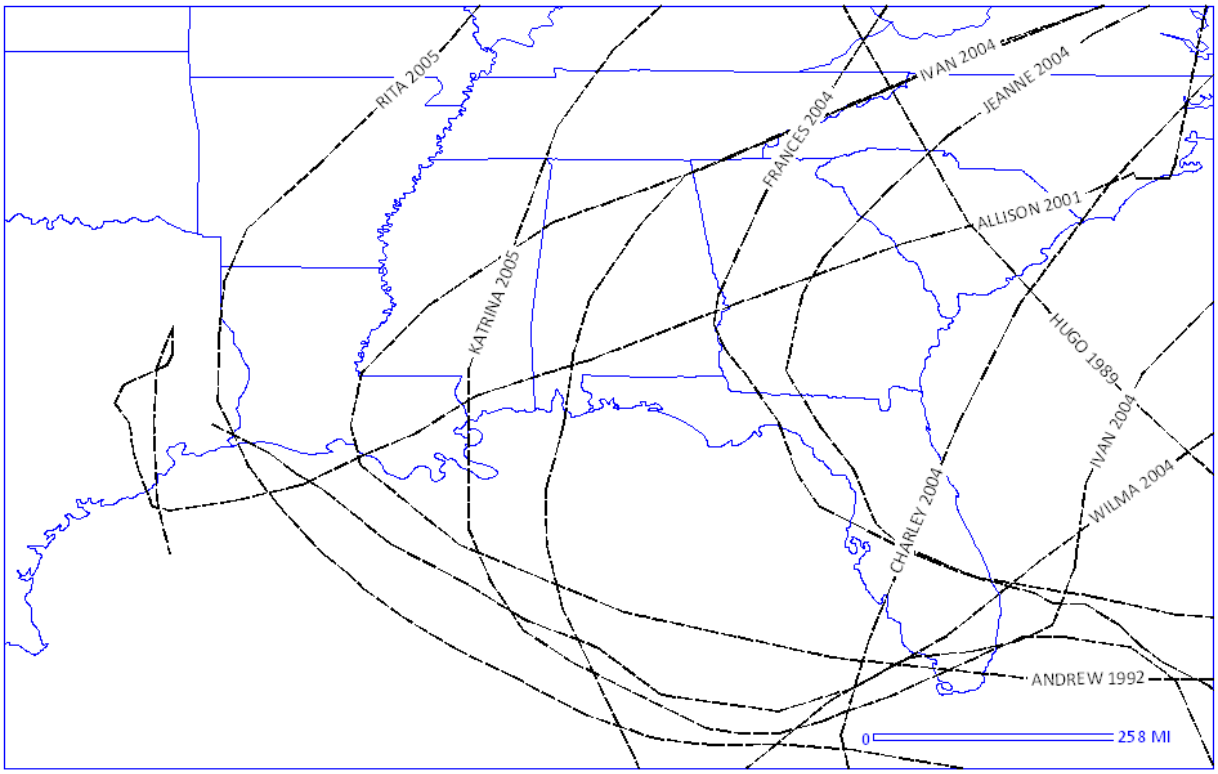

Figure 1-4. Paths of 10 Costliest United States Tropical Cyclones

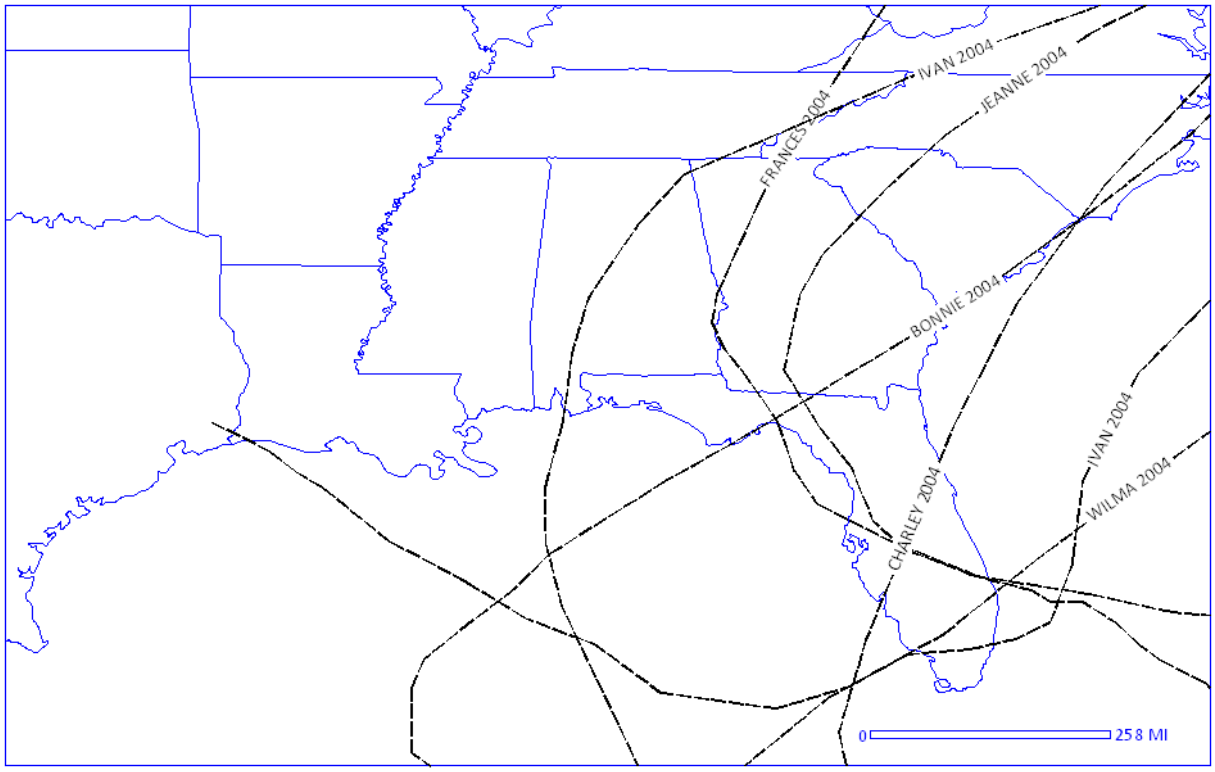

Figure 1-5. Florida Impacting Hurricanes of 2004

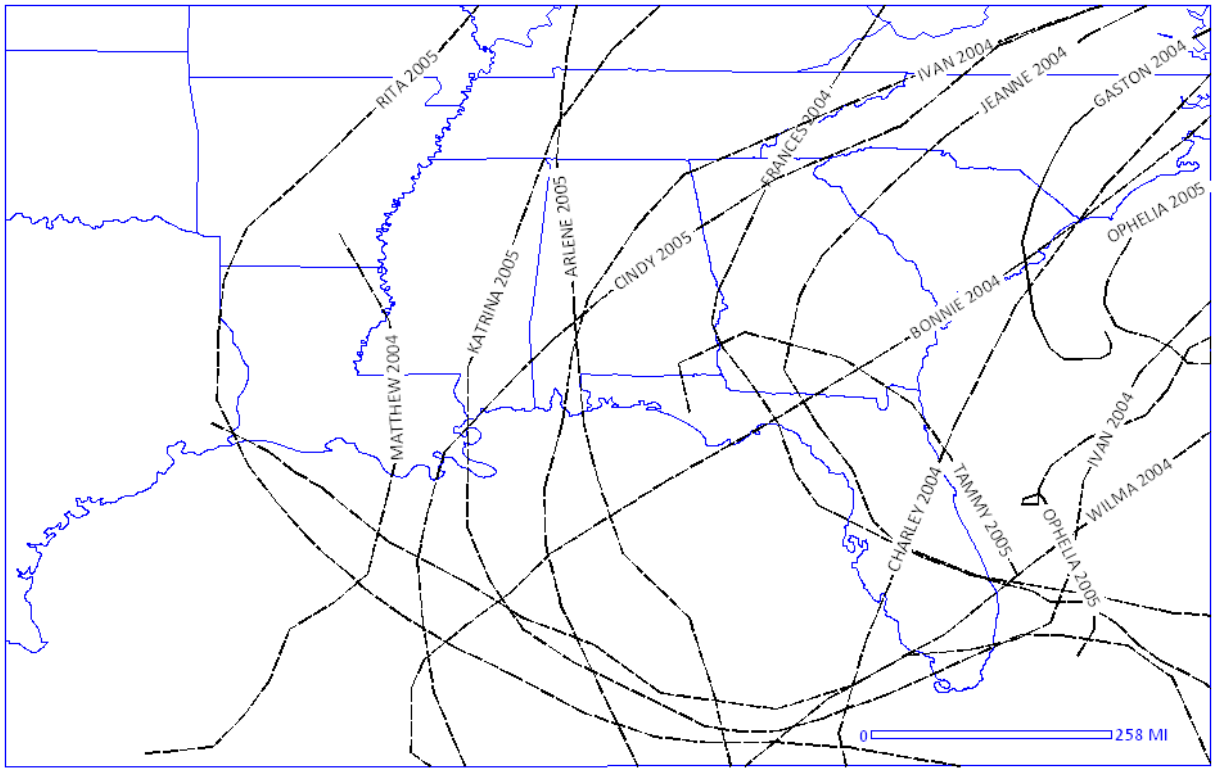

Figure 1-6. Hurricane Activity of 2004 and 2005 Seasons

CHAPTER 2
WIND-DRIVEN RAIN INGRESS THROUGH THE BUILDING ENVELOPE

Wind driven rain has been an active research topic for over a century [19]. In the area of building science, research of the effects of wind driven rain on building components has remained a difficult task for scientists. This is mainly due to the rapid progress of new and innovative construction materials and practices. This imbalance has directly led to the inability of building assemblies to withstand WDR loading, yielding water ingress. To explain this phenomenon, this chapter will discuss the major factors of WDR leading to water ingress through the building façade.

Rainfall Intensity

Extreme wind-driven rain events begin with the occurrence of rainfall accompanying wind events. Rainfall rates as well as drop size distributions can vary throughout the duration of a storm as well as from storm to storm [37]. Rainfall intensity (referred to in different literature as unobstructed rainfall intensity) is defined as the depth of rainfall accumulated per unit of time. Extreme short duration rainfall rates can reach 1872.0 mm/hr (73.7 in/hr, for one minute in Maryland, 1956) and 432.0 mm/hr (17.0 in/hr for 42 min in Missouri, 1947) [37]; however, statistical design rainfall rates are better representations. Technical Paper 40 from the National Weather Service prescribes a maximum of 127.0 mm/hr (5.0 in/hr) for a 100 year return 60 min rain event while most common test standards refer to a prescribed wetting of 203.0 mm/hr (8.0 in/hr, e.g. ASTM E331-00 [41], ASTM E1105-00, ASTM E2268-04 [44], and ASTM E547-00 [42]). This is the application required to cause water to sheet over a curtain wall, and is the rainfall intensity used in this experiment. There also exists a higher specified rainfall intensity of 274.0 mm/hr (10.8 in/hr, 100 year return 5 min rain event [35]). These design scenarios seem to well encompass rainfall in the northern hemisphere which rarely exceeds 144.0 mm/h (5.7 in/hr)

(0.01% of the time during the rainiest month) [37] and rainfall intensities gathered from tropical cyclones during the 2004-2006 Atlantic hurricane seasons that were a mean of 57.0 mm/h (2.4 in/hr) and a mean hydrometeor diameter of 1.7 ± 0.3 mm (.07 in ± .01 in) [36].

Raindrop Size Distribution

Raindrop size is an important factor in the wetting of the façade. As the next section explains raindrop size affects the trajectory of rain. However, before analyzing rainfall trajectory it is necessary to understand the effect different micrometeorological factors have on raindrop size distribution.

Raindrop size and raindrop size distribution is dependent on wind speed and rainfall intensity. Given a fixed liquid water content, the average hydrometeor size (figure 2-2) is expected to increase proportionally with wind speed. Raindrop size also varies with number of drops (i.e. the number of raindrops increases as the drop size decreases [27]. Other less significant factors that affect the drop size distribution include the type of rain, and position relative to the center of the storm.

Traditionally rainfall distribution has been presented as a function of only rainfall rate and drop size. Work performed by Best explains this relationship in the distribution expressed in equation 2-1.

$$1 - F = e^{-(2r/a)^{2.25}} \tag{2-1}$$

Where:

$$a = 1.30 I^{0.32}$$

$$G = 67 I^{0.846}$$

In this equation F is the fraction of liquid water in the air consisting of raindrops of radii < r (mm), I (mm/hr) is the rainfall intensity, and G (mm^3/ m^3) is the volume of liquid water per unit of volume of air. In this assumption, number of drops increase as drops size decreases.

Another rainfall intensity dependant distribution is the modified Γ-distribution (Equation 2-2) where N(D) is the concentration of drops having diameter D, N_G is the concentration parameter, Λ is the slope parameter, α is the curvature parameter, and D_0 is the median volume diameter [37].

$$N(D) = N_G D^{\alpha} e^{-\Lambda D} \tag{2-2}$$

Where:

$D_0 = 0.1571 M^{0.1681}$

$\Lambda = 5.5880 / D_0$

$\alpha = 2.160$

$N_G = \frac{512.85 M \times 10^{-6}}{D_0^4} (\frac{1}{D_0})^{2.160}$

Willis and Tattelman [37] sought to validate this distribution by comparing it to approximately 14,000 ten sec samples collected from hurricanes and tropical storms from 1975-1982 at 3000.0 m (9843.0 ft) and 450.0 m (1476.0 ft). What they found is that the model very reasonably characterized the observed distributions collected in rainfall rates of upwards of 225.0 mm/hr (8.9 in/hr). However, they also found unexplained differences in the distributions taken at 3000.0 m (9843.0 ft) and 450.0 m (1476.0 ft).

Rainfall Trajectory

Rainfall trajectory varies primarily due to two factors: raindrop size and wind speed. For a particular drop size the forces that act to change its flight pattern are gravity and drag. The drag forces are Reynolds (Re) number dependent, which are determined from the size of the droplet. As droplets form, they are small nearly spherical, due to surface tension dominating over the pressure forces. As their velocity increases in higher wind velocities they collide forming larger drops, and the unequal pressure distribution distorts the droplet as shown in figure 2-2. Through

out the fall of the droplet these collisions and droplet separations occur multiple times yielding different sized drops. Smaller sized drops are also susceptible to evaporation throughout [37].

Figure 2-1 depicts the rain vector, which has components of horizontal and driving rain intensity [18]. In the freestream case, as the droplets fall downwards through the boundary layer, the rain droplets are assumed to be moving at the gradient wind speed horizontally and falling at terminal velocity which effectively is a function of the drag coefficient. The trajectory, once reaching the obstructed wind flow area, becomes more complicated as does the wind flow. As droplets approach the building, the trajectory of the smaller particles changes more sharply. In contrast the higher inertia, larger droplets have a less oblique trajectory as well as a more rectilinear trajectory nearing the windward wall of the building [18]. In regards to the experiment described herein, the trajectory of rain droplets impinging on the specimens was assumed to be horizontal as it is assumed to be the worst case scenario for water intruding through vertically mounted fenestration.

Wetting of the Building Façade

The distribution of wetting on the building façade is highly non-uniform due to the flow characteristics around the building and the trajectory of the rain, which is sensitive to the raindrop size distribution [23, 26]. The flow around a building is dependent on upstream conditions, including surface roughness, orientation of the building in the flow field, and geometric shape. As different buildings are built to different aspect ratios, the varying local flows affect the deposition of droplets on the building façade. Hence the flow around a structure has to be calculated using a computational fluid dynamics model in which the three dimensional wind velocities are derived and then used to obtain the raindrop trajectories [26].

Quantifying the effect of WDR on a particular structure is accomplished by calculating the Local Effect Factors (LEFs) and Local Intensity Factors (LIFs) used by Choi. Other literature

may refer to LEFs and LIFs as specific catch ratio η_d and catch ratio η respectively. The LEF is the ratio of the wetting of a particular location on the structure to the unobstructed rainfall intensity in the free stream for a single hydrometeor diameter, d, and is illustrated in equation 2-3 [24,25].

$$LEF(t) = \frac{R_{dr}(d,t)}{R_h(d,t)} \tag{2-3}$$

The equivalent parameter for all raindrop sizes on the structure is the LIF. The LIF is obtained by integrating the LEFs over all hydrometeor diameters in equation 2-4 [24,25].

$$LIF(t) = \frac{R_{dr}(t)}{R_h(t)} \tag{2-4}$$

With the velocity data obtained from the flow model, the trajectories are computed at every point for each raindrop size by iteratively solving their equations of motion (Equation 2-5 through 2-7) in which m is mass of the droplet, r is radius, ρ_a is the air density, ρ_w is the water density, and μ is the air viscosity [26] and x is the along wind direction, y is the cross wind direction and, z is the vertical direction [24, 25].

$$m\frac{d^2x}{dt^2} = 6\pi\mu(U - \frac{dx}{dt}) - \frac{C_D R}{24} \tag{2-5}$$

$$m\frac{d^2y}{dt^2} = 6\pi\mu(W - \frac{dy}{dt}) - \frac{C_D R}{24} \tag{2-6}$$

$$m\frac{d^2z}{dt^2} = 6\pi\mu(V - \frac{dz}{dt}) - \frac{C_D R}{24} - mg(1 - \frac{\rho_a}{\rho_w}) \tag{2-7}$$

These equations of motion coupled with the drag coefficients of droplet sizes demonstrate that smaller diameter drops are greatly influenced by the flow closer to the structure. Choi demonstrated this with the use of drop size distributions by Best and Mualem [20, 21] to analyze a 4:1:1 ratio building. Choi demonstrated that for LEF values along the vertical outer thirds, the

top quarter decreases steadily upon increasing droplet size beyond 1.0 mm (0.04 in). In addition, the bottom three quarter LEF values increased steadily upon increasing droplet size beyond 1.0 mm (0.04in). Given raindrop sizes below 1.0 mm (0.04 in), the lower three quarters reach a minimum LEF value at 0.5mm (0.02 in), while the top quarter continues to decrease steadily. Furthermore in all cases, buildings demonstrated greater LIF values along the vertical outer thirds and substantially larger LIF values at the top quarter [24, 25].

Among the factors that affect WDR intensity, the most dominant are the location on the structure (as explained above), building geometry, and wind speed. The effect of varying building geometry, in particular width to height ratios, changes the blockage effect to the wind flow. For higher ratios the number of drops diverted away from the structure increases. This was also demonstrated by Choi's investigation in which a narrow (H:W:D=4:1:1) building exhibited higher LIF values than a wider (H:W:D= 4:8:2) building (assuming similar drop sizes).

Wind speed, as in the free stream case, also affects droplet trajectory by forcing droplets to acquire a larger horizontal velocity. The higher the wind speed the greater the driving rain intensity, therefore more droplets are susceptible to striking the building surface. Choi found that changing wind velocity from 5.0 m/s to 30.0 m/s (11.2 mph to 67.1 mph) can substantially increase LIF values 10 times for the top quarter of a 4:1:1 ratio building. That is to say, increasing wind velocity will increase the effect of all raindrop sizes on the building façade particularly in the top quarters.

Water Ingress through the Building Façade

Once rain droplets strike a building façade, they begin to collect and move across the building face. If unobstructed, the accumulation of water will simply runoff. However, if a penetration through the building envelope exists (e.g., microcracks in stucco [31]), water will

infiltrate due to the pressure differential, kinetic energy of rain droplets, and gravity and capillary forces [29].

This is a problem that persists although newer building codes and standards have yielded considerable declines in structural damage. In Florida this was evident during the 2004 hurricane season, which yielded over 1,000 complaints from new homeowners of water intrusion [30]. The causes for water intrusion in many of these cases were particularly perplexing due to the lack of obvious infiltration paths (e.g., damaged roofing materials, fenestration products, or evidence of flooding [30]).

Under commission from the Home Builders Association of Metro Orlando and the Florida Home Builders Association, Lstiburek conducted a study to identify the factors contributing to the failure of water penetration resistance in structures. In this study he identified the primary faults to be those of the performance of stucco claddings, water resistant barriers, windows and doors, service penetrations, soffit vent assemblies, and paint and coating techniques [31].

Blackall and Baker [29] stated that for the case of fenestration "there will almost always be paths for water to penetrate" unless much effort is put forth in the design and construction. Additionally once fenestration products have been installed they are susceptible to "building movement causing wracking forces on the casings" which will likely open paths for water infiltration.

Gurley et al. [17] found that the percentages of homes experiencing water damage due to water intruding through the exterior windows during the 2004 hurricane season were approximately 23% for homes built between 1994-1998, 24% for homes built between 1999-2001, and 12% for homes built between 2002-2004 [17].

Water penetration resistance performance has prompted several studies to identify the primary contributors of moisture problems. RDH Building and Engineering Ltd. [32, 33] sought to identify the contribution of building codes, standards, testing protocols and certification processes in a study that analyzed the performance of 113 laboratory and 127 field specimens. Their study identified five key issues:

- The need to address in-service exposure conditions
- Adequately address water penetration control at the window to wall interface
- Better address leakage directly associated with the manufactured window assembly
- Durability of water penetration performance
- Provide rational maintenance and renewals guidance for the installed window assembly

The research herein builds on the RDH study by (1) evaluating water penetration resistance in hurricane conditions and (2) taking a "systems" approach to evaluate the performance of a finished wall with integrated fenestration.

Summary

Wind-driven rain has three major factors that affect the wetting of structures: rainfall intensity, drop size distribution, and trajectory. Each factor has been reviewed to better represent the phenomenon of WDR and analyze current test standards as well as the performance of the specimens. The following chapter will provide an overview and commentary of existing water penetration test methods

.

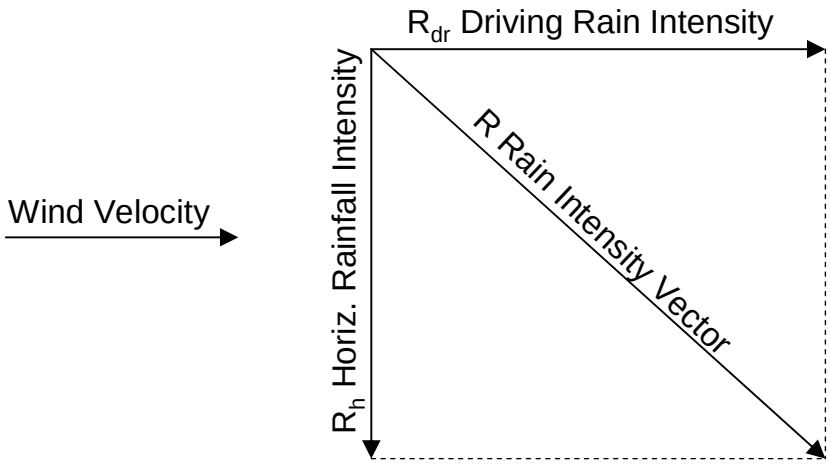

Figure 2-1. Components of the Rain Intensity Vector

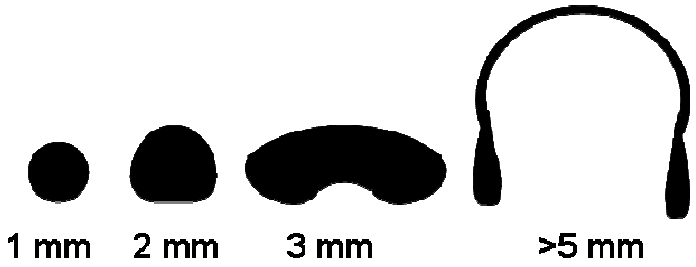

Figure 2-2. Typical Drop Size Shapes

CHAPTER 3
WATER PENETRATION RESISTANCE TEST METHODS

During tropical cyclones, fenestration products are subjected to extreme wind loads and WDR. Hence, governing bodies of many hurricane prone regions mandate that these products be evaluated by an accredited laboratory for structural and water penetration resistance. To assess product performance these laboratories employ repeatable, simplified test methods. The following chapter will provide an overview of these tests.

Uniform Static Air Pressure Difference

Uniform static air pressure tests are widely used in the product approval process (e.g., ASTM E331-00 [41]) and in diagnostic assessment of leakage paths in existing structures (Procedure A of ASTM E1105-05 [43]). Procedure A in ASTM E1105-05 [43], applies a specified static air pressure over 15 s and maintains that pressure for 900 s while the test subject receives a specified rate of water spray. ASTM E331-00 [41] preserves the same load time history however it states that "test-pressure difference or differences at which water penetration is to be determined, unless otherwise specified, shall be 137.0 Pa (2.86 psf)." (see figure 3-1). For the case of all ASTM tests water penetration is defined as "penetration of water beyond a plane parallel to the glazing (the vertical plane) intersecting the innermost projection of the test specimen, not including interior trim and hardware, under the specified conditions of air pressure difference across the specimen."

In Florida, Testing Application Standard (TAS) 202-94 [47] evaluates the structural and water penetration performance of fenestration products. It closely resembles ASTM E331-00 [41]. TAS 202-94 structurally tests a window to 150% of the rated design pressure, observing maximum and permanent deflections during testing (see figure 3-2). In regards to water infiltration the fenestration must not exhibit any intrusion when 15% of the design pressure is

applied with a constant water spray applied to the window specimen (see Section 5.2.6 of TAS 202-94 [47]).

Cyclic Static and Cyclic Air Pressure Difference

Cyclic static pressure tests are also used in the laboratory and the field to evaluate water penetration resistance (e.g. Procedure B of ASTM E1105-05 [43], ASTM E547-00 [42], ASTM E2268-04 [44], JIS A 1517 [46], and AS/NZS 4284:1995 [45]). The two major static cyclic pressure tests are ASTM E1105-05 [43] Procedure B, and ASTM E547-00 [42]. Both are a determination of water penetration of installed exterior windows, skylights, doors, and curtain walls, however; the major difference is ASTM E1105-05 [43] is strictly a field test.

ASTM E1105-05 [43] procedure B is also very similar to its counterpart, ASTM E1105-05 [43] procedure A, in that it doesn't specify a pressure median. The difference lies in the loading regime where the duration of the pressure cycle shall be 5 min followed by a decrease to ambient pressure in a period of not less than 1 min (see figure 3-4). The number of cycles is also unspecified and left to the governing body requesting the test. However, it stipulates that "In no case shall the total time of pressure application be less than 15 min" resulting in a minimum of 3 cycles. ASTM E547-00 [42] is a variation of ASTM E331-00's [41] loading function. The difference is the time of load has to be specified as well as the number of cycles (see figure 3-5).

ASTM E2268-04 [44] is a cyclic pressure test defined by a rapid pulsed air pressure difference. ASTM E2268-04 [44] is similar to the Japanese Industrial Standard JIS A 1517 [46] which uses the same loading function, however; it states that the "median test-pressure difference or differences at which water penetration is to be determined, unless otherwise specified, shall be 137.0 Pa (2.86 psf)" (see figure 3-3). The loading function JIS A 1517 [46] is a modulation limited to ± 50% of the median pressure with pulse lengths of 2 seconds.

Salient points of these tests are now discussed.

- Fenestration products come in a wide variety of design pressures and all have the potential to perform differently. A default minimum of 137.0 Pa (2.86 psf), in existing static pressure tests, rather than a percentage of the design pressure may not suit the requirements necessary in all areas. This issue becomes apparent in a location such as Florida where the lowest pressure rating for any window sold is approximately 1440.0 Pa (30.0 psf) and 15% of which is 216.0 Pa (4.5 psf). Therefore all windows intended for use in Florida would pass ASTM E331-00 [41] without meeting their lower bound infiltration criteria. While this issue is accounted for in TAS 202-94 [47] by specifically stating that the pressure shall not be less than 15% of the design pressure, it is a standard that is only used in Florida.

- TAS 203-94 [48] excludes the use of 137.0 Pa (2.86 psf) as a passing criteria for water intrusion. It is done intrinsically by mandating the successful completion of TAS 202-94 [47] prior to performing TAS 203-04 [48]. It should be noted that this is only for Florida. Additionally there is no stipulation on how to test for, quantify or record any water infiltration. Infiltration rates or observing minimum pressures at which the products exhibit water infiltration are not observed.

- ASTM E2268-04 [44] section 5.3 states: "As the specified or median test pressure is increased, the maximum test pressure in this procedure is also increased to 1.5 times the specification median test pressure. This higher maximum test pressure may not be representative of actual building service conditions. For this reason the maximum recommended median test pressure is 480.0 Pa (10.0 psf), which corresponds to a maximum test pressure of 720.0 Pa (15.0 psf)." Testing of products to 720.0 Pa (15.0 psf) to view water penetration behavior may not be sufficient and requires further research and discussion.

- No distinction in performance is made from product to product. Factors such as infiltration rates or minimum pressures at which the products do exhibit water infiltration are not observed. Such factors may play a major role in the insurable damage incurred and merit further study which cannot be obtained from minimum performance standards.

- The test pressure load varies considerably from in situ dynamic pressures. This is an issue which has been commented studies such as chapter 4 of Summary Report on Building Performance: 2004 Hurricane Season [10].

- There are no strategies or stipulations provided for different wind-driven rain exposure conditions (i.e. climate zones). This raises the question if water penetration resistance should be related directly to wind exposure zones and merits further research.

- Age effects are not considered. UV, ozone, and environmental exposures, over time, adversely affect the water penetration resistance of fenestration components such as weather-stripping and sealants [13]. Aging of the finished wall system may also yield new infiltration paths. The benefits of testing artificially aged assemblies merits further study [13, 50, 51, 52]

- These standards test specimens in isolation. Testing of the fenestration product as well as the interface is necessary to assess the performance of the assembly.
- These standards do not account for the loads fenestration products are exposed to when installed in structure. Fenestration products are inherently susceptible to the movement structures experience [29] (due to different physical loads, expansion due to heat, etc.). This redistribution of loading may open new migration paths for water and merits further research.

The American Architectural Manufacturers Association made similar notes of existing standards and has recently drafted a Voluntary Specification for Rating the Severe Wind Driven Rain Resistance of Windows, Doors and Unit Skylights (AAMA 520 [40]). The concept is to apply a spectrum of pulsating pressure and rain loads to determine how well a product performs in wind driven rain over a range of severities. The product receives a "score" on a scale of 1 to 10 based on its ability to prevent a volume of water greater than 15mL from entering the structure (see table 3-2 and figure 3-6). This is a significant departure from the usual practice of test standards, which are based on pass/fail criteria (minimum performance standards).

Pseudo-Dynamic Pressure

In 2005, AAMA drafted a voluntary specification that tests products for water penetration using dynamic pressure (AAMA 501.1-05 [39]). It utilizes a spray system in compliance with ASTM E331-00 [41] and "a wind generating device, such as an aircraft propeller, (that) shall be capable of producing a wind stream equivalent to the required wind velocity pressure." The wind generating device is calibrated to produce minimum of 3 test pressures (from 300 Pa, 380Pa, 480 Pa, 580 Pa, and 720 Pa) at four radially equidistant locations. The wind speed tolerance shall be within ±1.1 m/s (±2.5 mph) of the desired calculated wind speed. The test consists of applying the specified wind stream and spray for a period of 15 minutes. Water infiltration is then documented, quantified, and defined as "as any uncontrolled water that appears on any normally

exposed interior surfaces, that is not contained or drained back to the exterior, or that can cause damage to adjacent materials or finishes."

While this test attempts to more accurately reproduce field conditions, it raises a concern by allowing wind generators such as a propeller. Intrinsically by using a propeller without a method for flow straightening, the flow field is radially non-uniform and possesses significant vorticity. The velocity field produced by the propeller increases radially outward from the center of the propeller, resulting in pressures at the perimeter being much greater than those nearing the center. In extreme cases there may even be a flow reversal near the center of propeller. Given this phenomenon the calibration procedure is not effective since pressure measurements are taken at locations are that are radially equidistant from the center and by definition should yield similar pressures. In addition there is an induced spiral component of motion to rain droplets which would wet the face of the specimen unnaturally and may cause or inhibit water intrusions that are representative of service conditions.

Summary

In most hurricane-prone regions, fenestration must be tested by an accredited laboratory to determine its capacity to resist uniform static pressure loads and water ingress. Products must meet or surpass the requirements in these existing standards (a summary is given in table 3-3). The intention is that these products shall provide sufficient resistance to wind forces as to maintain the integrity of the building envelope. The next chapter will comment on the experimental procedure adopted and its development.

Table 3-1. Draft AAMA 520 Performance Levels

Performance Level	Lower Limit	Median	Upper Limit
1	239.4 Pa (5.0 psf)	478.8 Pa (10.0 psf)	718.2 Pa (15.0 psf)
2	284.3 Pa (6.0 psf)	574.6 Pa (12.0 psf)	852.8 Pa (18.0 psf)
3	335.2 Pa (7.0 psf)	670.3 Pa (14.0 psf)	1005.5 Pa (21.0 psf)
4	383.0 Pa (8.0 psf)	766.1 Pa (16.0 psf)	1149.1 Pa (24.0 psf)
5	340.9 Pa (9.0 psf)	861.9 Pa (18.0 psf)	1022.8 Pa (27.0 psf)
6	378.8 Pa (10.0 psf)	957.6 Pa (20.0 psf)	1136.4 Pa (30.0 psf)
7	526.7 Pa (11.0 psf)	1053.4 Pa (22.0 psf)	1580.0 Pa (33.0 psf)
8	574.6 Pa (12.0 psf)	1149.1 Pa (24.0 psf)	1723.7 Pa (36.0 psf)
9	622.4 Pa (13.0 psf)	1244.9 Pa (26.0 psf)	1867.3 Pa (39.0psf)
10	670.3 Pa (14.0 psf)	1340.7 Pa (28.0 psf)	2011.0 Pa (42.0 psf)

Table 3-2. Summary of Existing Testing Protocols

Test Name	Type of Load	Specified Load	Specified Number of Cycles	Objective	Product Applicability
ASTM E331	Static	137 Pa (2.86 psf)	N/A	Water penetration	Exterior windows, skylights, doors, and curtain walls
ASTM E1105-05 Procedure A	Static	Unspecified	N/A	Field determination of water penetration	Exterior windows, skylights, doors, and curtain walls
TAS 202-94	Static	75%, 150%, and 15% of DP	N/A	Structural, water penetration, air infiltration, forced entry	Any external component which helps maintain the integrity of the building envelope
ASTM E1105-05 Procedure B	Cyclic Static	Unspecified	Minimum of 3	Field determination of water penetration	Exterior windows, skylights, doors, and curtain walls
ASTM E547-00	Cyclic Static	137 Pa (2.86 psf)	Unspecified	Water penetration	Exterior windows, skylights, doors, and curtain walls
ASTM	Cyclic	206.0 Pa (2.5	300	Water	Exterior

E2268-04		psf), 137.0 Pa (2.86 psf), 69.0 Pa 1.4 psf		penetration	windows, skylights, and doors
AAMA 520	Cyclic	See table 3-2	300 per level see table 3-2	Water penetration	Windows, doors and unit skylights
AAMA 501.1-05	Pseudo-Dynamic	300.0 Pa (6.2 psf), 380.0 Pa (8.0 psf), 480.0 Pa (10.0 psf), 580.0 Pa (12.0 psf), and 720.0 Pa (15.0 psf)	One 15 min cycle at a time	Water penetration	Windows, curtain walls and doors

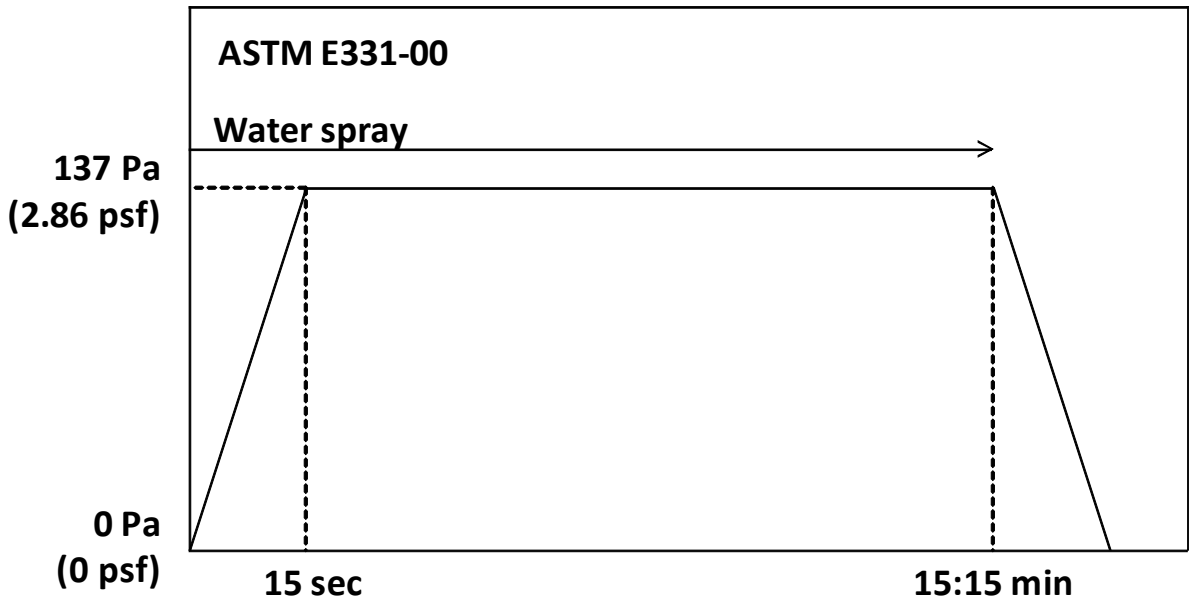

Figure 3-1. ASTM E331-00 [41] Pressure Loading History

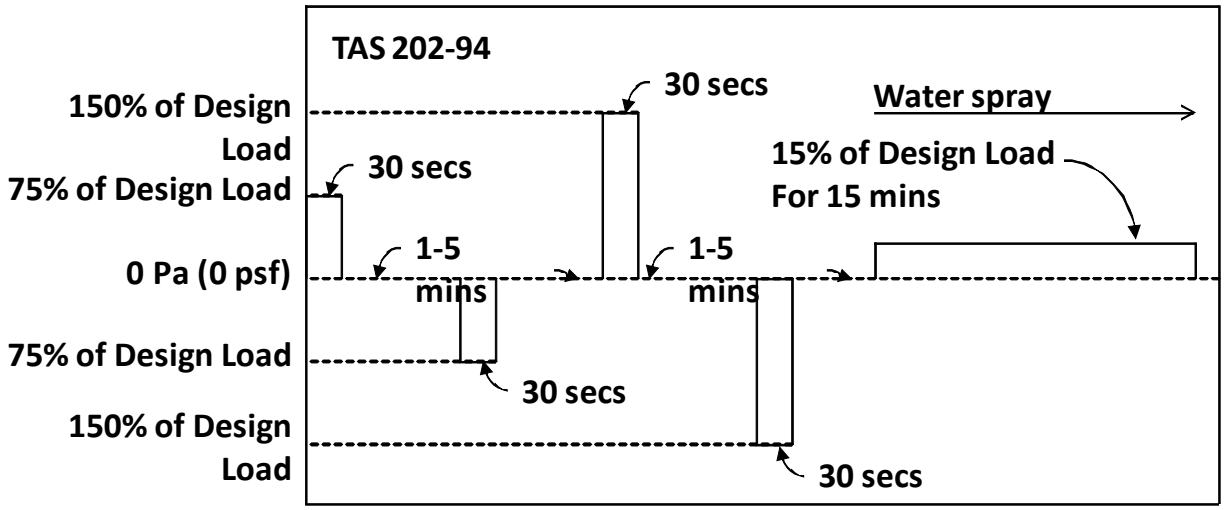

Figure 3-2. TAS 202-94 [47] Pressure Loading History

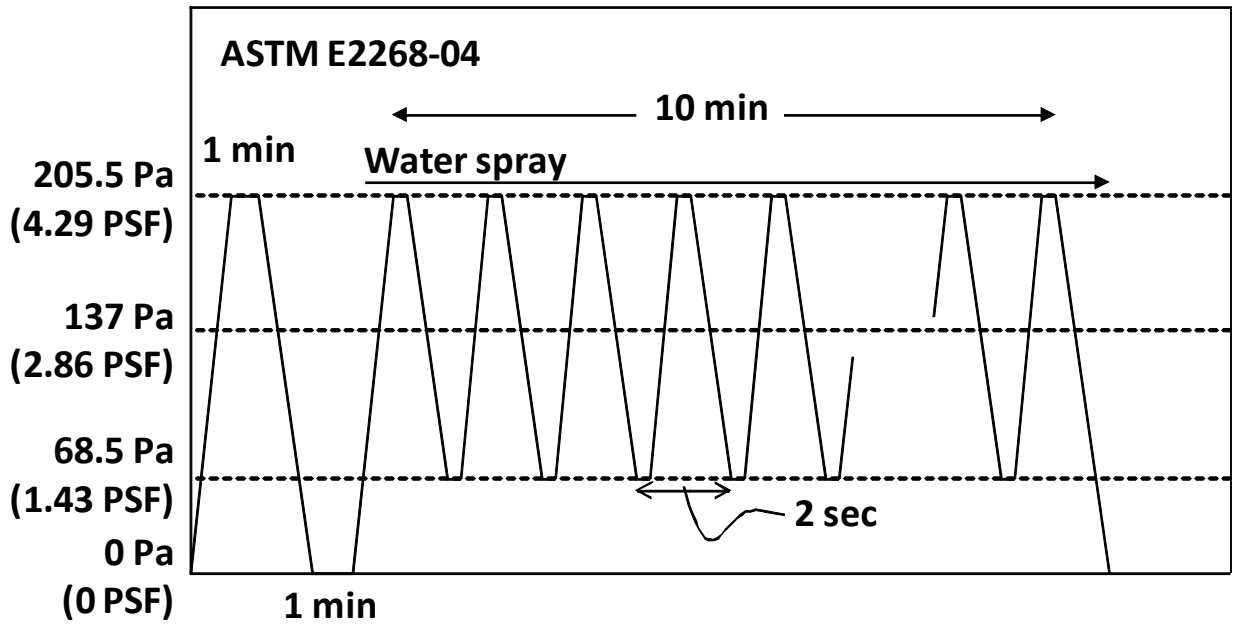

Figure 3-3. ASTM E2268-04 [44] Pressure Loading History

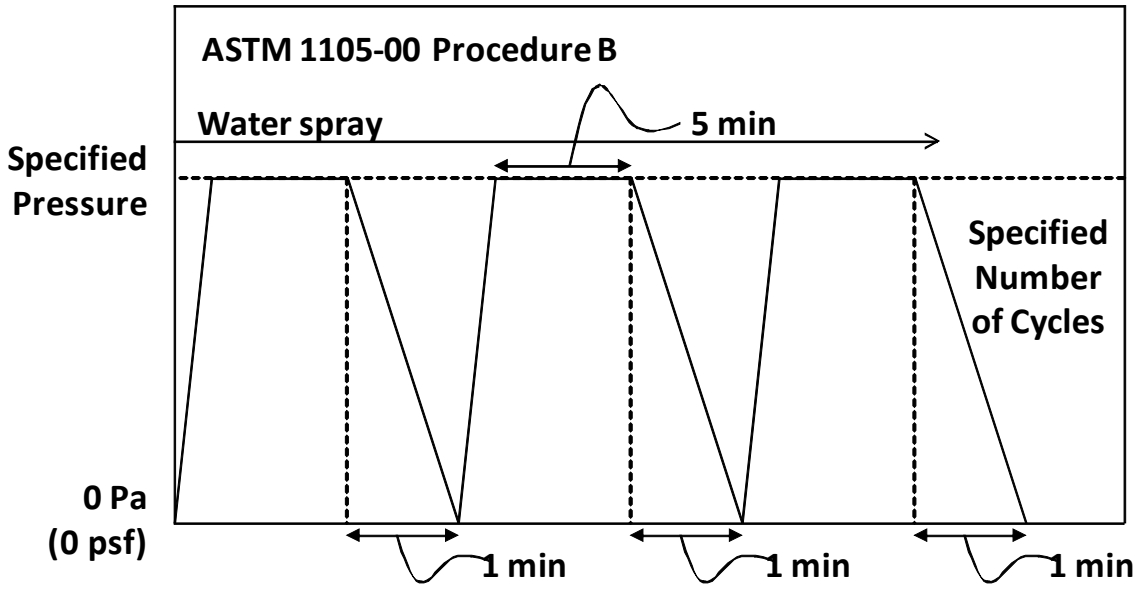

Figure 3-4. ASTM 1105-00 [43] Procedure B Pressure Loading History

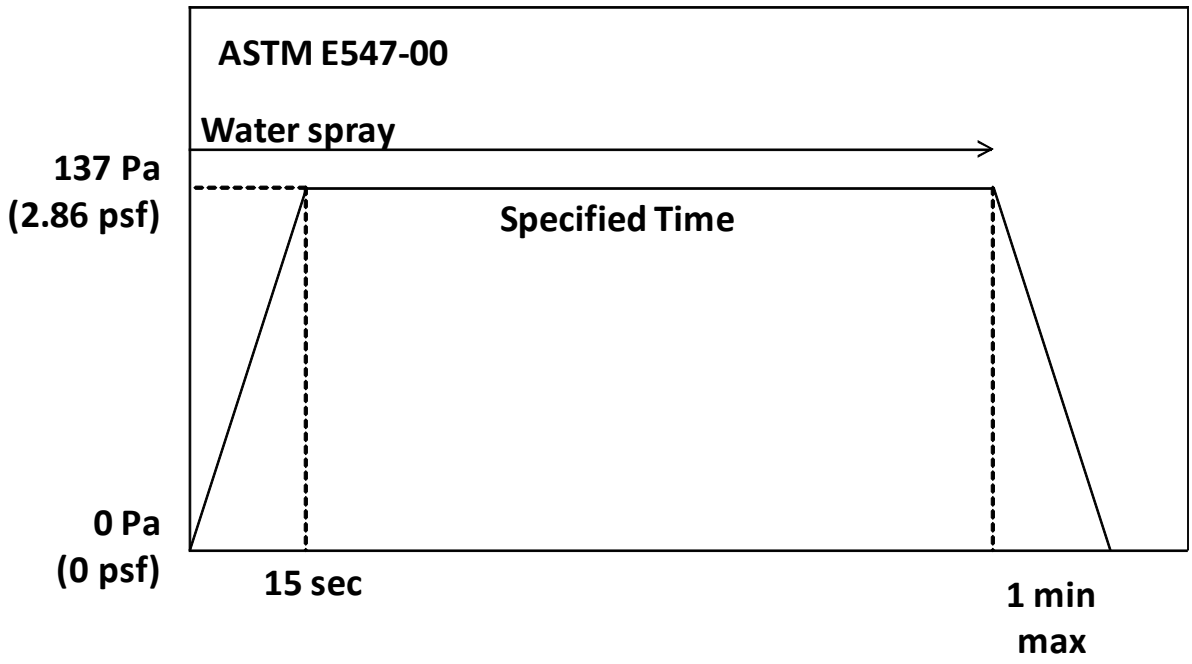

Figure 3-5. ASTM E547-00 [42] Pressure Loading History

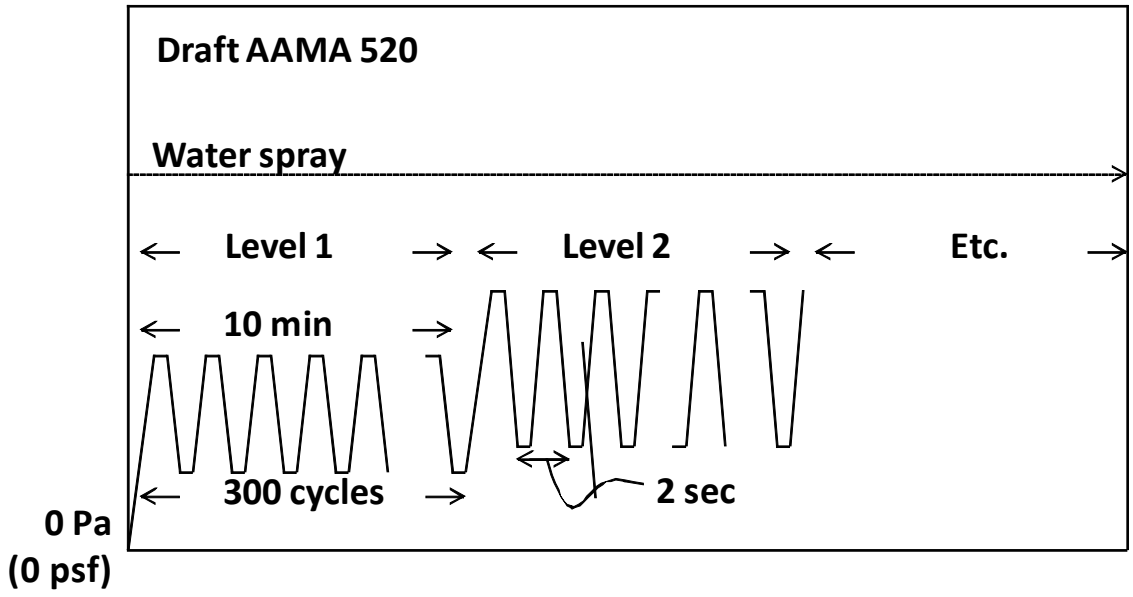

Figure 3-6. Draft AAMA 520 [40] Pressure Loading History

CHAPTER 4
EXPERIMENTAL PROCEDURE

Testing Apparatuses

This chapter presents information about the custom-built experimental apparatuses constructed to perform the static, cyclic and dynamic load tests. Two static air pressure chambers were constructed to simulate positive and negative (suction) loads, and both configurations allow for uniform and cyclic pressures. These apparatuses were constructed with the oversight of two product approval laboratories: Certified Testing Laboratories, Orlando, FL, and Architectural Testing Inc., York, Pennsylvania. Their input was sought to achieve one of the objectives of this research, which was to adapt the research grade testing for simplified product approval testing. Finally, dynamic testing was performed on a full scale residential house mockup, which was designed to accommodate removable wall sections. UF's Hurricane Simulator was then used to subject the specimens to a designed load history. Descriptions of each testing apparatus are as follows.

Negative (Suction) Air Pressure Chamber

UF constructed a negative air pressure chamber, which consists of a 26.4 mm (1 in) thick acrylic sheet mounted on a steel frame measuring 2.4 m x 2.4 m x 0.3 m (8.0 ft x 8.0 ft x 1.0 ft). It was designed to have a large unobstructed viewing area with minimal steel reinforcement while maintaining a maximum deflection of 1.6 mm (1/16 in) during the peak design pressures of 2873.0 Pa (60.0 psf) (see figure 4-1). HP-33 series Cadillac centrifugal blowers operating in parallel provide the required pressure and airflow (function of leakage). The blowers are capable of producing a pressure differential of about 2394.0 Pa (50.0 psf) at approximately 4.3-5.6 m^3/min (150.0 – 196.0 CFM), which exceeds 50% of the highest pressure rating of any specimens in this study. Pressure was modulated by two 106.0 mm (4.0 in) Bray Series 20

electro-pneumatic valves operated by a custom active control system under the control of National Instruments Labview 8.5 software (shown in figure 4-2). One valve controls the suction line from the chamber to the blowers, and the other valve vents the chamber to the atmosphere. These valves work in unison in order to perform the test cycles. Pressure feedback is provided by an Ashcroft XLdp transducer accurate to 6.2 Pa (0.1 psf). Two Baluff bod63m-lb02-f115 laser distance measurement devices monitor specimen deflection. One of the lasers measures total deflection of the glazing and the other measures the total deflection of the rough opening (R.O.). Subtracting the R.O. displacement from the glazing displacement yields the deflection of the window relative to the frame.

Simulated rain was transmitted from a spray rack composed of nozzles spaced on a uniform grid to wet the entire specimen evenly. The rack was spaced a fixed distance from the specimens and calibrated (with aid of a pressure gauge) to deliver 3.4L/m2*min (5.0 U.S.gal/ft2*hr) in accordance with ASTM E1105-05 [43]. Calibration of the rack was achieved by placing a 610.0 mm (24.0 in) catch box, divided into four even sections, at the at both upper corners and at the quarter point of the horizontal centerline of the spray system and 50.8 mm (2.0 in) from the specimen (see figure 4-3). When the calibration was completed the water pressure to the inlet of the spray rack was recorded to insure the calibration for every test. A sump pump in the catch basin of the rain chamber collected the water and recirculated through a filter back to a 757 L (200 gal) tank. A fluorescent yellow, ultra-violet tracer dye was added to the reservoir to improve the detection of leaks (see figure 4-1C).

Positive (Stagnation) Air Pressure Chamber

Several window manufacturers on the oversight committee raised the issue that water intrusion rates may be dependant of load direction (i.e., application of positive pressure to the exterior produces different ingress rates than suction being applied to the interior). Thus, a

positive pressure chamber capable of achieving 3830.0+ Pa (80.0+ psf) was constructed. To minimize flexing of the frame, 14 gauge galvanized sheet steel lined the inside of a frame consisting of 51.0 mm x 51.0 mm x 3.0 mm (2.0 in x 2 in x 1/8 in) HSS steel tubing spaced at a maximum of 711.0 mm (28.0 in). The spray rack used in the suction chamber was relocated to this chamber. A Spencer single stage centrifugal blower capable of a pressure of 3984.0 Pa (83.2 psf) and an airflow rate of 11.3 m^3/min (400 CFM) created the loads. The pressure was modulated through the same electromechanical valves used in the suction chamber.

The chamber in its entirety was then transported (with the aid of casters) to the specimen. The specimens were fixed to a stationary truss prior to attachment with the pressure chamber. In addition the mobility of the chamber allowed for the tightest seal around the specimen (See figure 4-4).

Hurricane Simulator

UF constructed a 2.09 MW (2800 hp) hurricane simulator capable of replicating turbulent wind and rain loads on a full-size, low-rise structure [49]. It is powered by four 522 kW (700 hp) Detroit Diesel marine engines, which were rebuilt and maintained by UF staff and students. Each engine is attached to two tandem Linde 135 cc hydraulic pumps that spin at 2300 rpm. Pressure is then delivered through 165.47 Pa (24,000 PSI) burst pressure hoses to hydraulic motors producing approximately 201.3 kW (270 bhp). The direct drive hydraulic motors (see figure 4-5) in turn spin a 4x2 array of vaneaxial fans arranged in a 25.6 m (84.0 ft) circular radius (3.5° angle between fans see figure 4-6). Each Aerovent manufactured fan measures 1.37m (54 in), and equipped with nine adjustable pitch blades delivers 1,700 m^3/min (160,000 CFM). The fans collect air through specially designed venture inlets that force the air to travel perpendicular to the fan disc for maximum efficiency. The flow is then accelerated through a contraction section reducing the cross-sectional area from 6.1 m x 3.1 m (20.0 ft x 10.0 ft), at the fans, to the

test segment of 2.9 m x 2.9 m (9.5 ft x 9.5 ft). Six, custom designed, steel reinforced, neutral shape NACA airfoils are mounted at the trailing edge of the contraction and introduce lateral turbulence as well as rain. The airfoils are computer controlled with the use of a 100Hz, 138.3 N-m (1000.0 ft-lb) hydraulic rotary actuator and a custom active control system built with National Instruments Labview 8.5 software. Water is conveyed through an internal network of pipes and injected into the wind field along the trailing edge through spray nozzles (see figure 4-7). The pressure regulated nozzles can be calibrated to produce 203.2-1117.6 mm/hr (8.0-44.0 in/hr) and are arranged in a grid to provide even wetting. The entire fan array rests on a trailer, making it the largest mobile hurricane simulator in the world. It is hauled by a tanker truck that also doubles as a 1,8930.0 L (5000.0 gal) radiator. The result of all the components is an actively controlled hurricane simulation capable of wind-driven rain and 1675.8 Pa (35.0+ psf) stagnation pressures (approximately 58.17 m/s, 130mph wind velocities, see figure 4-8).

Full Scale House Mockup

To test each of the specimens with the Hurricane Simulator, a 4.6 m x 9.8 m x 4.9 m (15.0 ft x 32.0 ft x 16.0 ft) model residential structure was constructed. The house mockup was designed in accordance to the Wood Frame Construction Manual (WFCM-2001) to withstand wind loads prescribed in ASCE 7 for 67+m/s (150+mph), ensuring its durability. The roof system was to be a standing seam metal roof system, to avoid repair after every test, and the roof trusses were designed and manufactured by a truss company to withstand the same loads. To place the specimens in the correct location of the impinging air flow, the mockup had to be elevated 1.7 m (5.5 ft) on a steel structure built up of 50.8 mm x 50.8 mm x 3.18 mm (2.0 in x 2.0 in x 1/8 in) square tubing. Raising the specimens into place was accomplished by employing a 27.0 KN (6,000lb) rated hydraulic lift installed under the mockup (figure 4-9). Once raised the specimens were connected to the roof assembly with a removable pin connection (figure 4-10).

Finally, the model was also placed on casters which roll along a track to permit centering of the specimens in the flow field, as well as to clear the area for other testing.

Air Caster Cart

Transportation of the specimens was also of concern because 25 of the specimens received an application of stucco or decorative cementitious coating. Cracking of the specimens during transportation would negate the validity of test results. Consequently a custom designed air caster cart was fabricated to transport specimens from testing station to testing station as well as into the storage facility. The air caster cart is a steel frame that can be assembled and disassembled around specimens (see figure 4-11). It rests on four air casters rated for 17.8 KN (4,000 lbs) each, the heaviest of the specimens being approximately 17.8 kN (4,000 lbs). Once loaded, the air casters are pressurized and the specimens are floated on a cushion of air 3.2 mm (1/8 in) thick. In case of accidental depressurization, the cart along with the specimen would slowly drop as the casters deflate. These measures insured the utmost care.

Testing Protocols and Sequencing

Specimens were subjected to four rounds of pressure loading and water testing. Static, cyclic as well as amplitude- and frequency-modulated sinusoidal pressure load sequences were applied, followed by a repeat of the static test to ensure that the specimens were not permanently damaged during testing (e.g. cracks forming in the joinery). Such failures would have compromised the investigation team's ability to compare results between the test methods. Therefore as a preventative measure, all of the following tests were limited to 50% of the windows' design pressure. The following static and cyclic pressure tests were composed of their existing counterpart to view their effectiveness as compared to dynamic pressure tests, as well as an amended version to investigate if newer modified test methods can more closely replicate those obtained from dynamic pressure testing.

Static Air Pressure Difference

The static pressure test method borrows from Procedure A of ASTM E1105-05 [43] and ASTM E331-00 [41]. ASTM E1105-05 [43] specifies three consecutive 300 s cycles while ASTM E331-00 [41] specifies a default of 137.0 Pa (2.86 psf) for uniform static pressure loading. Combination of both yielded the initial five minute cycle. A linear increase to 50% of the window's design pressure for the subsequent 15 minutes concluded the test (as shown in figure 4-12).

The rationale for linearly increasing the pressure over an extended time to 50% of the design pressure is to incorporate the ability to isolate the pressure at which individual infiltrations are first initiated. This pressure, along with the location where the infiltration occurred, can be used in comparison with the same data from any other experiment to view the efficacy of the test (i.e. observe when similar paths are observed and compare the recorded pressures). This data also provides a level of performance for each specimen by later comparing it to data recorded from other specimens and observing the differences in pressure for the initial water intrusions.

Specimen definition also changed from the original test methods. In ASTM E1105-05 [43] and ASTM E331-00 [41], the specimen consists of a fenestration product only. In the test methods employed, the specimen consists of the fenestration product integrated into a finished wall assembly.

By testing fenestration in isolation, products are not subjected to loads that they would be otherwise. In the field fenestration products are subjected to different loads, by means of building movement and temperature changes. These loads contribute to the overall water penetration resistance and merit acknowledgement.

Results from this test were considered the datum for damage incurred to the specimen since it was the first test performed. After cyclic and dynamic pressure tests, this test was reemployed to compare results and detect if damage to the specimen had occurred. That is to say, if an infiltration that occurred in the primary static test occurred earlier in the second, or a new infiltration occurred in the second that was unobserved in the first, damage had transpired.

Cyclic Static Air Pressure Difference

The cyclic pressure test was based on a modified version of ASTM E2268-04 [44] and the draft AAMA 520 [40] specification. The specimen was preloaded to 50% of the design pressure for one minute, followed by no load for one minute as is the case in ASTM E2268-04 [44]. Cyclic loading immediately followed. The series of cycles included those in AAMA 520 [40], although they are preceded by four custom series (see table 4-1). During testing the last series of cycles took place when the upper limit of the cycle approached 50% of the design pressure (see figure 4-13 for illustration).

This test method more realistically simulates the dynamic nature of extreme wind and rain events by recreating sinusoidal patterns based on the energy cascade. In this test method, performance can be quantified by the level at which the specimen exhibited water infiltration. However, pressure can only be defined over a range, in contrast to the static pressure test method. Therefore, specimen performance can only be compared through fourteen different levels. This still is a great improvement from current methods which are minimum performance standards and only test to 205.5 Pa (4.3 psf) or in some cases 720.0 Pa (15.0 psf) (see figure 3-3) which may not be sufficient.

Dynamic Pressure

The UF Hurricane Simulator was used to perform the dynamic testing of the specimens. The loads were designed using 10 minute wind speed observations collected by the Florida

Coastal Monitoring Program that were converted to velocity pressures. It was conservatively assumed that there was perfect aerodynamic admittance between the free stream velocity pressure and the stagnation pressure on the windward wall. Records with a mean velocity > 20 m/s (44.74 mph) were extracted and detrended. The longitudinal velocity component was calculated and passed through nine bandpass filters in 0.1 Hz passband increments. The peak amplitude for each passband was recorded and divided by the record's 10 minute mean velocity to get a peak amplitude / mean ratio. Data was stratified into three turbulence intensity regimes, of which the middle turbulence range (0.15 – 0.20) was used. The 50th percentile peak values were employed to construct a sinusoidal loading pattern at three different velocity thresholds that correspond to 239.0, 479.0, and 718.0 Pa (5.0, 10.0 and 15.0 psf). Figure 4-14 illustrates the sequence.

Water Infiltration Rates

Four wall specimens were subjected to a staircase negative and positive pressure load time histories while a spray rack applied 3.4L/m^{2}min (5.0 gal/ft^{2}hr) wetting to the exterior face (in accordance with ASTM E1105-05 [43]). Water that penetrated the window assembly was collected over a specified duration and weighed to quantify the rate of ingress.

It was hypothesized the rate of water ingress might behave differently given the progression of loading, particularly in the lowest pressure regime. Thus the load sequence (shown in figure 4-15) was applied forward (incrementing load steps) and backward (decrementing load steps). Specimens were allowed to dry between the series. The lower and upper bounds of the pressures were confined to the lowest pressure at which the specimen exhibited water ingress and 50% of the window's design pressure in all cases. Step size was determined by dividing the range from the lower to upper bound into equal increments. However if the specimen exhibited any peculiar behavior the step size was decreased further.

Once the data acquisition system registered the desired pressure level, research personnel monitored the instantaneous flow rate to determine when the infiltration flow had stabilized. This process normally took several minutes. Figure 4-16 shows the flow for each of the target pressures on the descending load curve of specimen 017C. As is shown in figure 4-17 each of the flows is nearly constant throughout the last 25% of the collection time, assuring an accurate measurement of flow. During the test adequate time was allotted between pressure steps to allow the water to drain from the collection system and specimens before continuing to the subsequent pressure.

A collection chamber was designed to collect water that penetrated through the operable portion of each window assembly. This is not to say that water could not migrate from the cavity between the window and the rough opening; however, water penetration through the window-wall interface was excluded because of the difficulty of collecting such minute volumes, what is in some cases, droplets of water or minimal continuous infiltrations through cracks. The collection chamber was also designed to allow the water to continuously transfer (outside of the pressure chamber when performing negative pressures) at the same rate at which it infiltrated the interior side of the specimen. This allowed continuous recording and monitoring (at 10Hz) by means of an Omega WSB-8150 weight scale connected to the same custom active control system (built with National Instruments Labview 8.5 software) that modulated the suction pressure. After the conclusion of the test, pressure and weight data were post processed using a routine that removes the outliers (noise) in the data. The first 75% of the data collected is also discarded to remove any variation in flow do to the initialization of mass collection. Figure 4-18 illustrates the flow rate using the filtered weight data.

Summary

The research team at the University of Florida designed and constructed testing apparatuses to apply modified versions of current test methods. Results from the modified test methods were then analyzed to view particular strengths and limitations and to assess their effectiveness at replicating the dynamic nature of wind and wind-driven rain. The results of this analysis are discussed in chapter 6.

Table 4-1. Pressure Series for Cyclic Pressure Test Method

Performance Level	Lower Limit		Median		Upper Limit	
	Pa	psf	Pa	psf	Pa	psf
1*	67.0	1.4	136.5	2.85	205.9	4.3
2*	95.8	2.0	191.5	4.0	287.3	6.0
3*	143.6	3.0	287.3	6.0	430.9	9.0
4*	191.5	4.0	383.0	8.0	574.6	12.0
1	239.4	5.0	478.8	10.0	718.2	15.0
2	284.3	6.0	574.6	12.0	852.8	18.0
3	335.2	7.0	670.3	14.0	1005.5	21.0
4	383.0	8.0	766.1	16.0	1149.1	24.0
5	340.9	9.0	861.9	18.0	1022.8	27.0
6	378.8	10.0	957.6	20.0	1136.4	30.0
7	526.7	11.0	1053.4	22.0	1580.0	33.0
8	574.6	12.0	1149.1	24.0	1723.7	36.0
9	622.4	13.0	1244.9	26.0	1867.3	39.0
10	670.3	14.0	1340.7	28.0	2011.0	42.0

A 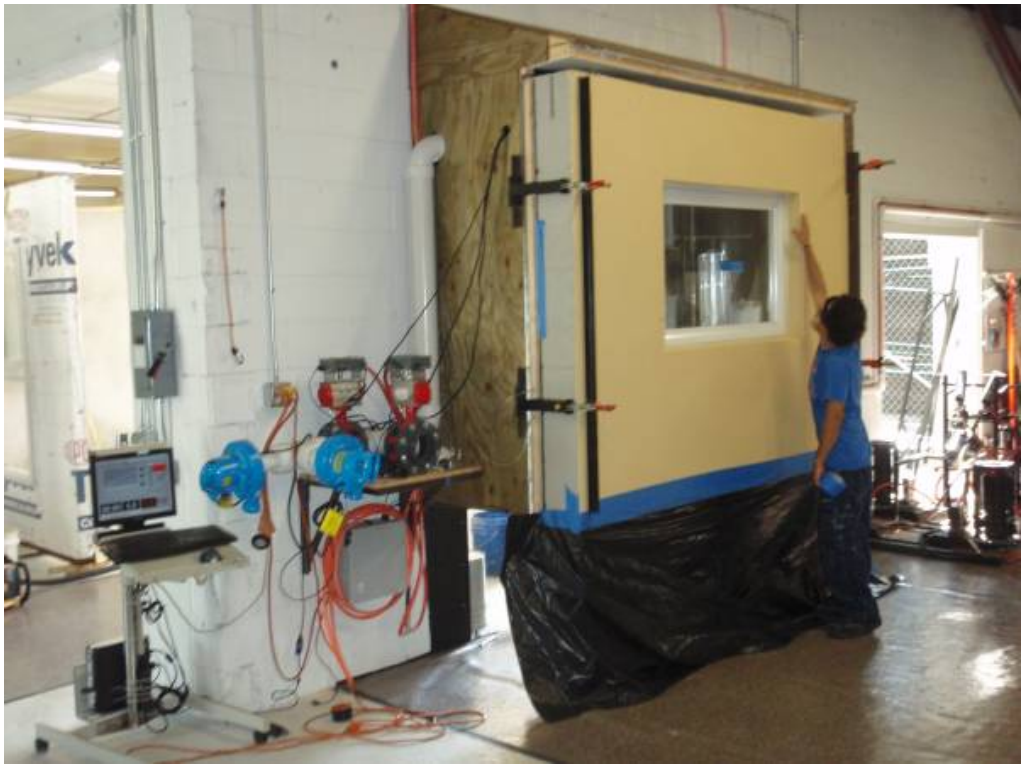

B 

C 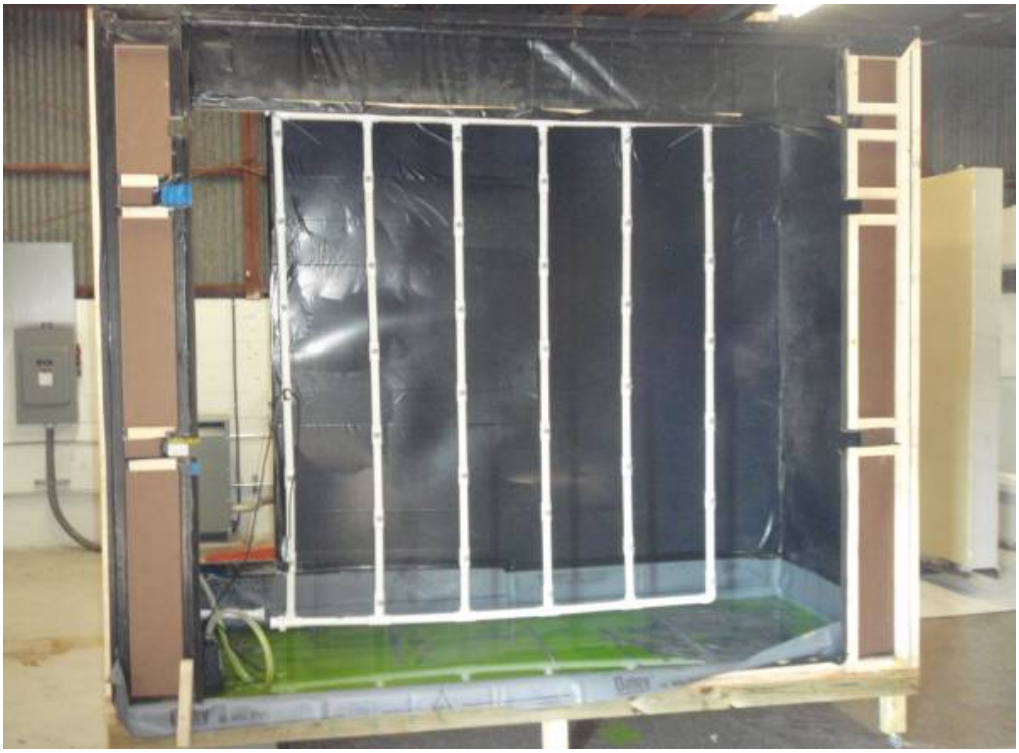

D 

Figure 4-1. Negative Pressure Chamber: A) Wall attached to the pressure chamber. Suction is applied to the interior. B) Interior view of the wall specimen looking through 25.4 mm (1.0 in) acrylic. C) Rain Chamber containing the spray rack. D) Spray Rack is mounted to the wall exterior and sealed to collect water.

Figure 4-2. Electro-Pneumatic Valves

Figure 4-3. Calibration Catch Box

A 

B 

C 

D 

Figure 4-4. Posivie Pressure Chamber: A.) Wall on permanent stands attached to the fixed truss. B.) Rain Chamber containing the spray rack calibrated to produce prescribed (8.0 – 17.6 in/hr) wetting. C.) Side view of mounted wall D.) Attached chamber.

Figure 4-5. Direct Drive Hydraulic Motor

Figure 4-6. Van-Axial Fan

Figure 4-7. Nozzle

A 

B

C

Figure 4-8. Hurricane Simulator: A) Tuned inlets that connect to industrial vaneaxial fans. B) Side view of simulator. The inlets and contraction can be removed for travel. C) Hurricane Simulator, residential model and specimen being prewetted.

Figure 4-9. Hydraulic Lift

Figure 4-10. Roof to Wall Connection

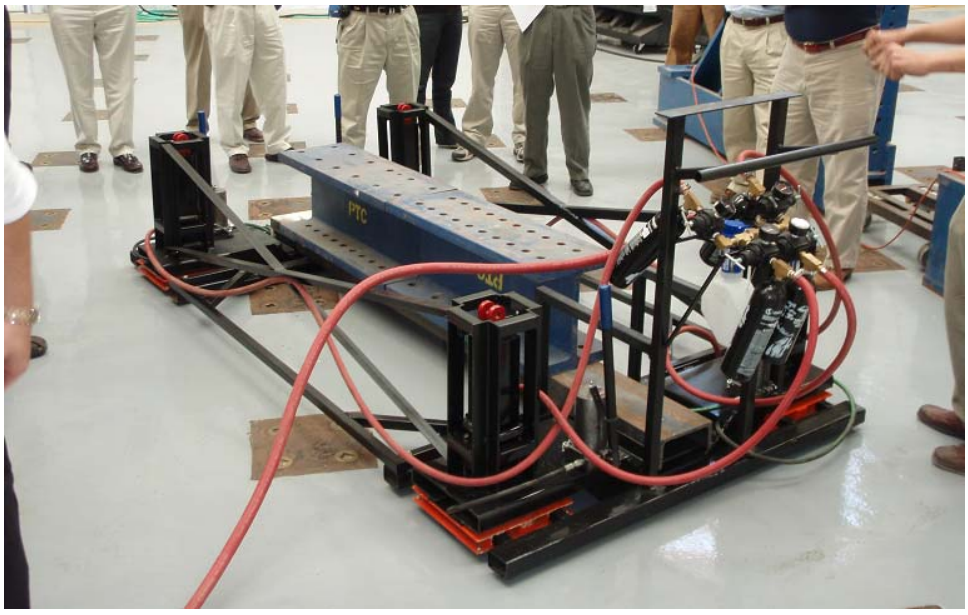

Figure 4-11. Air Caster Cart

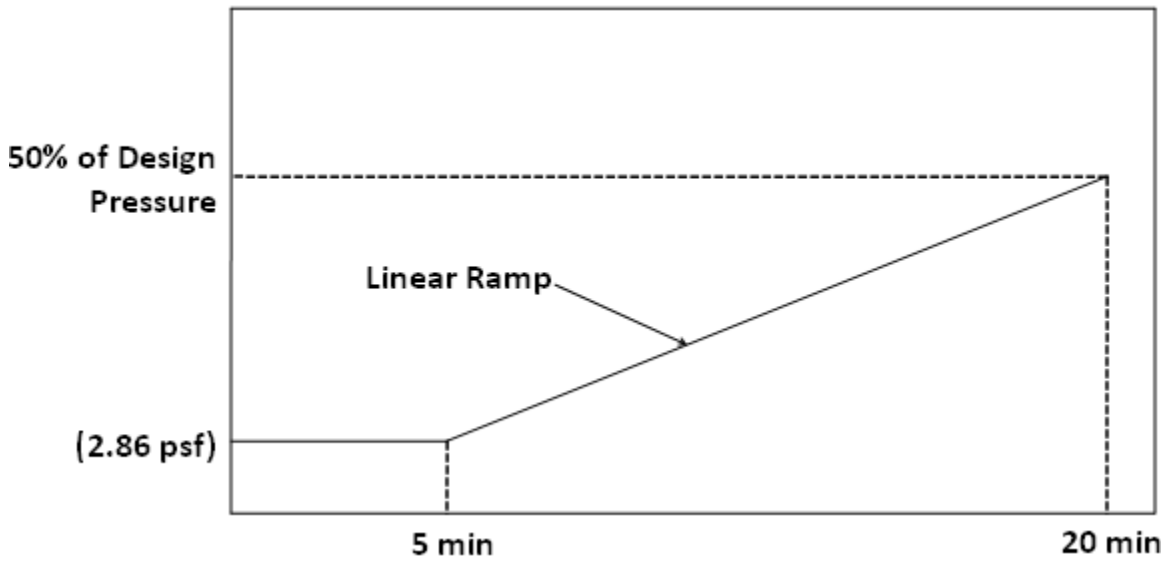

Figure 4-12. Static Pressure Load Sequence

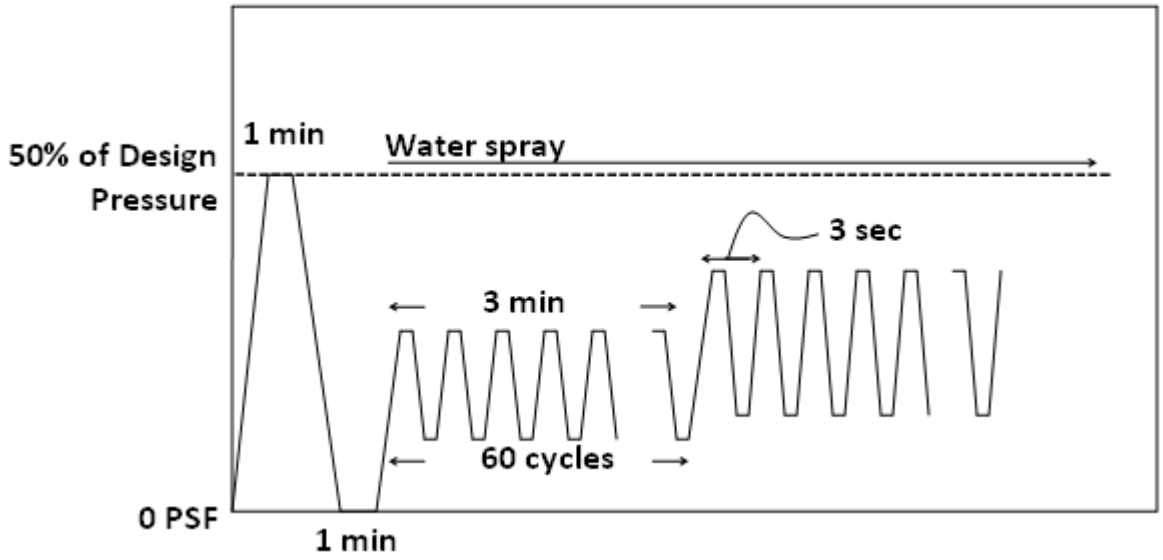

Figure 4-13. Cyclic Pressure Load Sequence

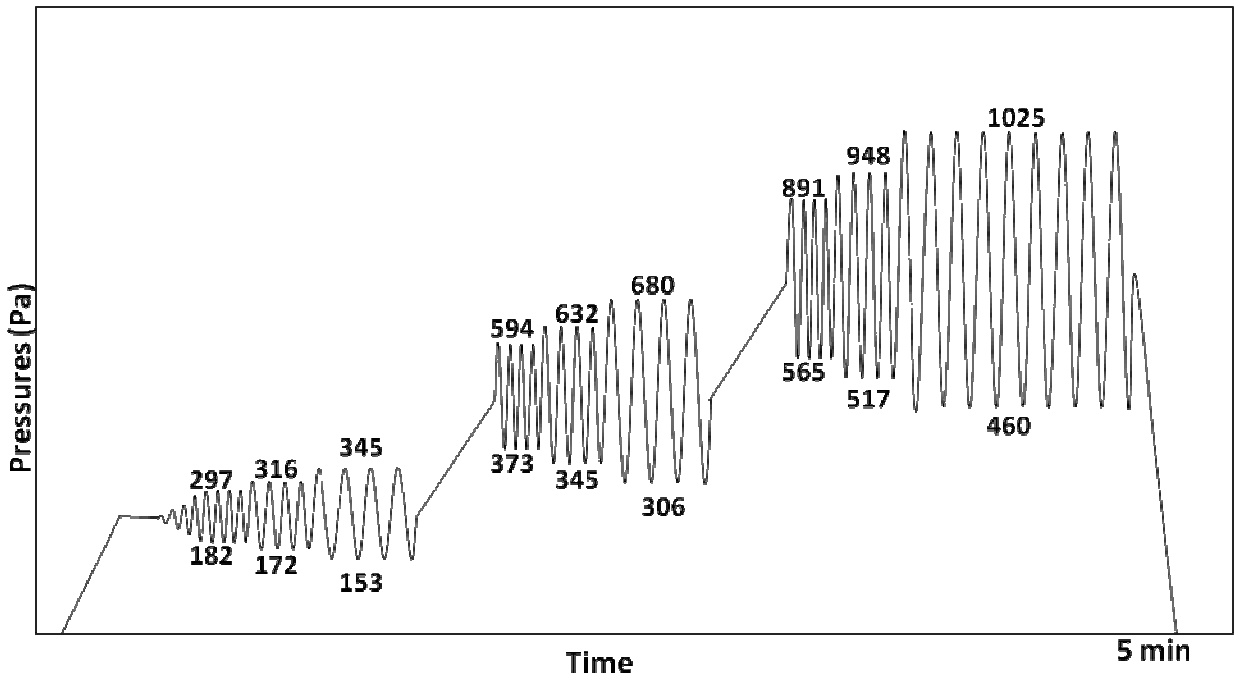

Figure 4-14. Pressure Time History for Dynamic Test

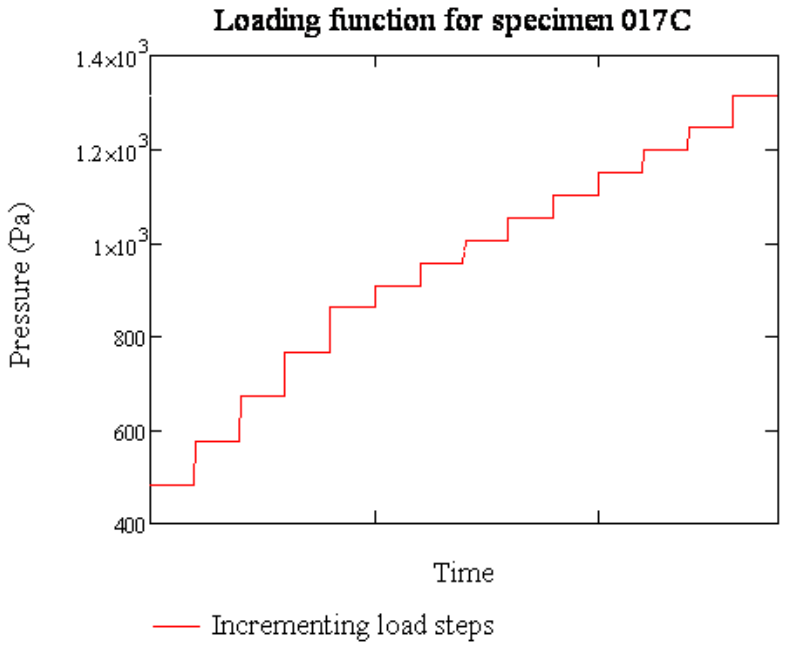

A

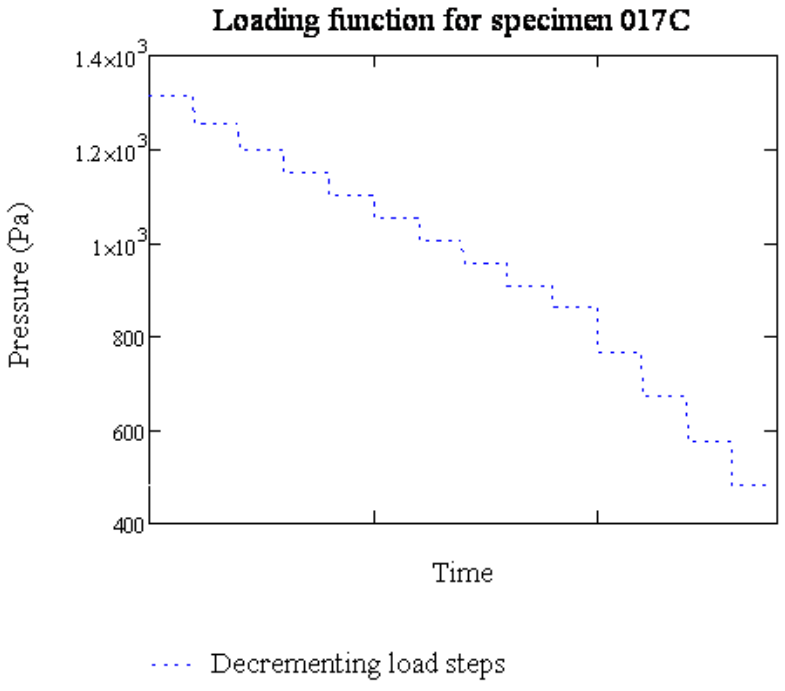

B

Figure 4-15. Loading Functions for Specimen 017C

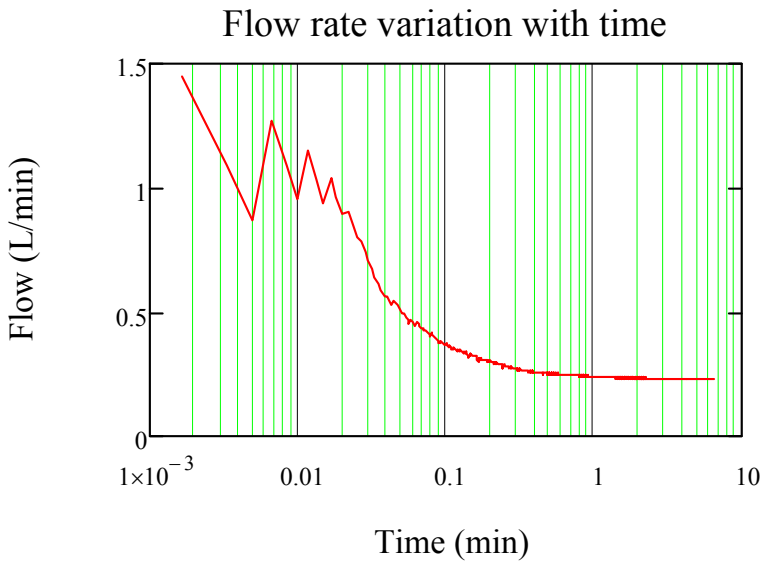

Figure 4-16. Flow Data for Increasing Load Curve (1149.0 Pa/ 24.0 psf step of specimen 017C)

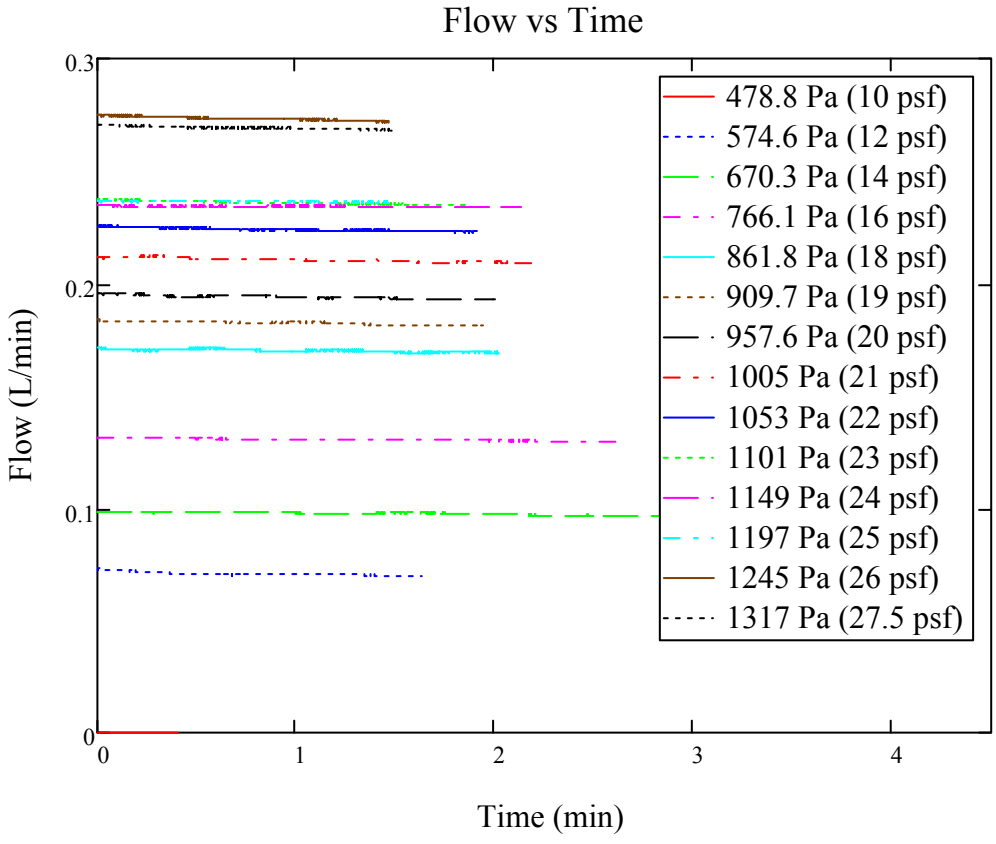

Figure 4-17. Last 25% of Data for All Pressure Steps (decreasing pressure curve of specimen 017C)

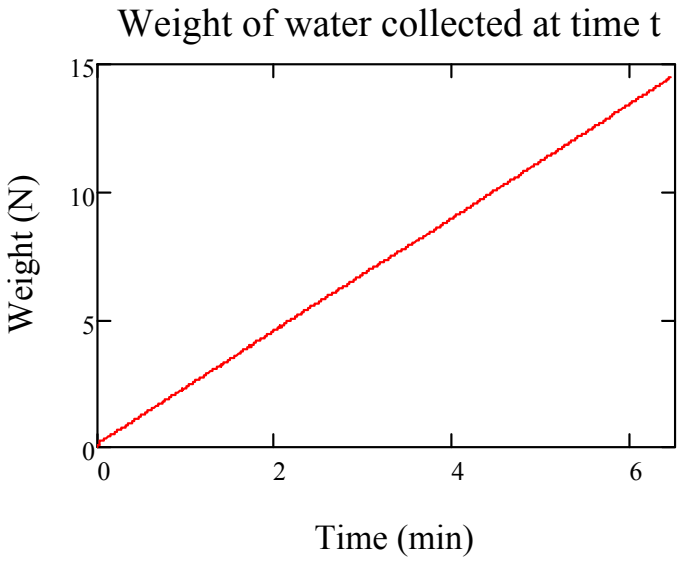

Figure 4-18. Filtered Weight Data (1149.0 Pa/ 24.0 psf Step of Specimen 017C)

CHAPTER 5
SPECIMEN DESIGN AND CONSTRUCTION

The 16 wall specimens in table 5-1 were specifically constructed for this research, and are discussed in this chapter. Eighteen additional wall specimens were constructed for a companion project, which is detailed in [53]. The specimen matrix from that project is reprinted in table 5-2. Each specimen has a unique combination of window operator type (see figures 5-5 through 5-8), window dimensions, window material, window interface (i.e. different installation methods), wall construction (wood frame and concrete masonry) and finish (decorative cementitious coating, stucco, or fiber cement board). Among different variants chosen for the specimens, considerations were also made to safely transport and store the specimens. Specimens were designed to be tested post-cure, therefore they were stored in a warehouse where moisture and sunlight were kept to a minimum in order to avoid unintended aging.

Under advisement from the task force it was decided that wall construction should be limited to those typical in residential construction. Hence, wood framed walls were designed to 209 kmph (130mph) wind loading and concrete masonry walls were designed to 225 kmph (140mph) wind loading.

Wood Frame Wall Specimens

Wood frame wall specimens were constructed offsite by a residential contractor using design specifications provided by the American Forest & Paper Association (AF&PA) for minimum code conforming wood frame walls. This was done with the intention of allowing the walls to flex as much as permitted while still meeting deflection requirements set forth for stucco finishes.

Once framed, these specimens were sheathed with 11.1 mm (7/16 in) oriented strand board and the exterior was wrapped in commercial wrap. They were then finished in either fiber

cement board or a three coat (scratch, brown, and finish coats) stucco application, 13.0 mm (1/2 in) thick, over lath.

To simulate a wall to slab connection and to keep the walls from deflecting unintentionally, each wall had a steel channel bolted to the bottom plate (see figure 5-1). Each specimen was braced to the apparatus of every test, as well as the air caster cart, through the channels. This precaution allowed handling and transportation of the specimen without damaging the finish or any other component. Specimens were also kept elevated from the ground approximately 101.6 mm (4.0 in) to access them for transport.

Masonry Wall Specimens

CMU wall specimens were built onsite, upon a rigid steel channel, by a licensed masonry contractor. The CMU channel had #5 rebar welded at one fourth and three fourths of its length to reinforce the masonry (see figure 5-3). Two 15.9 mm x 254.0 mm (5/8 in x 10.0 in) bolts were also welded to the channel in order to resist any moment that was developed between the masonry and the channel. Both the rebar and bolts are intended to help transfer load to the channel, which in turn will transfer the load safely out of the specimen. Each CMU wall was also equipped with grouted cells at the ends and at either side of the window rough opening (see figure 5-4). Rough opening tolerance was in compliance with ACI 530.

Upon completion by the mason, the walls were finished with either a decorative cementitious coating (varied from a paint thickness to 6.4 mm, 1/4 in), or a three coat (scratch, brown, and finish coats) stucco application (13.0 mm, 1/2 in) over lath. The stucco application of these specimens was selected with the assistance of Construction Code Specialists (CCS) and the National Concrete Masonry Association (NCMA).

Testing Matrix

In residential construction it is common that a single home may contain a number of different window sizes and operator types. With a wide range of window options available, the selection of a window is often based on the architectural appearance as well as the functionality it may serve in the desired application. These functions include egress requirements where designers deem necessary, in case of an emergency, as well as giving occupants control of the interior environment by natural ventilation. It would be unreasonable to test all possible permutations of window size and type; therefore, under guidance of leading manufacturers, careful consideration was made to limit the window variants to those most representative of coastal construction practice in the south-eastern U.S. For operator types, single hung, horizontal sliding, out-swing casement, and awning windows were selected for evaluation. Each of which were limited to one representative window size based on minimum gateway sizes from residential performance classes provided in AAMA/WDMA/CSA 101/I.S.2/A440 [38]. Within similar operator types and dimensions there are also varying drainage types from window to window (e.g., windows with built-in weep holes). Window material (aluminum and vinyl) was also varied to observe their respective water infiltration resistance. In addition, all of the windows were installed to manufacturer's guidelines. Two installation methods for windows were also employed (performances of which were analyzed in [53]).

Summary

Sixteen specimens were evaluated to observe their respective water infiltration resistance. Each specimen was unique its combination of window; operator type, material, size, installation, and wall; material, and finish. These individual permutations were subjected to the aforementioned test methods and results were then analyzed.

Table 5-1. Test Specimen Matrix

Specimen	Wall Construction	Finish	Operator	Window Dimension	Material	DP
001	Wood	Stucco	Fixed	110.49 cm X 158.75 cm 43.5” X 62.5”)	Aluminum	40
006	Wood	FCB	Casement	90.17 cm X 151.13 cm (35.5” X 59.5”)	Aluminum	40
011	CMU	DCC	Hor. Sliding	158.75 cm X 110.49 cm (62.5” X 43.5”)	Aluminum	45
020B	CMU	Stucco	Fixed	110.49 cm X 158.75 cm (43.5” X 62.5”)	Aluminum	40
022	Wood	FCB	Single Hung	110.49 cm X 158.75 cm (43.5” X 62.5”)	Vinyl	40
025	Wood	Stucco	Casement	90.17 cm X 151.13 cm (35.5” X 59.5”)	Vinyl	40
032	CMU	Stucco	Hor. Sliding	158.75 cm X 110.49 cm (62.5” X 43.5”)	Vinyl	40
019D	CMU	DCC	Fixed	110.49 cm X 158.75 cm (43.5” X 62.5”)	Aluminum	40
043	CMU	DCC	Single Hung	110.49 cm X 158.75 cm (43.5” X 62.5”)	Aluminum	60
048	CMU	Stucco	Casement	90.17 cm X 151.13 cm (35.5” X 59.5”)	Aluminum	60
049	Wood	Stucco	Hor. Sliding	158.75 cm X 110.49 cm (62.5” X 43.5”)	Aluminum	60
054	Wood	FCB	Awning	120.65 cm X 74.93 cm (47.5” X 29.5”)	Aluminum	60
064	CMU	Stucco	Single Hung	110.49 cm X 158.75 cm 43.5” X 62.5”)	Vinyl	50
067	CMU	DCC	Casement	90.17 cm X 151.13 cm (35.5” X 59.5”)	Vinyl	55
070	Wood	FCB	Hor. Sliding	158.75 cm X 110.49 cm (62.5” X 43.5”)	Vinyl	60
073	Wood	Stucco	Awning	120.65 cm X 74.93 cm (47.5” X 29.5”)	Vinyl	60

Table 5-2. Test Specimen Matrix

Specimen	Wall Construction	Finish	Operator	Window Dimension	Material	DP
017	Wood	Stucco	Fixed	110.5 cm X 158.8 cm (43.5” X 62.5”)	Aluminum	40
017B	Wood	Stucco	Fixed	110.5 cm X 158.8 cm (43.5” X 62.5”)	Aluminum	40
017C	Wood	Stucco	Single Hung	110.5 cm X 158.8 cm (43.5” X 62.5”)	Aluminum	55
017D	Wood	Stucco	Fixed	110.5 cm X 158.8 cm (43.5” X 62.5”)	Aluminum	40
017E	Wood	Stucco	Fixed	110.5 cm X 158.8 cm (43.5” X 62.5”)	Aluminum	40
018	Wood	FCB	Fixed	110.5 cm X 158.8 cm (43.5” X 62.5”)	Aluminum	40
018B	Wood	FCB	Fixed	110.5 cm X 158.8 cm (43.5” X 62.5”)	Aluminum	40
018C	Wood	FCB	Fixed	110.5 cm X 158.8 cm (43.5” X 62.5”)	Aluminum	40
018D	Wood	FCB	Fixed	110.5 cm X 158.8 cm (43.5” X 62.5”)	Aluminum	40
018E	Wood	FCB	Fixed	110.5 cm X 158.8 cm (43.5” X 62.5”)	Aluminum	40
019	CMU	DCC	Fixed	110.5 cm X 158.8 cm (43.5” X 62.5”)	Aluminum	40
019B	CMU	DCC	Fixed	110.5 cm X 158.8 cm (43.5” X 62.5”)	Aluminum	40
019C	CMU	DCC	Fixed	110.5 cm X 158.8 cm (43.5” X 62.5”)	Aluminum	40
035	CMU	DCC	Fixed	120.7 cm X 74.9 cm (47.5” X 29.5”)	Vinyl	52.7
020	CMU	Stucco	Fixed	110.5 cm X 158.8 cm (43.5” X 62.5”)	Aluminum	40
016	CMU	Stucco	Fixed	120.7 cm X 74.9 cm (47.5” X 29.5”)	Aluminum	52.7
020C	CMU	Stucco	Fixed	110.5 cm X 158.8 cm (43.5” X 62.5”)	Aluminum	40
020D	CMU	Stucco	Fixed	110.5 cm X 158.8 cm (43.5” X 62.5”)	Aluminum	40

A 

Figure 5-1. Bolted Channels to Wood Frame Walls

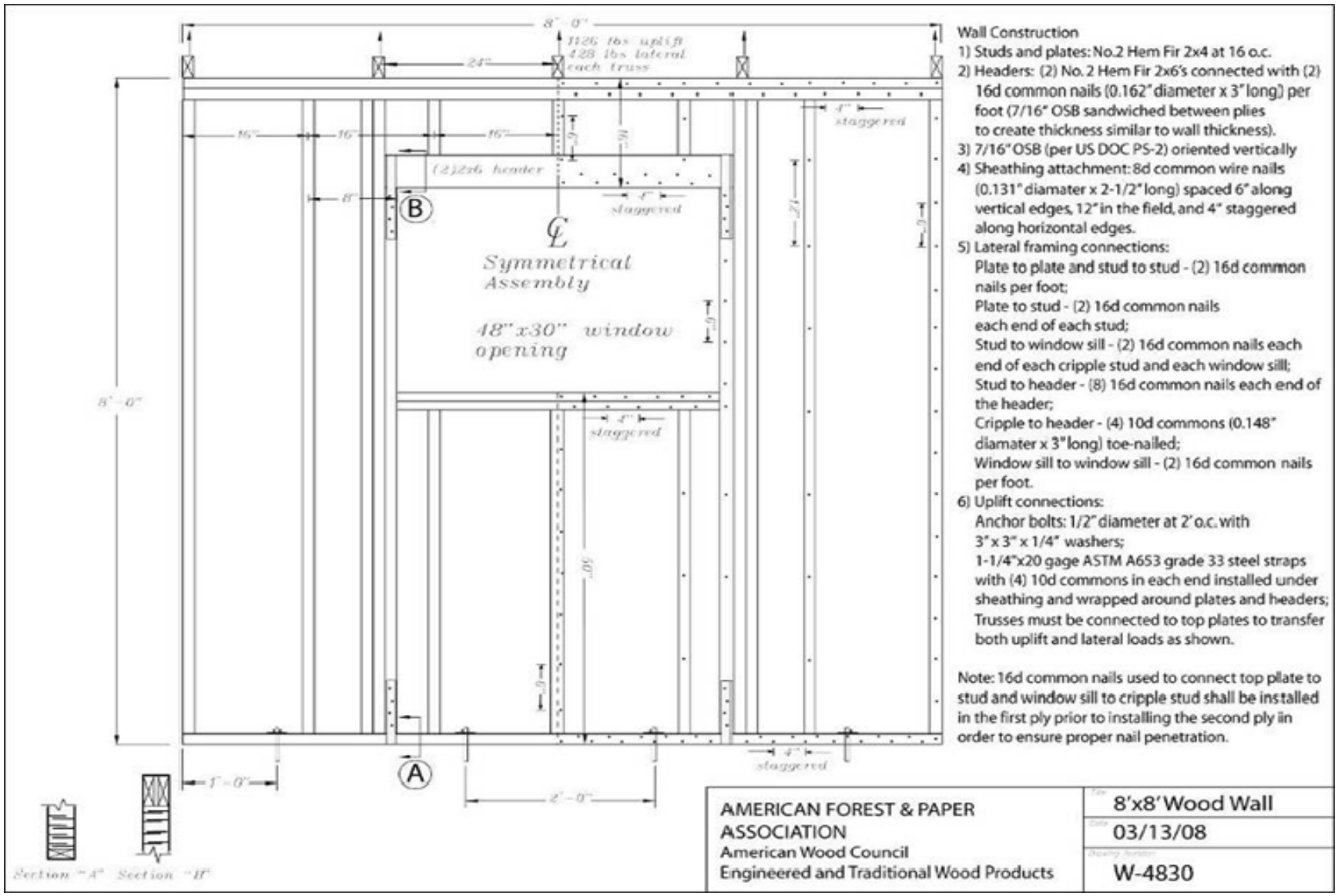

Figure 5-2. Designs for Wood Frame Walls.

A

B

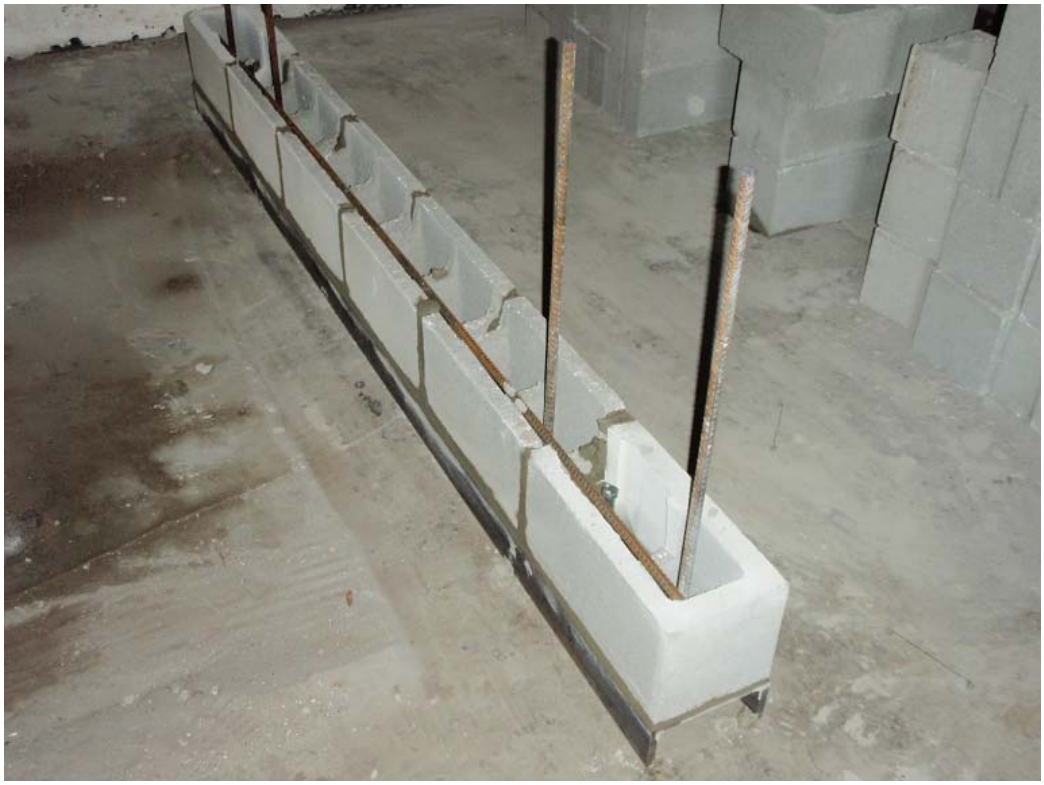

Figure 5-3. CMU Wall Specimen Stabilization Channel

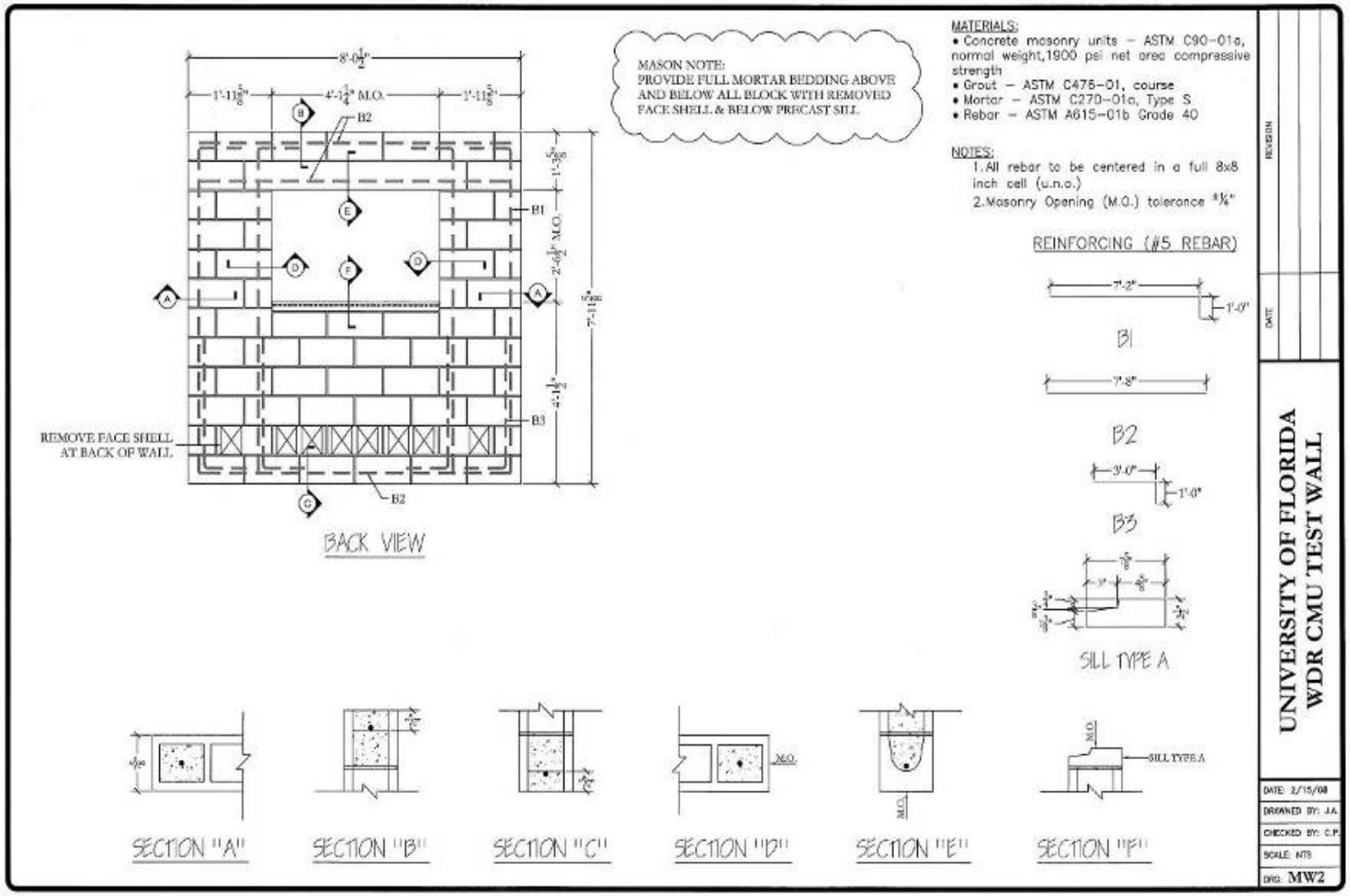

Figure 5-4. Designs for CMU Wall

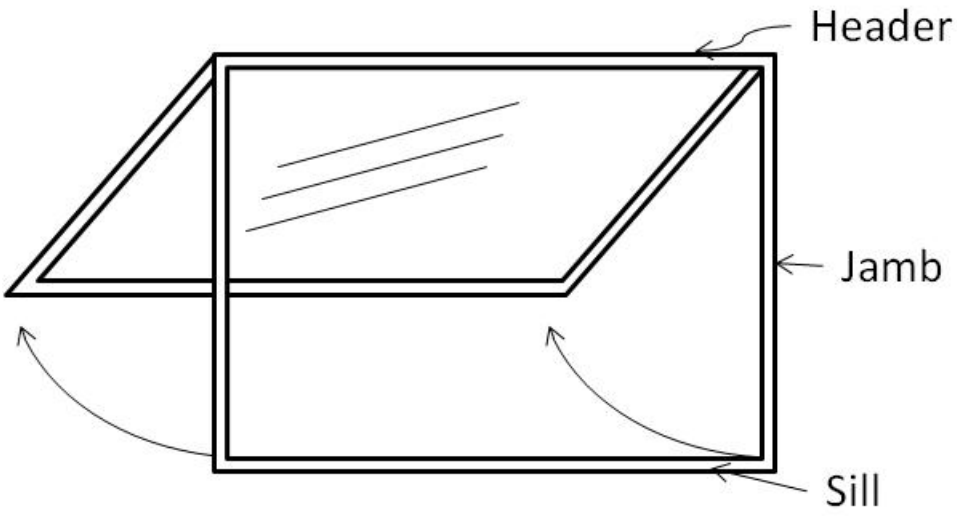

Figure 5-5. Awning Window

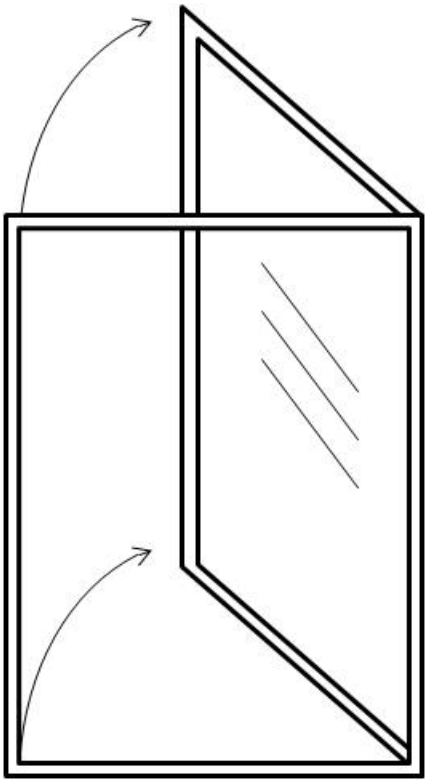

Figure 5-6. Casement Window

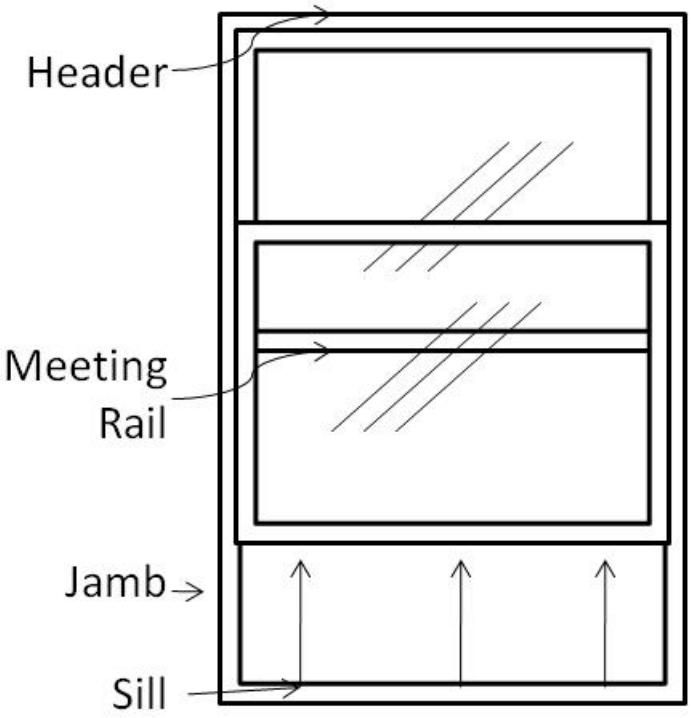

Figure 5-7. Single Hung Window

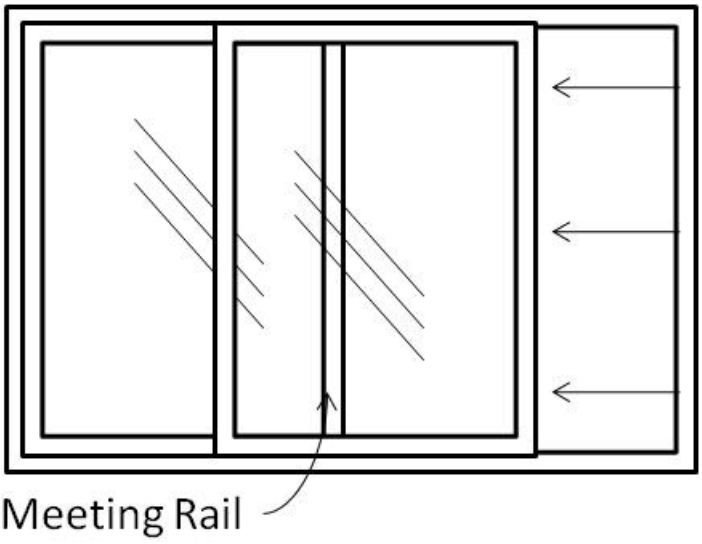

Figure 5-8. Horizontal Sliding Window

CHAPTER 6
RESULTS

The specimens were subjected to four independent rounds of testing to investigate the effects of differing loading conditions. The specimens were monitored for instances of water intrusion, which is defined as "any liquid water observed from the interior side of the wall assembly to have bypassed the moisture barrier of the window/wall system." This chapter discusses the repeatability of test results, its relationship to damage accumulation, and compares the diagnostic abilities of the various tests to detect leakage. The water penetration resistance of each operator type is evaluated, with particular focus on the performance of compression and sliding seals. Finally, the results of positive and negative pressure testing are compared to investigate whether or not anecdotal claims that the direction of pressure loading affects leakage and can be repeated experimentally.

Assessment of Repeatability during the Test Series

Test specimens were subjected to three water penetration resistance test methods with different pressure loading scenarios, and had to be transported to each of the testing apparatuses and their storage locations. Thus it was necessary to determine if successive testing and/or transport caused any permanent damage before results could be compared.

Two measures were taken to obviate this issue. First, the maximum pressure applied was intentionally set at half of the window's rated design pressure (DP) to avoid permanent damage to the wall assembly, seals, and window components, which would in turn change water penetration resistance. Second, a custom built air caster cart was developed to literally float the walls from one location to the next. This system worked well; the investigators have no cause to believe that any of the specimens were damaged during transport.

To address the potential outcomes from successive testing, the first test was repeated after the static, cyclic, and dynamic tests (performed in this order). All other factors being equal (e.g., identical mechanical response of the valves, temperature, relative humidity, etc.), the two static pressure tests should produce the same results if the specimens were not permanently damaged in previous tests.

The results of the first and last uniform static pressure tests are now discussed. The test data for this project may be found in tables 6-1 and 6-2 (The reader should refer to [53] for the test data from the companion project specimens found in table 5-2). Table 6-1 contains initial infiltration paths that occurred at recorded pressures during the separate rounds of static testing. Each row in the tables corresponds to an isolated location where infiltration was observed. Table 6-2 contains the number of leakage paths observed in each test.

Each specimen that exhibited either a large change in the pressure threshold associated with the first sign of leakage and/or number of leaks from the first static pressure test to the last were reanalyzed using other recording methods used during testing (e.g. photographic and video), to determine if indeed damage accumulation had occurred. The salient points from the re-inspection are listed below.

- Specimens 019, 020B and 070 exhibited new infiltration paths through the window/wall interface during the second static pressure test, demonstrating damage. These test results will be disregarded.
- Specimen 011 exhibited new infiltration paths through the window assembly during the second static pressure test. Its test results will be disregarded.
- Specimen 067 exhibited new infiltration paths through the precast sill at a lower pressure in the second static test, demonstrating damage. Its test results will be disregarded.
- Specimen 064 should be identified as the only specimen that was subjected to 1675.8 Pa (35.0 psf) during the dynamic pressure test. These pressures were substantially beyond the test protocol of 50% of the design pressure (1197.0 Pa /25.0 psf), hence the specimen was deemed to have sustained damage and its results will be disregarded.

- During the initial static pressure testing, research personnel prematurely terminated 2 of the 9 specimen tests (032 and 049) because of concern that the rate of water infiltration might damage the specimen or overload the drainage capacity of the testing apparatus. These were the first tests performed in this project. Further investigation showed that rates of infiltration observed were typical and no damage had occurred. In subsequent tests, the testing was carried out through the full duration.

- Regarding specimens 020D and 025, it is the opinion of the research team that the infiltration paths documented in the second static pressure test were minute and possibly overlooked in the first static pressure test. They are judged to not be indicative of permanent damage.

Summarizing, six out of the 34 wall specimens exhibited a change in performance sufficiently large to warrant their removal from subsequent analysis. For practical purposes it may be assumed that the remaining specimens exhibited repeatable performance characteristics and that the results are intercomparable.

Comparison of Results from Static, Cyclic and Dynamic Test Methods

Comparing the diagnostic ability of static, cyclic and dynamic testing was the principal objective of this project. The ultimate goal is to determine if full-scale dynamic testing should replace the simplified test methods used today or if the simplified tests are sufficient to evaluate water penetration resistance in their current form (or with minor modifications). It is important to note that these questions are being asked in the context of "systems" testing. Today, products are tested in isolation, which many professionals feel is a major shortcoming.

This new understanding is the key to improving simplified, but highly repeatable, test protocols to bridge the gap between what can be physically accomplished and duplicated in commercial testing labs, and what actually occurs in a windstorm (or perhaps, a research-grade windstorm simulation facility).

Dynamic pressure testing using the hurricane simulator was assumed to be the better representation of loads exhibited by a windstorm, although it is noted that there still remain many deficiencies with the ability of full-scale simulators to recreate hurricane force winds and wind-

driven rain. The field is still in its infancy, and projects such as this one are required for experimentalists to hone these techniques. That being said, the system was calibrated to a simplified representation of actual field data collected in hurricanes and true "wind-driven" rain was applied (in contrast to the pressure chamber tests where water is sprayed on the specimen while a pressure gradient is created across the specimen).

Table 6-3 contains information about the specimens that exhibited leakage in the first three rounds of testing. Specimens that did not leak or experienced permanent damage during the testing are omitted. The number of common leakage paths identified through both dynamic and static testing is listed in the first data column. The second data column contains the number of leakage paths observed in the cyclic and dynamic tests. The dynamic test results compare more favorably to the cyclic test than the static pressure test. Table 6-4 contains the number of leakage paths observed in static and cyclic tests that were not observed in the dynamic testing. It also contains the number of leakage paths observed exclusively in the dynamic test, but did not manifest in the static or cyclic tests. The counts are nearly identical (7,7,8) for the three test methods, which indicates there is no clear advantage to the dynamic testing.

Summarizing, adapting conventional testing techniques to holistically test wall systems appears to work well based on the results of these experiments. It should be noted that this observation is only strictly valid for the type of construction evaluated in this research, namely single-family residential finished wall systems with integrated fenestration.

Intercomparison of Window Operator Water Penetration Resistance

The water penetration resistance of the specimens with operable windows is listed in table 6-5. They are grouped by operator type: awning (016, 035, 054, 073), casement (006, 025, 048), single hung (017C, 022, and 043) and horizontal sliding (032, 049). Summary statistics are provided in table 6-6.

All of the operable windows met the requirement that the water penetration resistance must be greater than or equal to the 15% of the design pressure (stipulated in Section 5.3.3.2 of AAMA/WDMA/CSA 101/I.S.2/A440 [38] and Section 5.2.6 of TAS 202-94 [47] in Florida) using the leakage definition set forth in ASTM E 331. ASTM E 331 states that leakage is the "penetration of water beyond a plane parallel to the glazing (the vertical plane) intersecting the innermost projection of the test specimen, not including interior trim and hardware, under the specified conditions of air pressure difference across the specimen." Water was observed to collect in the bottom slider track earlier in the test, thus for completeness, a second pressure threshold is included in table 6-5. This water would have to reach a sufficient elevation head to overtop the back dam to qualify as leakage using the ASTM E 331 definition.

The results summarized in table 6-5 demonstrate that those windows that use a compression seals exhibit better watertightness than the sliding seal windows. None of the awning windows leaked, which based on the limited results of this research, indicates that the awning style is the preferable option for area prone to severe wind driven rain. Two of the three casement windows leaked, but a larger pressure than the sliding seal windows. The single hung windows leaked at the lowest pressures, but the flow rate through the horizontal sliders was much greater.

Operable Window Infiltration Rate Testing

The testing application standards typically allow for two load configurations. A suction load can be applied to the interior of the specimen, or a positive pressure can be applied to the exterior of the specimen. In either case, the opposite side of the specimen is open to the free atmosphere. Thus, all other factors being the same, the pressure gradient should be the same across the specimen.

It has been speculated that the direction of loading can affect the water penetration resistance (vis-à-vis test results on identical products using both load scenarios that do not agree). This issue was specifically addressed in one of the stakeholder oversight meetings, which prompted further testing using a positive pressure chamber (all of the tests results discussed so far were obtained using a negative pressure chamber).

Four test specimens were tested again using the two pressure chambers. The loads were incremented in a stepwise pattern while the infiltration rate, through the window assembly alone, was monitored. Results from the testing, which appear in figure 6-1 and figure 6-2, are virtually identical. It should be noted that because the infiltration rate was measured through the window, specimen 070 (deemed to have sustained damage through the window wall interface) was reintroduced. It should also be noted that compression seal operator type windows were intentionally left out of this experiment because of the difficulty of collecting and measuring the minute volumes of infiltrated water (e.g. figure 6-3). These data suggest that there is no basis to the claim that the direction of loading affects the infiltration rate given that flow rates were nearly identical for a large range of pressures. Moreover, the lowest pressure threshold for which infiltration occurred for both tests compared very favorably. A summary of infiltration flow rates is given in figure 6-4 and typical infiltration paths are provided in figures 6-5 through 6-8.

Least squares curve fitting was performed on the data. The infiltration rate through the hung windows appears to be directly proportional to the pressure load, while the relationship between the pressure and infiltration rate through the horizontal sliders is non-linear. Equations for flow and their respective coefficients of determination are as shown in equations 6-1 through 6-4 for specimens 017C, 022, 049, and 070 respectively. P-Pressure(Pa), Q-Flow rate (L/min).

$$Q = 3.28 \times 10^{-5} P - .76 \quad (6\text{-}1)$$
$$R^2 = 0.964$$

$$Q = 1.90 \times 10^{-3} P - 0.76 \quad (6\text{-}2)$$
$$R^2 = 0.982$$

$$Q = 0.67 e^{6.8 \times 10^{-4} P} - 3.8 \times 10^{-4} e^{-0.01P} \quad (6\text{-}3)$$
$$R^2 = 0.979$$

$$Q = 0.61 e^{3.7 \times 10^{-4} P} - 24.11 e^{-8.2 \times 10^{-3} P} \quad (6\text{-}4)$$
$$R^2 = 0.995$$

An investigation as to whether water penetration behavior is dependant on prior load rate (i.e. target pressures are achieved from greater or lower pressures) was also conducted. In figures 6-1 and 6-2 the infiltration rates are compared as loads are applied in a step wise fashion. It was theorized that once a specimen was brought up to a certain pressure, infiltration rates at any subsequent lower pressure would be greater; however, the data in these figures suggests that infiltration rates are independent of prior pressure levels.

Summary

Specimens were subjected to static, cyclic as well as amplitude- and frequency-modulated sinusoidal pressure load sequences, followed by a repeat of the static test to ensure that the specimens were not permanently damaged during testing. Six of the 34 test specimens exhibit different leakage characteristics between the first and last tests. These results were omitted from further analysis (with the exception of specimen 022, which was reintroduced for isolated window testing). It was found that adapting conventional testing techniques to holistically test wall systems appears to work well based on the results of these experiments. Compression seal windows are more watertight than sliding seal windows, with awning windows being the superior option. Finally, positive and negative pressure loading were performed on test

specimens. It was shown that the direction of loading has no effect on the infiltration rates and pressure threshold associated with the first sign of leakage.

Table 6-1. Time to Leakage and Corresponding Pressure in Uniform Static Pressure Tests

Specimen	First Static Test			Second Static Test			Difference	
	Time	Pa	psf	Time	Pa	psf	Pa	psf
001	10:54	450	9	DNL	DNL	DNL	N/A	N/A
016	DNL	DNL	DNL	DNL	DNL	DNL	N/A	N/A
017	DNL	DNL	DNL	DNL	DNL	DNL	N/A	N/A
018	18:17	867	18	DNL	DNL	DNL	N/A	N/A
018B	DNL	DNL	DNL	DNL	DNL	DNL	N/A	N/A
018C	DNL	DNL	DNL	DNL	DNL	DNL	N/A	N/A
018D	DNL	DNL	DNL	DNL	DNL	DNL	N/A	N/A
018E	DNL	DNL	DNL	DNL	DNL	DNL	N/A	N/A
019B	DNL	DNL	DNL	DNL	DNL	DNL	N/A	N/A
019D	DNL	DNL	DNL	DNL	DNL	DNL	N/A	N/A
020	DNL	DNL	DNL	DNL	DNL	DNL	N/A	N/A
035	DNL	DNL	DNL	DNL	DNL	DNL	N/A	N/A
048	16:22	1489	31	DNL	DNL	DNL	N/A	N/A
054	03:13	1226	26	DNL	DNL	DNL	N/A	N/A
073	04:51	139	3	DNL	DNL	DNL	N/A	N/A
020D	10:45	503	11	11:09	522	11	19	0
017C	15:00	948	20	15:40	977	20	29	1
064	08:40	402	8	11:22	431	9	29	1
043	09:12	474	10	09:56	527	11	53	1
049	11:25	847	18	10:57	795	17	-53	-1
025	12:40	565	12	11:36	503	11	-62	-1
017B	17:45	843	18	20:00	958	20	115	2
019C	07:20	273	6	06:00	192	4	-81	-2
017E	06:20	215	5	03:18	139	3	-77	-2
020C	06:38	239	5	04:15	139	3	-101	-2
006	15:15	699	15	10:40	828	17	129	3
032	09:30	527	11	11:11	675	14	148	3
017D	19:30	943	20	17:27	819	17	-124	-3
011	10:30	493	10	09:11	369	8	-124	-3
022	07:21	345	7	10:25	603	13	259	5
070	10:12	450	9	11:49	728	15	278	6
019	15:00	958	20	08:55	354	7	-603	-13
067	15:34	977	20	03:57	139	3	-838	-18
020B	DNL	DNL	DNL	11:10	474	10	N/A	N/A

Table 6-2. Number of Leakage Paths Observed in Uniform Static Pressure Tests

Specimen	First Static Test	Second Static Test	New Path in Second	Location of New Path
001	1	0	0	Through sealant
016	0	0	0	
017	0	0	0	
018	1	0	0	Joinery bottom right corner
018B	0	0	0	
018C	0	0	0	
018D	0	0	0	
018E	0	0	0	
019B	0	0	0	
019D	0	0	0	
020	0	0	0	
035	0	0	0	
048	1	0	0	Through weather stripping
054	1	0	0	Small drop through window wall interface
073	1	0	0	Window wall interface
020D	2	3	1	Screw in right jamb
017C	3	3	0	
064	5	5	2	Head jamb, left jamb sash interface
043	3	3	0	
049	5	6	2	Lock assembly, head jamb
025	4	4	1	Through compressible seal top left
017B	1	1	0	
019C	2	1	0	Through sealant
017E	2	2	0	
020C	1	1	0	
006	3	2	0	Joinery of operable pane
032	1	3	2	Above operable pane, meeting rail
017D	1	1	0	
011	5	6	3	Joinery bottom left corner, joinery top right, Meeting rail
022	4	4	0	
070	3	7	3	Sealant, lock assembly, meeting rail
019	1	2	1	Jamb bucking
067	1	1	0	Precast sill
020B	0	1	1	Jamb bucking

Note: Damaged specimens are highlighted

Table 6-3. Leakage Paths Observed in Static, Cyclic and Dynamic Tests

Specimen	Similar Paths in Primary Static and Dynamic Tests	Similar Paths in Cyclic and Dynamic Tests
001	2	2
006	2	2
017B	0	0
017C	2	3
017D	0	0
017E	1	1
018	0	1
019C	2	2
020C	0	1
020D	2	4
022	3	4
025	3	4
032	1	3
043	3	3
048	1	0
049	5	4
054	0	0
073	1	1
Total	28	35

Table 6-4. Leakage Path Detection Comparison

Specimen	Paths in Static Not Detected in Dynamic	Paths in Cyclic Not Detected in Dynamic	Paths Detected Exclusively in Dynamic	Description of Paths Not Detected in Dynamic	Description of Paths Detected Exclusively in Dynamic
001	1	0	1	Through sealant at window fin	Through sealant at window fin
006	0	1	0	Through joinery	
017	0	0	3		Sill joinery, Jamb wall interface, Joinery of head jamb
017B	1	2	0	Window/flashing interface	
017C	0	0	0		
017D	1	1	0	Sealant/flashing interface	
017E	0	0	0		
018	1	0	0	Sealant/flashing interface	
019C	0	0	0		
020C	1	1	0	Skip in sealant	
020D	0	0	0		
022	0	0	1		Meeting rail
025	1	1	1	Crank assembly	Through joinery
032	0	0	1		Top of meeting rail
043	0	0	0		
048	0	0	0		
049	0	0	1		Through joinery of operable pane at top right corner
054	1	1	0	Window/flashing interface	
073	0	0	0		
Total	7	7	8		

Table 6-5. Evaluation of Operable Windows With Respect to Pressure of First Leakage Path

Operator type	Pressures (Pa/psf)				% of DP
	Static	2nd Static	Lowest	DP(Pa/psf)	
Awning					
054	DNL	DNL	DNL	2872.8/60	N/A
016	DNL	DNL	DNL	2523.3/52.7	N/A
073	DNL	DNL	DNL	2872.8/60	N/A
035	DNL	DNL	DNL	2523.3/52.7	N/A
Casement (067 removed)					
048	DNL	DNL	DNL	2872.8/60	N/A
006	699.0/14.6	828.3/17.3	699.0/14.6	1915.2/40	36.5%
025	565.0/11.8	502.7/10.5	502.7/10.5	1915.2/40	26.3%
Single Hung (064 removed)					
043	474.0/9.9	526.7/11.0	474.0/9.9	2872.8/60	16.5%
017C	670.32/14.0	1149.1/24.0	670.32/14.0	2633.4/55	25.5%
022	890.6/18.6	785.2/16.4	785.2/16.4	1915.2/40	41.0%
Hor. Sliding (leak per definition in Chapter 6* 011 and 070 removed)					
049	138.9/2.9	138.9/2.9	138.9/2.9	2872.8/60	4.8%
032	138.9/2.9	138.9/2.9	138.9/2.9	1915.2/40	7.3%
Hor. Sliding (leak defined per ASTM E 331**, 011 and 070 removed)					
049	847.5/17.7	794.8/16.6	794.8/16.6	2872.8/60	27.7%
032	N/A	675.1/14.1	675.1/14.1	1915.2/40	35.3%

Note: Two sets of data for Horizontal Sliding operator type to differentiate the definitions of leakage.

* Any liquid water observed from the interior side of the wall assembly to have bypassed the moisture barrier of the window/wall system

** Penetration of water beyond a plane parallel to the glazing (the vertical plane) intersecting the innermost projection of the test specimen, not including interior trim and hardware, under the specified conditions of air pressure difference across the specimen

Table 6-6 Average Percentage of Design Pressure for Which Leakage Occurred

Operator type	Average percentage of DP when infiltration occurred
Awning	Did not leak
Casement	37.6% (Note: One did not leak and one was damaged)
SH/DH	27.7%
Horizontal Sliding	6.1% (first sign of leakage)
Horizontal Sliding	31.5% (per ASTM E 331)

\

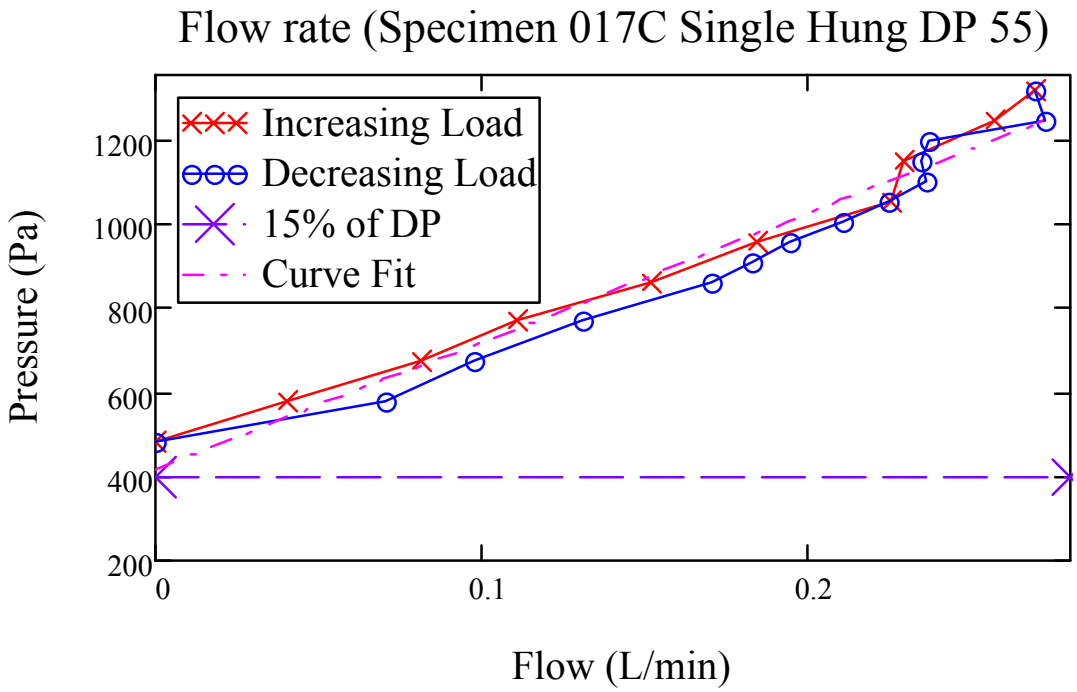
Flow rate (Specimen 017C Single Hung DP 55)
Increasing Load
Decreasing Load
15% of DP
Curve Fit
Pressure (Pa)
1200
1000
800
600
400
200
0
0.1
0.2
Flow (L/min)

A

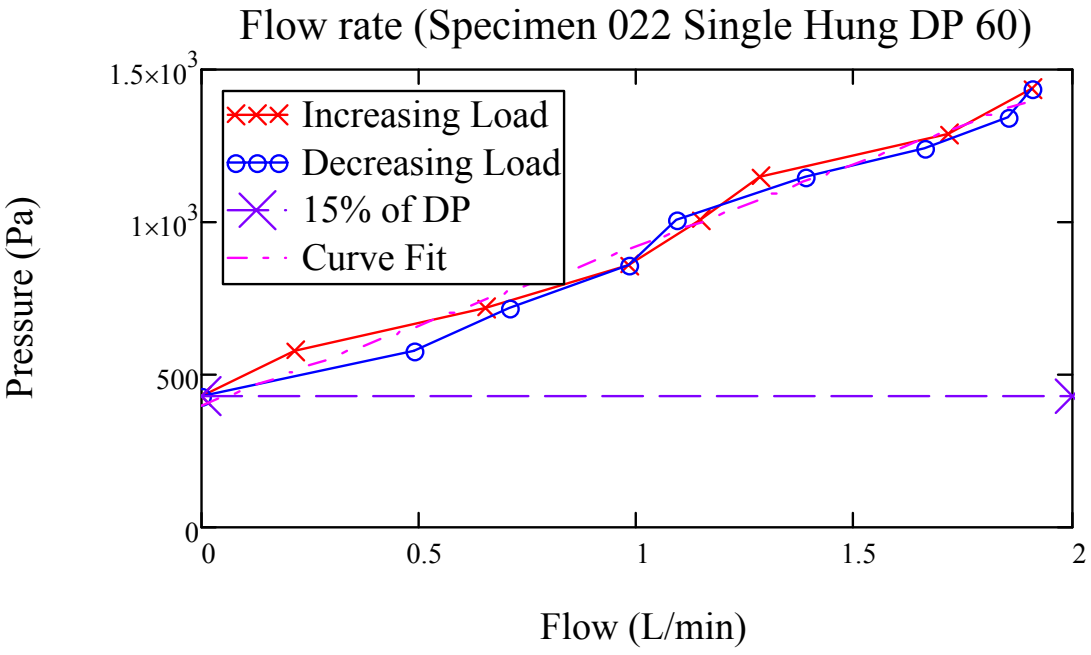
Flow rate (Specimen 022 Single Hung DP 60)
Increasing Load
Decreasing Load
15% of DP
Curve Fit
Pressure (Pa)
1.5×10^3
1×10^3
500
0
0
0.5
1
1.5
2
Flow (L/min)

B

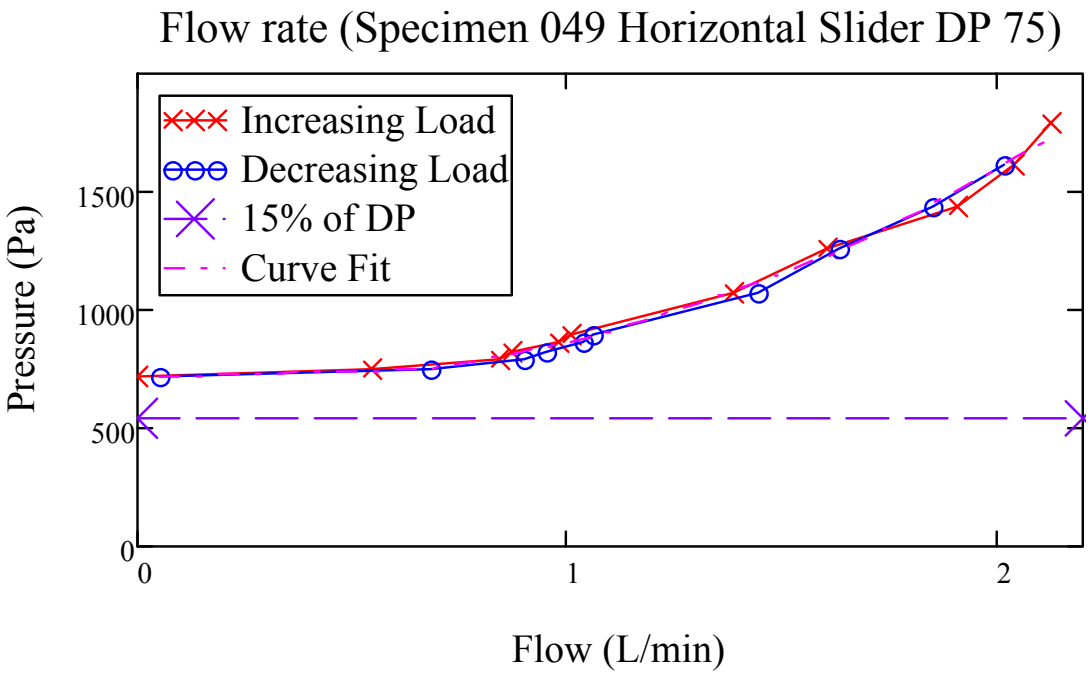

C

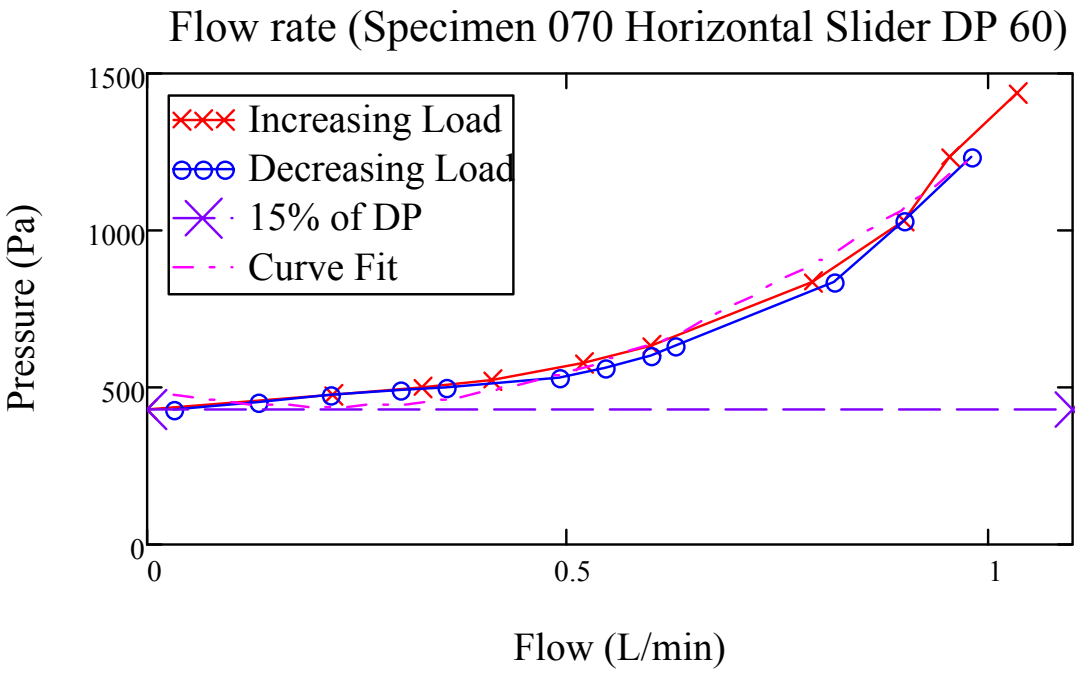

D

Figure 6-1. Load and Unload Curves for Operable Windows Under Negative Load

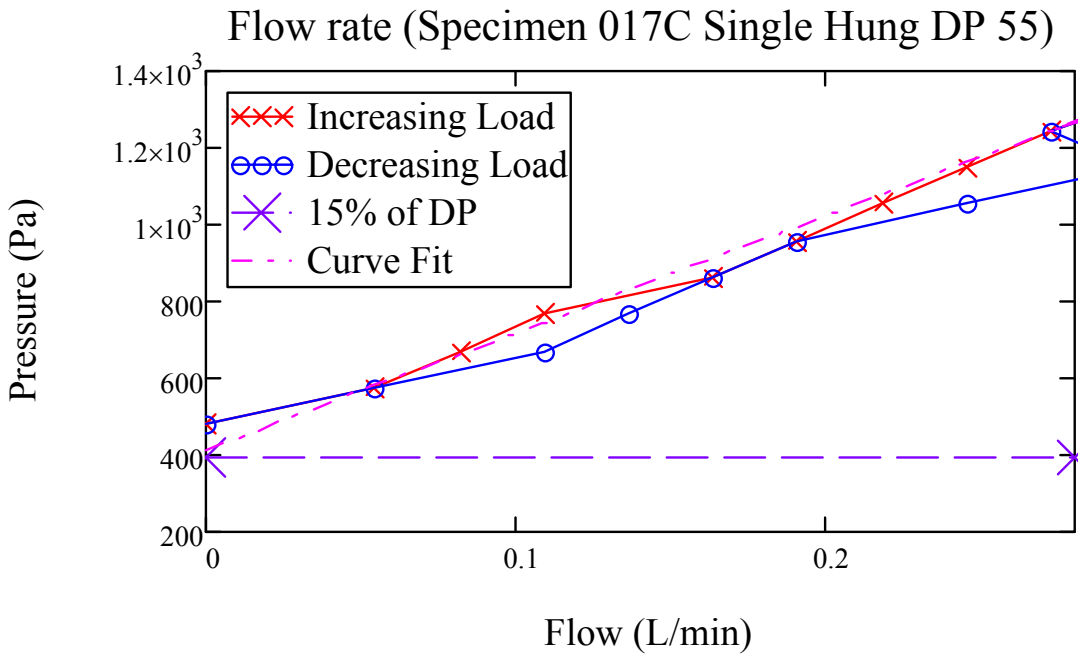
Flow rate (Specimen 017C Single Hung DP 55)
Pressure (Pa)
1.4×10^3
1.2×10^3
1×10^3
800
600
400
200
0
0.1
0.2
Flow (L/min)
Increasing Load
Decreasing Load
15% of DP
Curve Fit

A

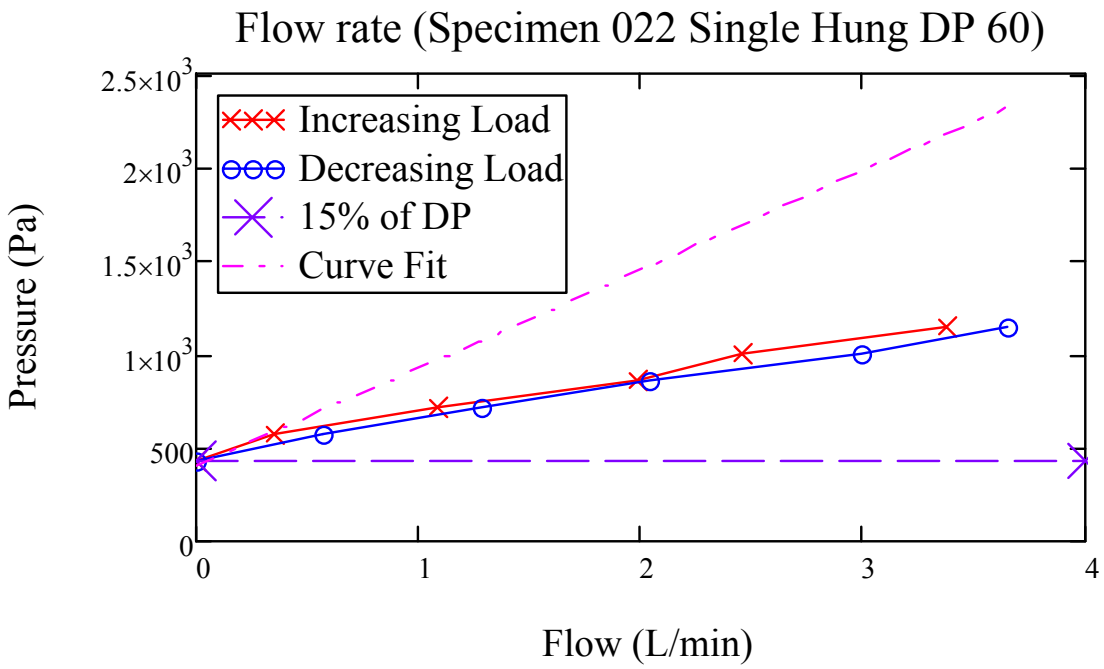
Flow rate (Specimen 022 Single Hung DP 60)
Pressure (Pa)
2.5×10^3
2×10^3
1.5×10^3
1×10^3
500
0
0
1
2
3
4
Flow (L/min)
Increasing Load
Decreasing Load
15% of DP
Curve Fit

B

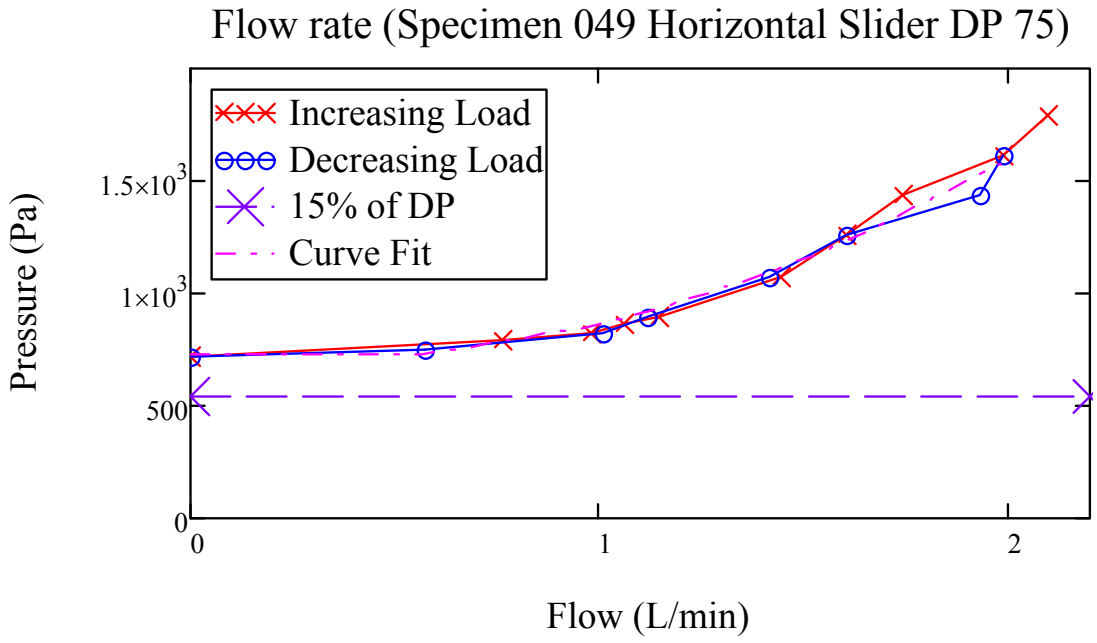

C

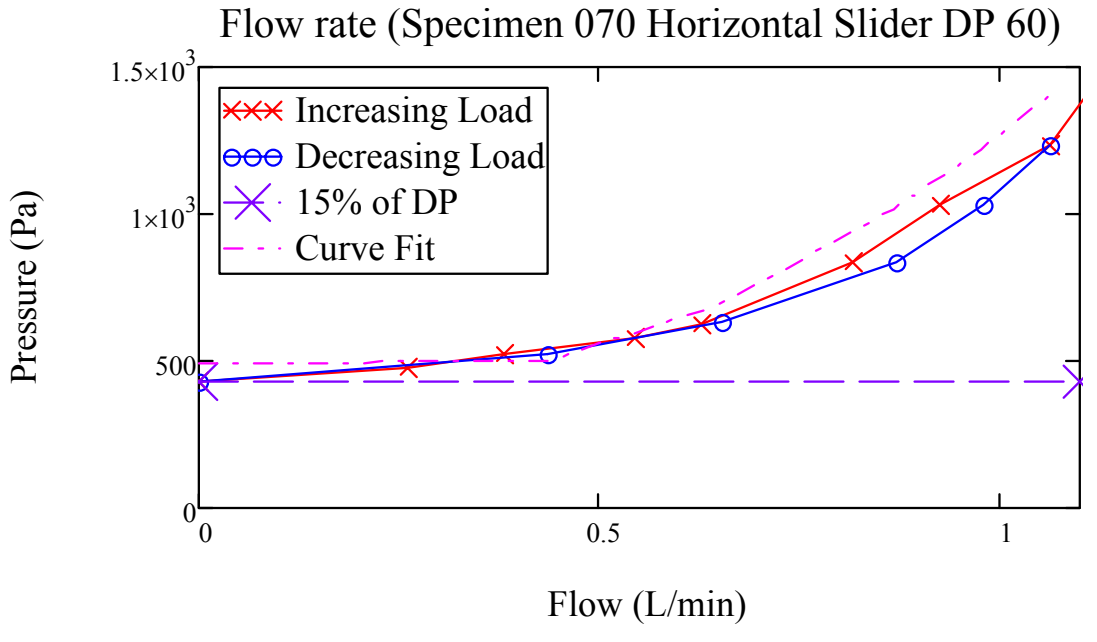

D

Figure 6-2. Load and Unload Curves for Operable Windows Under Positive Load (Curve-fit is from negative pressure testing)

Figure 6-3. Water Infiltrated at the End of Static Pressure Test (bottom left corner of specimen 006/ Casement window)

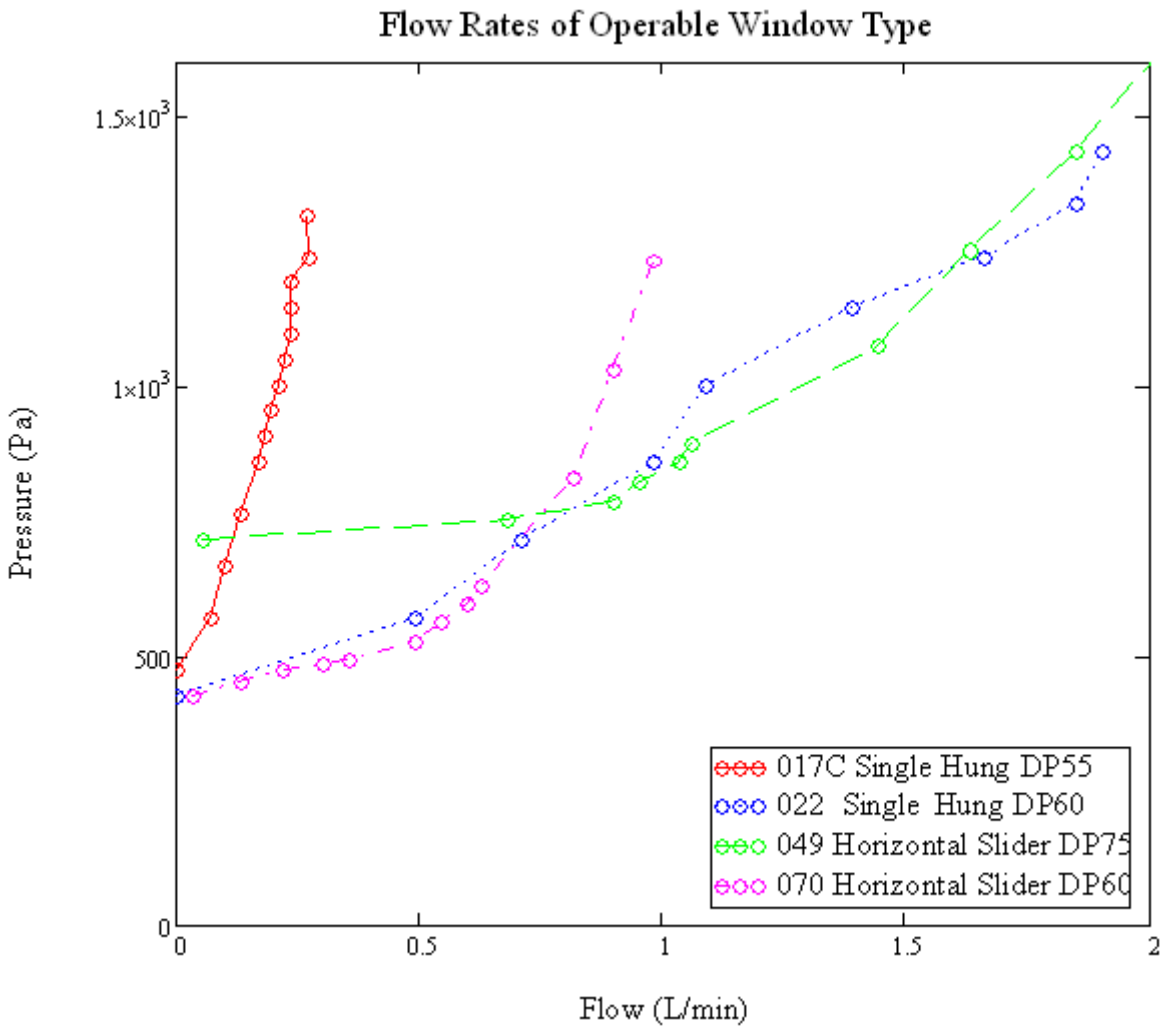

Figure 6-4. Comparison of Performance of Operable Window Assemblies

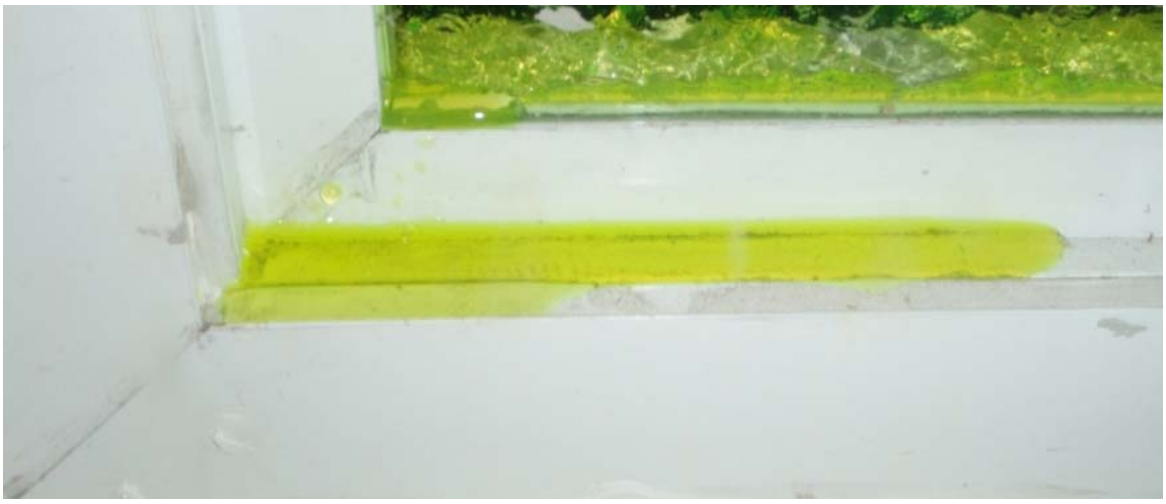

Figure 6-5. Typical Infiltration for Casement Windows (Bottom left corner above sill)

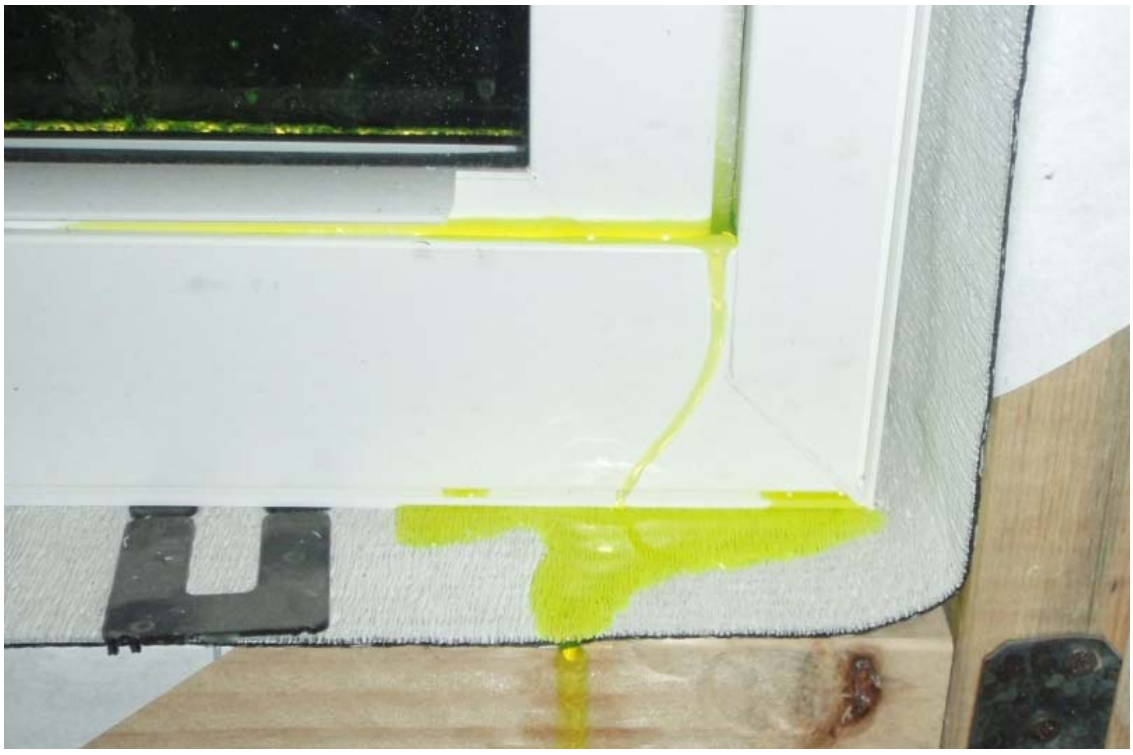

Figure 6-6. Typical Infiltration for Single Hung Windows (Bottom right corner above sill)

Figure 6-7. Typical Infiltration for Single Hung Windows (Left side of meeting rail)

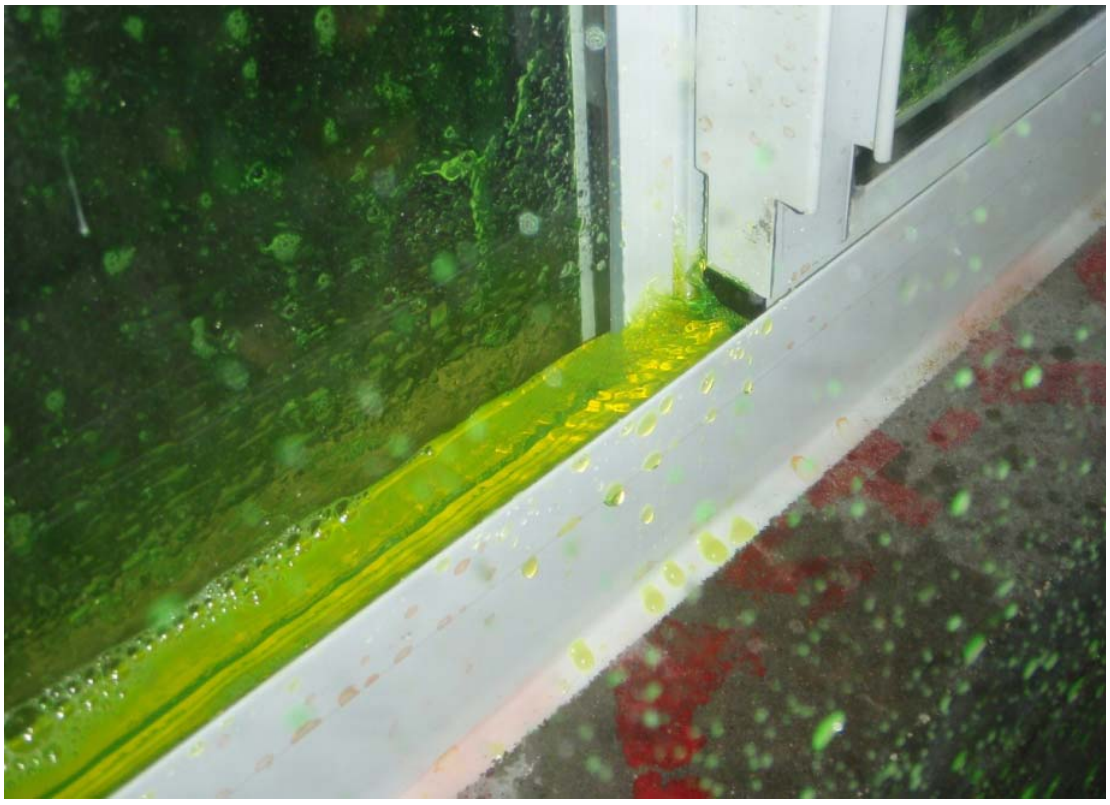

Figure 6-8. Typical Infiltration for Horizontal Sliding Windows

CHAPTER 7
KEY FINDINGS

Comparison of Test Methods

Specimens were subjected to static, cyclic as well as amplitude- and frequency-modulated sinusoidal pressure load sequences to observe water infiltration behavior. Analysis of the data compiled from the 34 specimens generated the following key observations regarding the testing methods:

- The current water penetration test methods for fenestration evaluate residential window performance in isolation. The results of this testing unequivocally demonstrate that additional leakage paths can occur in the wall and at the window-wall interface, which clearly indicates that the modern product approval process is deficient in addressing "real-world" leakage in the context of building systems performance.

- Based on the limited testing discussed herein, no clear advantage in diagnostic capability was found using dynamic simulation to evaluate the water penetration resistance of wall systems with integrated windows. This conclusion is only strictly valid for single family residential systems. It is presently unknown if these results are extensible to cladding and curtain wall systems, and these results likely have absolutely no bearing on roof systems, which are subjected to entirely different turbulent load conditions. Moreover, it is expected that in order to simultaneously compare wall and roof system performance in a laboratory setting, it will be necessary to implement full-scale dynamic testing at sufficient scale to envelope an entire building.

- The cyclic pressure test yielded more infiltration paths than the static pressure test, but the static pressure is a better choice to identify smaller leaks once they form (see figure 7-1 for an example). The pulsating pressure load causes an oscillating movement in the window assembly not recreated in the static test. Thus inertial effects are captured, which more closely resembles the expected response of a flexible system being acting upon by a buffeting load. Thus it may be useful to combine tests, with the static component following the cyclic testing

- The direction of loading (positive vs. negative pressure application) was found not to affect steady leakage rate nor the pressure threshold associated with the first sign of leakage. Tests were conducted in a highly controlled environment using research grade equipment, thus it is recognized that other logistical issues associated with experimental testing might create conditions that produce different results for each direction of loading.

- The current cyclic pressure testing methods prescribe a square wave load function. It is strongly suggested that a sinusoidal function should be substituted. The rationale is as follows. First, reproducing a square wave is physically unrealizable. Mechanical systems cannot simulate discontinuous pressure loading functions. Second, a "ramp" up or down is

required to shift from one pressure state to another. As the duration of this ramp becomes shorter, the possibility of overshooting the target pressure value becomes larger, which is highly problematic. Third, the most common practice in atmospheric science and wind engineering is to decompose wind and pressure into sinusoidal functions using a Fourier transform. Deviating from this practice is unnecessary and puts unnecessary experimental burden on the testing laboratories.

Performance of Window Assemblies

As expected, operable window assemblies exhibit larger rates of water infiltration than fixed windows. The test methods performed aimed to observe the effects that different components had on the water penetration resistance of the window assembly. Among the variables were wall material, window material, window design pressure, and window operator type. Analysis of the data compiled from the 16 specimens that had operable windows installed, generated the following key observations regarding the water penetration resistance:

- Specimens utilizing windows with compression seals performed better than those with sliding seals (table 6-6). Awnings performed the best of all specimens. In windows utilizing sliding seals, it was observed that the operable pane separated from the seal. This allowed a gap for air and water to intrude along the interface (e.g. through jamb/sash interface for single hung window)

- Compression seal operator type windows exhibited a substantial improvement in relative water penetration resistance (i.e. infiltration occurring at percentages of design pressure) with increased design pressure: Of the eight different compression seal operator type windows only the lowest rated (1915.0 Pa/ 40.0 psf design pressure) exhibited water infiltration (table 6-5). However it is unclear whether sliding seal operator type windows demonstrate depreciation or improvement in relative water penetration resistance (i.e. infiltration occurring at percentages of design pressure) with increased design pressure.

- Design pressure should not be considered an indication of performance in regards to infiltration flow rate, particularly given higher pressures: It is more of a dependence on operator type. During these tests it was observed in some cases, that the highest design pressure rated specimen exhibited the highest flow rates. Figure 6-1 shows that horizontal sliding operator type windows follow a non linear pressure to flow relationship, and single hung operator type windows follow a first order, linear pressure to flow relationship.

A

B

Figure 7-1. Infiltration Paths Through the Right Side of the Operable Sill of Specimen #032. A) End of the cyclic test B) End of the static test.

001

Wall:	Wood	**Ext. Finish:**	Stucco	**Sill:**	Flush Sill
Window:	Fixed	**DP Rating:**	40	**Material:**	Aluminum
Installation:	ASTM 2112	**Flashing:**	4" self-adhered	**Interior Seal:**	N/A

Time	Pressure (psf)	Location	Description	Leakage
STATIC				
10:54	9.4	jamb/ wall intf	leak through installation bottom left corner	Installation
CYCLIC				
N/A	N/A	N/A	No leaks observed	N/A
DYNAMIC				
4:30	9.6-21.4	below sill	Approximately 1 in from bottom right corner between frame and flashing	Installation
SECOND STATIC				
N/A	N/A	N/A	No leaks observed	N/A

Figure A1-1. Specimen 001 Records

006

Wall:	Wood	**Ext. Finish:**	Stucco	**Sill:**	Flush Sill
Window:	Fixed	**DP Rating:**	40	**Material:**	Aluminum
Installation:	ASTM 2112	**Flashing:**	4" self-adhered	**Interior Seal:**	N/A

Time	Pressure (psf)	Location	Description	Leakage
PRIMARY STATIC				
6:00	4.0	glazing intf	Through glazing interface at bottom left corner	Window
13:15	12.3	joinery	Through joinery of operable pane at bottom left corner	Window
15:15	14.6	sill corner	Over sill bottom left corner	Window
CYCLIC				
7:21	3-9	joinery	Through joinery of the operable pane at bottom right corner	Window
8:00	3-9	glazing int	Through glazing interface at the bottom left corner	Window
13:44	5-15	sill corner	Over sill bottom left corner	Window
20:20	7-21	sill	Over sill approximately 4" from bottom left corner	Window
DYNAMIC				
0:40	3.8-6.2	glazing intf	Through glazing interface at bottom left corner	Window
1:59	7.8-12.4	sill corner	Over sill at bottom left corner	Window
SECOND STATIC				
7:14	8.4	glazing intf	Through glazing interface at the bottom right corner	Window
10:40	17.3	sill corner	Over sill bottom left corner	Window
16:58	32.5	sill	Sill overflow	Window

Figure A1-2. Specimen 006 Records

011

Wall:	CMU	**Ext. Finish:**	DCC	**Sill:**	Flush Sill
Window:	Horizontal Slider	**DP Rating:**	45	**Material:**	Aluminum
Installation:	ASTM 2112	**Flashing:**		**Interior Seal:**	N/A

Time	Pressure (psf)	Location	Description	Leakage
STATIC				
0:01	2.9	Meeting rail	Through meeting rail at bottom	Window
6:20	4.9	Sill corner	Over sill at bottom right corner	Window
8:30	7.9	Sill	Over sill	Window
8:50	8.0	Jamb	Through jamb/sash interface at bottom right	Window
12:04	X.X	Jamb	Through jamb/sash interface at top right	Window
13:01	0.6	Joinery	Joinery of operable pane top left corner	Window
14:30	X.X		*Test stopped*	Window
CYCLIC				
0:01	1.4-4.3	Meeting rail	Through meeting rail at bottom	Window
6:50	3-9	Sill	Over sill	Window
6:55	3-9	Joinery	Through joinery of frame at bottom right corner	Window
9:17	4-12	Jamb	Through jamb/sash interface at bottom right	Window
10:00	4-12	Joinery	Through joinery of frame at bottom left corner	Window
11:40	4-12	Meeting rail	Through meeting rail at top	Window
12:00	5-15		Test stopped	Window
DYNAMIC				
0:22	3.8-6.2	Meeting rail	Through meeting rail at bottom	Window
1:00	3.6-6.6	Jamb	Through jamb/sash interface at XXX	Window
1:48	7.8-12.4	Sill	Sill overflow	Window
2:06	7.8-12.4	Meeting rail	Through meeting rail at top	Window
3:13	11.8-18.6	Head Jamb	Top of operable pane	Window
SECOND STATIC				
0:03	2.9	Meeting rail	Through meeting rail at bottom	Window
3:00	2.9	Below sill	Through window/wall interface, skip in sealant at bottom right corner	Installation
5:27	3.5	Joinery	Through joinery of frame at bottom left corner	Window
9:11	7.7	Sill	Sill overflow	Window
10:40	9.5	Precast Sill	Through precast sill at bottom right corner	Wall Assembly
14:06	13.3	Joinery	Through joinery of frame at top right corner	Window
16:30	X.X	Meeting rail	Through meeting rail at top	Window

Figure A1-3. Specimen 011 Records

019D

Wall:	CMU	**Ext. Finish:**	DCC	**Sill:**	Face Sill
Window:	Fixed	**DP Rating:**	40	**Material:**	Aluminum
Installation:	ASTM 2112	**Flashing:**		**Interior Seal:**	N/A

Time	Pressure (psf)	Location	Description	Leakage
STATIC				
N/A	N/A	N/A	No leakage observed	N/A
CYCLIC				
N/A	N/A	N/A	No leakage observed	N/A
DYNAMIC				
N/A	N/A	N/A	No leakage observed	N/A
SECOND STATIC				
N/A	N/A	N/A	No leakage observed	N/A

Figure A1-4. Specimen 019D Records

020B

Wall:	Wood	**Ext. Finish:**	FCB	**Sill:**	Flush Sill
Window:	Single Hung	**DP Rating:**	40	**Material:**	Vinyl
Installation:	AAMA 100	**Flashing:**	9" mech. attached	**Interior Seal:**	Low exp. foam

Time	Pressure (psf)	Location	Description	Leakage
STATIC				
N/A	N/A	N/A	No leakage observed	N/A
CYCLIC				
N/A	N/A	N/A	No leakage observed	N/A
DYNAMIC				
N/A	N/A	N/A	No leakage observed	N/A
SECOND STATIC				
11:10	9.9	Buck	Through the buck at bottom left corner	Installation

Figure A1-5. Specimen 020B Records

022

Wall:	Wood	**Ext. Finish:**	FCB	**Sill:**	Flush Sill
Window:	Single Hung	**DP Rating:**	40	**Material:**	Vinyl
Installation:	AAMA 100	**Flashing:**	9" mech. attached	**Interior Seal:**	Low exp. foam

Time	Pressure (psf)	Location	Description	Leakage
STATIC				
7:21	7.2	Jamb	Through jamb/sash interface at bottom right corner	Window
8:24	9.1	Jamb	Through jamb/sash interface at bottom left corner	Window
10:50	13.6	Jamb	Through jamb/sash interface, progressed through entire length of both jambs	Window
13:40	18.6	Meeting rail	Through meeting rail at right side	Window
14:21	19.9	Meeting rail	Through meeting rail at left side	Window
15:18	21.6	Below sill	Below the sill at mid length	Installation
18:58	28.2		Through XX at top right corner	
CYCLIC				
9:40	4-12	Jamb	Through jamb/sash interface at right side of operable pane	Window
11:20	4-12	Sill	Over sill at right side	Window
12:00	5-15	Sill	Sill overflow	Window
13:30	5-15	Jamb	Through left jamb/sash interface various spots	Window
13:59	5-15	Meeting rail	Through meeting rail right side	Window
15:00	6-18	Below sill	Below sill approximately 10" from bottom left corner	Installation
15:30	6-18	Meeting rail	Through meeting rail left side	Window
22:00	8-24		Test stopped	
DYNAMIC				
1:53	7.8-12.4	Sill	Sill overflow	Window
1:54	7.8-12.4	Meeting rail	Through meeting rail at left side	Window
2:35	6.4-14.2	Meeting rail	Through meeting rail at right side	Window
2:48	6.4-14.2	Jamb	Through jamb/sash interface of operable pane at right side	Window
2:48	6.4-14.2	Jamb	Through jamb/sash interface of operable pane at left side	Window
SECOND STATIC				
9:01	10.2	Sill corner	Sill overflow at bottom right corner	Window
10:22	10.9	Sill corner	Sill overflow at bottom left corner	Window
10:25	12.6	Jamb	Through jamb/sash interface at approx 18" up from both bottom left corner	Window
10:25	12.6	Jamb	Through jamb/sash interface at approx 18" up from both bottom right corner	Window
12:27	16.4	Meeting rail	Through meeting rail at left side	Window
12:27	16.4	Meeting rail	Through meeting rail at right side	Window
15:27	21.8	Meeting rail	Meeting rail at left side worsened considerably	Window

Figure A1-6. Specimen 022 Records

025

Wall:	Wood	**Ext. Finish:**	Stucco	**Sill:**	Flush Sill
Window:	Casement	**DP Rating:**	40	**Material:**	Vinyl
Installation:	AAMA 100	**Flashing:**	4" self adhered	**Interior Seal:**	Backer rod and sealant

Time	Pressure (psf)	Location	Description	Leakage
STATIC				
12:40	11.8	Sill	Over sill at bottom left corner	Window
15:05	14.5	Glazing Intf.	Through glazing interface at bottom right corner	Window
15:05	14.5	Glazing Intf.	Through glazing interface at bottom left corner	Window
15:05	14.5	Crank	Through crank assembly	Window
CYLIC				
5:00	2-6	Crank	Through crank assembly	Window
6:12	3-9	Sill	Over sill at bottom left corner	Window
11:40	4-12	Joinery	Through joinery of operable pane at bottom right corner	Window
14:30	5-15	Sill	Over sill at bottom right corner	Window
15:45	6-18	Sill	Sill overflow	Window
16:45	6-18	Glazing Intf.	Through glazing interface at bottom right corner	Window
18:22	7-21	Glazing Intf.	Through glazing interface at bottom left corner	Window
19:20	7-21	Joinery	Through joinery of operable pane at bottom right corner	Window
DYNAMIC				
2:30	6.4-14.2	Sill	Over sill at bottom left corner	Window
3:03	11.8-18.6	Joinery	Through joinery of operable pane at bottom right corner	Window
3:19	11.8-18.6	Glazing	Through glazing interface at bottom right corner	Window
3:19	11.8-18.6	Glazing	Through glazing interface at bottom left corner	Window
3:25	10.8-19.8	Sill	Over sill at bottom right corner	Window
3:25	10.8-19.8	Joinery	Through joinery of sill at bottom right corner	Window
SECOND STATIC				
11:36	10.5	Sill	Sill overflow at bottom left corner	Window
11:48	10.7	Glazing	Through glazing interface at bottom left corner	Window
15:30	14.8	Glazing	Through glazing interface at bottom right corner	Window
20:00	20.0	Head Jamb	Above operable pane at top left corner	Window

Figure A1-7. Specimen 025 Records

032

Wall:	CMU	**Ext. Finish:**	Stucco	**Sill:**	Flush Sill
Window:	Horizontal Sliding	**DP Rating:**	40	**Material:**	Vinyl
Installation:	ASTM E2112	**Flashing:**		**Interior Seal:**	N/A

Time	Pressure (psf)	Location	Description	Leakage
STATIC				
0:15	2.9	Meeting rail	Through meeting rail at bottom	Window
9:30	11.0		Test stopped	
CYCLIC				
0:04	1.4-4.3	Meeting rail	Through meeting rail at bottom	Window
12:50	5-15	Sill corner	Over sill at bottom left corner	Window
13:36	5-15	Head jamb	Above operable pane at various locations	Window
14:57	5-15	Sill corner	Over sill at bottom right corner	Window
15:40	6-18	Sill	Sill overflow	Window
16:30	6-18		Test stopped	
DYNAMIC				
0:00		Meeting rail	Through meeting rail at bottom	Window
2:03	7.8-12.4	Meeting rail	Through meeting rail at top	Window
2:22	7.2-13.2	Head jamb	Above operable pane at various locations	Window
3:26	10.8-19.8	Sill	Sill overflow	Window
SECOND STATIC				
0:03	2.9	Meeting rail	Through meeting rail at bottom	Window
11:11	14.1	Sill	Sill overflow at meeting rail and right corner	Window
14:50	20.9	Head jamb	Above operable pane top right corner	Window
16:50	24.5	Meeting rail	Through meeting rail at top	Window

Figure A1-8. Specimen 032 Records

043

Wall:	CMU	**Ext. Finish:**	DCC	**Sill:**	Flush Sill
Window:	Single Hung	**DP Rating:**	60	**Material:**	Aluminum
Installation:	ASTM E2112	**Flashing:**		**Interior Seal:**	N/A

Time	Pressure (psf)	Location	Description	Leakage
STATIC				
6:54	6.0	Buck	Through buck/window interface at various locations on right jamb	Installation
9:12	9.9	Sill	Sill overflow	Window
16:19	21.5	Meeting rail	Through meeting rail at right side	Window
CYCLIC				
			Note: leaked during prewetting	
4:58	2-6	Buck	Through shim/sealant at 1' down from top right corner	Installation
12:09	5-15	Sill corner	Sill overflow at left side	Window
12:40	5-15	Meeting rail	Through meeting rail at right side	Window
22:40	8-24	Sill corner	Sill overflow at right side	Window
DYNAMIC				
0:30	3.8-6.2	Buck	Through buck/window interface at various locations on right jamb	Installation
1:55	7.8-12.4	Sill	Sill overflow	Window
2:15	7.2-13.2	Meeting rail	Through meeting rail at both sides	Window
SECOND STATIC				
4:04	2.9	Buck	Through shim/sealant at 1.5' down from top right corner (4th shim)	Installation
9:22	10.1	Meeting rail	Through meeting rail at right side	Window
9:56	11.0	Sill	Sill overflow	Window
13:40	17.5	Buck	Through shim/sealant appeared to be through a crack in sealant	Installation

Figure A1-9. Specimen 043 Records

Specimen 048

048

Wall:	CMU	**Ext. Finish:**	Stucco	**Sill:**	Flush Sill
Window:	Casement	**DP Rating:**	60	**Material:**	Aluminum
Installation:	ASTM E2112	**Flashing:**		**Interior Seal:**	N/A

Time	Pressure (psf)	Location	Description	Leakage
STATIC				
16:22	31.1	Sill	Drop between weather stripping and frame	Window
CYCLIC				
N/A	N/A	N/A	No leakage observed	N/A
DYNAMIC				
1:48	7.8-12.4	Sill	Drop between weather stripping and frame	Window
SECOND STATIC				
N/A	N/A	N/A	No leakage observed	N/A

Figure A1-10. Specimen 048 Records

049

Wall:	Wood	**Ext. Finish:**	Stucco	**Sill:**	Flush Sill
Window:	Horizontal Slider	**DP Rating:**	60	**Material:**	Aluminum
Installation:	AAMA 100	**Flashing:**	9" mech. attached	**Interior Seal:**	Backer rod and sealant

Time	Pressure (psf)	Location	Description	Leakage
STATIC				
2:54	2.9	Meeting rail	Through meeting rail at bottom	Window
6:20	6.2	Joinery	Through joinery of glazing stop at bottom right of right pane	Window
8:40	11.6	Meeting rail	Through meeting rail at 6" above bottom	Window
10:30	15.6	Window/wall	Through window/wall interface at bottom left corner	Installation
11:25	17.7	Sill	Sill overflow	Window
13:30	22.5		Test stopped	
CYCLIC				
0:05	1.4-4.3	Meeting rail	Through meeting rail at bottom	Window
6:00	3-9	Meeting rail	Through meeting rail at top	Window
6:30	3-9	Joinery	Through joinery of operable pane at bottom left corner	Window
12:40	5-15	Below Sill	Below sill at bottom left corner	Window
22:40	8-24	Sill corner	Sill overflow at right corner	Window
24:20	9-27	Sill	Sill overflow below moving pane	Window
DYNAMIC				
0:19	3.8-6.2	Meeting rail	Through meeting rail at bottom	Window
1:00	3.6-6.6	Meeting rail	Through meeting rail at top	Window
2:53	6.4-14.2	Window/wall	Through window/flashing interface at bottom left corner	Installation
3:40	10.8-19.8	Window/wall	Through window/flashing interface at various locations	Installation
4:15	9.6-21.4	Joinery	Through joinery of operable pane at top right corner	Window
SECOND STATIC				
0:00	2.9	Meeting rail	Through meeting rail at bottom	Window
10:57	16.6	Sill	Sill overflow	Window
11:27	18.0	Meeting rail	Through meeting rail at top	Window
12:09	19.5	Window/wall	Through window/flashing interface at bottom left corner	Installation
12:56	21.3	Head jamb	Above operable pane at various locations	Window
13:35	22.7	Lock	Through lock assembly	Window
15:19	27.7	Meeting rail	Through meeting rail at middle	Window

Figure A1-11. Specimen 049 Records

054

Wall:	Wood	**Ext. Finish:**	FCB	**Sill:**	Flush Sill
Window:	Awning	**DP Rating:**	60	**Material:**	Aluminum
Installation:	AAMA 100	**Flashing:**	4" self adhered	**Interior Seal:**	Low exp. foam

Time	Pressure (psf)	Location	Description	Leakage
STATIC				
3:13	25.6	Window/ flashing	Through window/flashing interface at bottom right corner	N/A
CYCLIC				
5:30	30.0	Window/ flashing	Through window/flashing interface at mid width	N/A
DYNAMIC				
N/A	N/A	N/A	No leakage observed	N/A
SECOND STATIC				
N/A	N/A	N/A	No leakage observed	N/A

Figure A1-12. Specimen 054 Records

064

Wall:	CMU	**Ext. Finish:**	Stucco	**Sill:**	Flush Sill
Window:	Double Hung	**DP Rating:**	50	**Material:**	Vinyl
Installation:	ASTM E2112	**Flashing:**		**Interior Seal:**	N/A

Time	Pressure (psf)	Location	Description	Leakage
STATIC				
8:40	8.4	Sill corner	Sill overflow at bottom left corner	Window
10:50	11.5	Sill corner	Sill overflow at bottom right corner	Window
11:50	13.1	Jamb/sash	Through jamb/sash interface of bottom pane at left sides	Window
13:00	14.8	Meeting rail	Through meeting rail at right side	Window
13:30	15.5	Jamb/sash	Through jamb/sash interface of top pane at both sides	Window
15:15	18.1	Sill	Sill overflow	Window
14:50		Meeting rail	Through meeting rail at left side	Window
17:00	20.6		Test stopped	
CYCLIC				
6:21	3-9	Jamb/sash	Through jamb/sash interface at bottom left corner of bottom pane	Window
10:00	4-12	Jamb/sash	Through jamb/sash interface at both sides of bottom pane	Window
12:00	5-15	Sill	Sill overflow at both corners	Window
14:10	5-15	Meeting rail	Through meeting rail at right side	Window
14:10	5-15	Jamb/sash	Through left jamb/sash interface of top pane	Window
20:11	7-21	Head jamb	Through weather stripping of top pane	Window
DYNAMIC				
1:12	3.2-7.2	Jamb/sash	Through jamb/sash interface at right side of top pane	Window
1:30	3.2-7.2	Sill corner	Sill overflow at bottom left corner	Window
1:50	7.8-12.4	Sill corner	Sill overflow at bottom right corner	Window
2:04	7.8-12.4	Meeting rail	Through meeting rail right side	Window
2:37	6.4-14.2	Jamb/sash	Through jamb/sash interface at right side of bottom pane	Window
2:59	6.4-14.2	Head jamb	Through head jamb at various locations	Window
3:22	10.8-19.8	Meeting rail	Through meeting rail at middle	Window
SECOND STATIC				
11:22	9.0	Sill corner	Sill overflow at bottom left corner	Window
13:40	11.2	Meeting rail	Through meeting rail at both sides	Window
15:40	13.1	Jamb/sash	Through jamb/sash interface at right side of top pane	Window
16:22	13.7	Head jamb	Through head jamb at various locations	Window
			Note: specimen couldn't hold pressure higher than 15psf	

Figure A1-13. Specimen 064 Records

067

Wall:	CMU	**Ext. Finish:**	DCC	**Sill:**	Flush Sill
Window:	Casement	**DP Rating:**	55	**Material:**	Vinyl
Installation:	ASTM E2112	**Flashing:**		**Interior Seal:**	N/A

Time	Pressure (psf)	Location	Description	Leakage
STATIC				
15:34	20.4	Precast Sill	Drops formed on surface of precast sill	Wall Assembly
CYCLIC				
9:19	12.0	Precast Sill	Water visible through precast sill	Wall Assembly
DYNAMIC				
0:00		Precast Sill	Precast sill leaked during prewetting and throughout test	Wall Assembly
SECOND STATIC				
3:57	2.9	Precast Sill	Water visible through precast sill	Wall Assembly

Figure A1-14. Specimen 067 Records

070

Wall:	Wood	**Ext. Finish:**	FCB	**Sill:**	Flush Sill
Window:	Horizontal Sliding	**DP Rating:**	60	**Material:**	Vinyl
Installation:	AAMA 100	**Flashing:**	9" mech. attached	**Interior Seal:**	Low exp. foam

Time	Pressure (psf)	Location	Description	Leakage
STATIC				
0:21	2.9	Meeting rail	Through meeting rail at bottom	Window
10:12	9.4	Sill corner	Sill overflow at left side	Window
12:15	16.1	Sill corner	Sill overflow at right side	Window
16:27	23.8	Head jamb	Above operable pane at right corner	Window
CYCLIC				
0:05	1.4-4.3	Meeting rail	Through meeting rail at bottom	Window
9:30	4-12	Lock	Through bottom lock assembly	Window
10:22	4-12	Head jamb	Above operable pane at various locations	Window
11:40	4-12	Sill corner	Sill overflow at bottom left corner	Window
22:00	8-24		Test stopped	
DYNAMIC				
0:20	3.8-6.2	Meeting rail	Through meeting rail at bottom	Window
2:50	6.4-14.2	Window/ flashing	Through window/flashing interface at bottom left corner	Installation
3:09	11.8-18.6	Meeting rail	Through meeting rail at top	Window
3:33	10.8-19.8	Sill	Sill overflow	Window
-		Head jamb	Above operable pane at various locations	Window
SECOND STATIC				
0:01	2.9	Meeting rail	Through meeting rail at bottom	Window
9:09	10.4	Sealant	Through sealant at bottom right corner	Installation
11:49	15.2	Sill	Sill overflow	Window
12:20	16.3	Head jamb	Above operable pane at right corner	Window
16:19	23.4	Lock	Through bottom lock assembly	Window
18:17	26.9	Meeting rail	Through meeting rail at top	Window
19:30	29.3	Window/ flashing	Through window/flashing interface at bottom right corner	

Figure A1-15. Specimen 070 Records

073

Wall:	Wood	**Ext. Finish:**	Stucco	**Sill:**	Flush Sill
Window:	Awning	**DP Rating:**	60	**Material:**	Vinyl
Installation:	AAMA 100	**Flashing:**	4" self adhered	**Interior Seal:**	Backer rod and sealant

Time	Pressure (psf)	Location	Description	Leakage
STATIC				
4:51	2.9	Window/ flashing	Through window/flashing interface at bottom right corner	Installation
7:20	7.3	Window/ flashing	Through window/flashing interface at 1' bottom left corner	Installation
17:13	25.0	Window/ flashing	Through window/flashing interface at bottom center	Installation
19:55	30.0	Window/ flashing	Through window/flashing interface at bottom left corner	Installation
CYCLIC				
3:32	2-6	Sealant	At jamb 4" from bottom at right corner through sealant	Installation
8:50	3-9	Window/ flashing	Through window/flashing at 16" right of bottom left corner	Installation
10:30	4-12	Window/ flashing	Through window/flashing interface at bottom left corner	Installation
26:07	9-27	Window/ flashing	Through window/flashing interface at 26" right from bottom left corner	Installation
DYNAMIC				
2:55	6.4-14.2	Window/ flashing	Through window/flashing interface at bottom right corner	Installation
SECOND STATIC				
N/A	N/A	N/A	No leaks observed	N/A

Figure A1-16. Specimen 073 Records

LIST OF REFERENCES

[1] NCDC. Billion Dollar Climate and Weather Disasters, 1980-2008. National Climatic Data Center (NCDC) 2008

[2] Insurance Services Office (ISO), 545 Washington Boulevard, Jersey City, NJ 07310

[3] Pielke RA, Landsea CW. Normalized Hurricane Damage in the United States: 1900-2005. Natural Hazards Review 2007. 9 (1); 621-631.

[4] Blake ES, Rappaport EN, Landsea CW. NWS TPC-5 The Deadliest, Costliest, and Most Intense United States Tropical Cyclones from 1851 to 2006 (and other frequently requested hurricane facts). National Weather Service; 2007.

[5a] US Census Bureau. Interim Projections of the Total Population for the United States and States: April 1, 2000 to July 1, 2030. US Census Bureau; 2008.

[5b] US Census Bureau. Cumulative Estimates of Resident Population Change for the United States, Regions, States, and Puerto Rico and Region and State Rankings: April 1, 2000 to July 1, 2008. US Census Bureau; 2008.

[6] Hartwig RP. Florida Property Insurance Facts. III Institute for Insurance Information; 2008.

[7] Hartwig RP. Florida Case Study: Economic Impacts of Business Closures in Hurricane Prone Areas. III Institute for Insurance Information; 2002.

[8] Executive Order 92-291. Governor's Commission on Hurricane Andrew, Executive order 92-291. Governor's Disaster Planning and Response Review Committee; 1992.

[9] FEMA. Building Performance: Hurricane Andrew in Florida. Federal Emergency Management Agency; 1992.

[10] FEMA. Summary Report on Building Performance: 2004 Hurricanes. Federal Emergency Management Agency; 2005

[11] NCDC. Climate of 2004 Atlantic Hurricane Season. National Climatic Data Center (NCDC); 2004.

[12] NCDC. Climate of 2005 Atlantic Hurricane Season. National Climatic Data Center (NCDC); 2005.

[13] Katsaros JD, Hardman BG. Failed Fenestration: New Materials Require New Techniques. In: Thermal Performance of the Exterior Envelopes of Whole Buildings X International Conference Proceedings, ASHRAE; 2007.

[14] Simpson RH. The Hurricane Disaster Potential Scale. Weatherwise, 1974; 27: 169-186.

[15] NOAA. Data for hurricane charts gathered from:

http://csc-s-maps-q.csc.noaa.gov/hurricanes/viewer.html . National Oceanographic and Atmospheric Association; Accessed 7-12-2008.

[16] Sparks PR, Schiff SD, Reinhold TA. Wind Damage to Envelopes of houses and Consequent Insurance Losses. Journal Wind Engineering and Industrial Aerodynamics, 1994; 53 (1-2): 145-155.

[17] Gurley K, Burton J, Abdullah M, Masters F, Reinhold T. Post 2004 Hurricane Field Survey-an Evaluation of the Relative Performance of the Standard Building Code and the Florida Building Code. Department of Civil and Coastal Engineering, College of Engineering, University of Florida, Structures Research Communication No. 53102-2, 2006.

[18] Blocken B, Carmeliet J. Spatial and Temporal Distribution of Driving Rain On A Low-Rise Building. Wind and Structures, 2002; 5(5): 441-462.

[19] Blocken B, Carmeliet J. A Review of Wind-Driven Rain Research in Building Science. Journal of Wind Engineering and Industrial Aerodynamics, 2004; 92: 1079–1130.

[20] Best AC. The Size Distribution of Raindrops. Quart. J. Roy. Meteorological Society, 1950; 76 (327): 16-36.

[21] Mualem Y, Assouline S. Mathematical Model for Rain Drop Distribution and Rainfall Kinetic Energy. Trans. Amer. Soc. Agric. Eng, 1986; 29 (2): 494-500.

[22] Karagiozis A, Hadjisophocleous G, Cao S. Wind Driven Rain Distributions on Two Buildings. Journal of Wind Engineering and Industrial Aerodynamics, 1997; 67(8): 559-572.

[23] Choi ECC. Simulation of Wind Driven Rain Around the Building. Journal of Wind Engineering and Industrial Aerodynamics, 1993; 46-47: 721-729.

[24] Choi ECC. Parameters Affecting the Intensity of Wind Driven Rain on the Front Face of a Building. Journal of Wind Engineering and Industrial Aerodynamics, 1994; 53(1-2): 1-17.

[25] Choi ECC. Determination of Wind Driven Rain Intensity on Building Faces. Journal of Wind Engineering and Industrial Aerodynamics, 1994; 51(1): 55-69.

[26] Choi ECC. Wind Driven Rain on Building Faces and the Driving Rain Index. Journal of Wind Engineering and Industrial Aerodynamics, 1999; 79(1-2): 105-122.

[27] Rodgers GG, Poots G, Page JK, Pickering WM. Theoretical Predictions of Rain Drop Impactions on a Slab Type Building. Building Science, 1974; 9: 181-190.

[28] Mualem Y, Assouline S. Mathematical Model for rain Drop Distrubution an Rainfall Kinetic Energy. Transactions of the American Society of Agricultural Engineering ASAE TAAEAJ, 1986; 29(2): 494-500.

[29] Blackall TN, Baker MC. Rain Leakage of Residential Windows in the Lower Mainland of British Columbia. Division of Building Research National Research Council of Canada; 1984.

[30] Mullens M, Hoekstra B, Nahmens I, Martinez F. Water Intrusion in Central Florida Homes during Hurricane Jeanne in September 2004. Report to U.S. DOE, University of Central Florida Housing Constructability Lab; 2006.

[31] J.W. Lstiburek. Rainwater Management Performance of Newly Constructed Residential Building Enclosures During August and September 2004. Prepared for the Home Builders Association of Metro Orlando and the Florida Home Builders Association; 2004.

[32] RDH. Water Penetration Resistance of Windows- Study of Codes, Standards, Testing, and Certification. RDH Building Engineering Limited; 2002.

[33] RDH. Water Penetration Resistance of Windows –Study of Manufacturing, Building Design, Installation and Maintenance Factors. RDH Building Engineering Limited; 2002. “

[34] Hershfield DM. Technical Paper No.40- Rainfall Frequency Atlas of the United States. National Weather Service; 1961.

[35] NOAA. NOAA Technical Memorandum NWS Hydro-35. National Oceanic and Atmospheric Administration (NOAA); 1977

[36] Tokay A, Bashor PG, Habib E, Kasparis T. Raindrop Size Distribution Measurements in Tropical Cyclones. American Meteorological Society- Monthly Weather Review, 2008; 136(5): 1669-1684.

[37] Willis PT, Tattelman P. Drop-Size Distribution Associated With Intense Rainfall. Journal of Applied Meteorology, 1989; 28: 3-15.

[38] AAMA/WDMA/CSA 101/I.S.2/A440-05. Standard specification for windows, doors and unit skylights. American Architectural Manufacturers Association/ Window and Door Manufacturers Association/ Canadian Standards Association; 2005.

[39] AAMA 501.1-05. Standard test method for exterior windows, curtain walls, and doors for water penetration using dynamic pressure. Illinois, USA: American Architectural Manufacturers Association; 2005.

[40] AAMA 520 (Draft). Voluntary specification for rating the severe wind driven rain resistance of windows doors and unit skylights. Illinois, USA: American Architectural Manufacturers Association; 2005.

[41] ASTM E331-00. Standard Test Method for Water Penetration of Exterior Windows, Skylights, Doors, and Curtain Walls by Uniform Static Air Pressure Difference. Pennsylvania, USA: American Society for Testing and Materials; 2000.

[42] ASTM E547-00. Standard Test Method for Water Penetration of Exterior Windows, Skylights, Doors, and Curtain Walls by Cyclic Static Air Pressure Difference. Pennsylvania, USA: American Society for Testing and Materials; 2000.

[43] ASTM E1105-05. Standard Test Method for Field Determination of Water Penetration of Installed Exterior Windows, Skylights, Doors and Curtain Walls Uniform or Cyclic Static Air Pressure. Pennsylvania, USA: American Society for Testing and Materials; 2005.

[44] ASTM E2268-04. Standard Test Method for Water Penetration of Exterior Windows, Skylights and Doors by Rapid Pulsed Air Pressure Difference. Pennsylvania, USA: American Society for Testing and Materials; 2004.

[45] AS/NZS 4284:1995. Testing of Building Façades. Homebush, Australia: Australia Standards; 1995.

[46] JIS A 1517. Test Method of Water Tightness for Windows and Doors. Tokyo, Japan: Japan Standards Association; 1984.

[47] TAS 202-94. Criteria for Testing Impact & Nonimpact Resistant Building Envelope Components Using Uniform Static Air Pressure. Florida, USA: Department of Community Affairs, Florida Building Code, Codes and Standards; 1994.

[48] TAS 203-94. Criteria for Testing Products Subject to Cyclic Wind Pressure Loading. Florida, USA: Department of Community Affairs, Florida Building Code, Codes and Standards; 1994.

[49] Masters FJ, Gurley KR, and Prevatt DO. Full-scale simulation of turbulent wind-driven rain effects on fenestration and wall systems. 3rd International Symposium on Wind Effects on Buildings and Urban Environment, Tokyo, Japan, March 4-5, 2008.

[50] Lindgren O. Climate Data OS Parameters for The Design of an Equipment for Accelerated Ageing of Windows and Other Wood-Based Products. Swedish Council for Building Research, 1984; 1: 195-199.

[51] Gjelsvik T. Apparatus for Accelerated Weathering of Building Materials and Components. Materials and Structures, 1983; 16(3): 209-211.

[52] Fazio P, Athienitis A, Marsh C, Rao J. Environmental Chamber for Investigation of Building Envelope Performance. Journal of Architectural Engineering, 1997; 3(2): 97-102.

[53] Salzano CT. Residential Window Installation Options for Hurricane-Prone Regions. Masters thesis presented to The University of Florida, 2009.

BIOGRAPHICAL SKETCH

Carlos Rodolfo Lopez was born in Bogota, Colombia. At the age of 5 he moved the state of Florida where he grew up. As the only child of a Business Administrator and Architect/Contractor he was exposed to the construction environment at a very young age. Upon graduating from John I. Leonard High School in June 2003 he began his pursuit of a Bachelor of Science degree in civil engineering, with a focus in Structures, from the University of Florida. While completing his B.S. he had the privilege of meeting great professionals from his field who shared his interests and passions. Upon completion of his degree in 2007 he sought the mentorship from one such professional, Dr. Forrest J. Masters. Under his mentorship he studied the behavior of building assemblies subjected to hurricane force wind and rain. In his study of building science he had the great opportunity of working side by side with professionals ranging from top executives of some the largest fenestration manufacturing companies to heads of the top trade organizations and leading legislative officials.

While completing his requirements for his Master of Engineering degree, Carlos also had the privilege participating in the Florida Coastal Monitoring Program (FCMP). The FCMP is a unique joint venture focusing on full-scale experimental methods that quantify low level hurricane wind behavior and the resultant loads on residential structures. As a team leader of the FCMP Carlos deployed to Hurricanes Gustav in Louisiana, Ike in Texas, and Tropical Storm Fay in Central Florida to set up instrumentation that quantified near surface hurricane behavior. Upon passing of the storms, Carlos also participated in teams that performed post-storm damage assessments.

Once fulfilling all requirements required for the Master of Engineering degree, Carlos will pursue a Doctor of Philosophy degree in civil engineering from the University of Florida.

Carlos R. Lopez is a student member of the American Association for Wind Engineering, the American Society of Civil Engineers, and American Concrete Institute.